AN ABSTRACT OF THE THESIS OF

Steven Neil Berris for the degree of Master of Science

in Forest Engineering presented on December 10, 1984

Title: Comparitive Snow Accumulation and Melt During Rainfall in Forest and Clearcut Plots in Western Oregon

Abstract approved: R. Dennis Harr

R. Dennis Harr

A study was conducted to compare snow accumulation and melt during rainfall in adjacent forest and clearcut plots in the transient snow zone of the western Cascade Range in Oregon. Snow accumulation differences were determined by comparing the water equivalents of forest and clearcut snowpacks. During rain-on-snow periods, energy balances were analyzed to evaluate the differences in energy transfers acting to melt snow in the two plots. In this way, snowmelt differences can be linked to the microclimatic alterations related to clearcut logging. Snowmelt estimated by energy balace analyses was compared with snowmelt determined by snowmelt lysimeter data and snow survey information.

The forest canopy played a strong role in controlling snow accumulation. Snow trapped in the forest canopy melted faster than snow that accumulated on the ground in the clearcut plot. Snow survey information indicated that the water equivalents of clearcut snowpacks averaged 29 mm, but were up to 74 mm greater than forest snowpacks.

For five rain-on-snow events during the winter of 1983-1984, four of which rainfall amounts were smaller than that called for in the study design, a comparison of snowmelt estimated by the three methods had variable results. Only during the last two rain-on-snow events, of which one was the annual rainfall event, did results from the three methods all show greater snowmelt in the clearcut plot. Snowmelt determined by lysimeter information was more reliable during these events than the previous three events because of improved rainfall sampling.

Snowmelt estimated by energy balance analyses was consistently greater in the clearcut plot. Longwave radiation was the greatest source of snowmelt for all events, contributing 38-88 percent of the total computed snowmelt of each event. Snowmelt attributed to net longwave radiation was 22-56 percent greater in the clearcut plot. However, the combined fluxes of latent and sensible heats accounted for a large portion of the snowmelt differential between the plots. Although the combined fluxes ranked second in importance as a source of heat for snowmelt (6-36 percent of the total snowmelt for each event), in the clearcut plot they were 226-300 percent of the combined fluxes in the forest plot.

During the largest rain-on-snow event (February 11-13, 1984), total snowmelt was 55-111 percent greater in the clearcut plot depending on the method of measurement. The increased snowmelt of the clearcut plot is attributed to (1) greater snow accumulation prior to the event and (2) greater energy inputs during the event.

COMPARITIVE SNOW ACCUMULATION AND MELT DURING RAINFALL IN FOREST AND CLEARCUT PLOTS IN WESTERN OREGON

by

Steven Neil Berris

A THESIS

Submitted to

Oregon State University

in partial fulfillment of
the requirements for the
degree of
Masters of Science

Completed December 10, 1984

Commencement June, 1985

Approved:

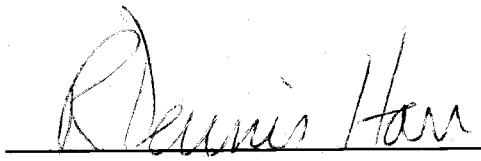

Professor of Forest Engineering in charge of major

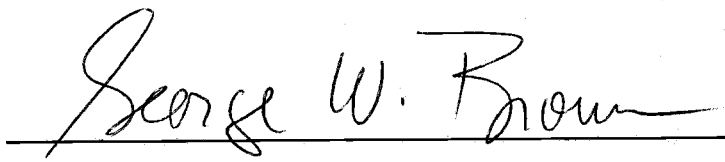

Head of Department of Forest Engineering

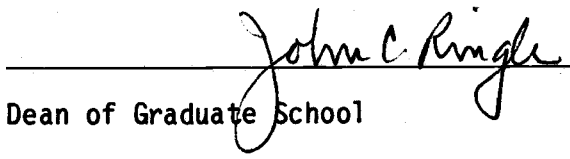

Dean of Graduate School

Date thesis is presented: December 10, 1984

Typed by Steven Neil Berris

ACKNOWLEDGEMENTS

I gratefully acknmowledge the guidance and suggestions of Dr. Robert Beschta and Dr. John Buckhouse. A special thanks to Don Henshaw for his assistance and patience pertaining to data processing and graphics. The technical expertise and thoughtful suggestions of Dr. Richard Holbo is appreciated. The assistance, professional experience, and timely humor of Dr. R. Dennis Harr helped make this experience especially pleasurable. The love and support of Deborah Clark throughout this study will never be forgotten. This master's thesis is dedicated to my parents, Ben and Elaine Berris for their support, guidance and love without which this would not be possible. This study was funded by USDA Forest Service, Pacific Northwest Forest and Range Experiment Station through Cooperative Agreement Supplement PNW-81-310.

TABLE OF CONTENTS

LIST OF FIGURES

LIST OF TABLES

COMPARITIVE SNOW ACCUMULATION AND MELT DURING RAINFALL IN FOREST AND CLEARCUT PLOTS IN WESTERN OREGON

INTRODUCTION

The hydrology of a snowpack is the product of the climatic characteristics of its geographic location. Snowpacks west of the Cascade Range crest can be described as "warm" snowpacks because their interior temperatures generally remain at or near 0°C (Smith, 1974). A state of delicate balance characterizes this type of snowpack because relatively little energy is necessary to initiate melt. Shallow snowpacks of lower elevations (350-1100 m) of the western Cascade Range in Oregon tend to be transient with time. Meltwater is quickly yielded from these snowpacks during warm or rainy periods due to their low capacity for storage of liquid water. It is not unusual for shallow snowpacks to melt completely during rainstorms.

The warm, transient snowpacks west of the Cascade crest are commonly subject to large amounts of rainfall. This is referred to as rain-on-snow. Rainstorms normally occur over a long duration (18-72 hrs) with low to moderate intensities (less than 6 mm/hr) (Harr et al., 1982). Extreme amounts of rainfall (more than 230 mm in 3 days) have resulted from warm, moist air originating from the vicinity of the Hawaiian Islands rising over the Cascade Range (Fredriksen, 1965; Harr, 1981). During rain-on-snow periods, water

output from these shallow snowpacks is derived from both the melting of the snowpack and the routing of rainwater through the snowpack. This water typically infiltrates into the forest soils where it is routed to stream channels as subsurface flow (Dyrness, 1969; Harr, 1977). Thus, peak flows are largely determined by the rate of water output from the snowpacks.

Rain-on-snow has been a dominant process shaping the geomorphology of drainage basins in western Oregon (Harr, 1981). During these events, soils quickly saturate resulting in positive pore pressures. As a result, the shear strength of these saturated soils may be reduced sufficiently to cause downslope movement. Soil mass movement may be imperceptibly small, such as creep, or failure may occur resulting in slumps, earthflows, or debris avalanches. In addition to altering the hillslope landscape, mass movement processes are the dominant mechanisms of sediment transport into stream channels in the Pacific Northwest (Swanston and Swanson, 1976).

High rates of subsurface flow which occur during rain-on-snow periods quickly increase the discharge of nearby streams (Harr, 1976). These streams may have the necessary power to transport channel sediment and debris, and induce serious channel erosion resulting in damaged aquatic habitats. Serious flooding may occur if sections of streambanks are eroded or if the flow capacities of channels are decreased by sediment and debris.

Historically, most of the damaging floods and many mass movement occurrences have occurred during rain-on-snow events. Of the 16 largest flood peaks on the Willamette River at Salem, Oregon between

1861 and 1981, 14 were associated with snowmelt during rainfall (Harr, 1981). Approximately 38 percent of the 18,900 km^2 Willamette River basin above Salem is in the transient snow zone. Similarly, 9 of the 12 largest peak flows in watershed 2 in the H.J. Andrews Experimental Forest in western Oregon were also associated with rain-on-snow (Harr, 1981). Snowmelt during heavy rainfall in December, 1964 caused massive damage by high peak flows, debris flows, and landslides in the H.J. Andrews Experimental Forest. Peak flows resulting from this storm and concurrent snowmelt caused the largest flows in over 100 years (Fredriksen, 1965). In the H.J. Andrews Experimental Forest, 83 percent of the road related failures, 10 of the 11 slope failures in clearcut areas, and 10 of the 11 debris torrents that could be accurately dated occurred as a consequence of snowmelt during rainfall (Harr, 1981).

THE PROBLEM

The effect of clearcut logging on snowmelt during rainfall may be large. When the forest canopy is removed, more snow generally accumulates in clearcuts due to the absence of canopy interception losses. Also, the altered microclimate of the clearcut allows increased exposure of the deeper snowpack to the warm, moist air that commonly occurs with rainfall. During windy periods, the heat and moisture from the air may be transferred to the snowpack causing increased energy inputs available for snowmelt. The warm, shallow snowpacks west of the Cascade Range crest may be especially sensitive to an altered microclimate because of their limited water holding capacities. This may result in the quick release of water from these snowpacks during rain-on-snow periods.

Few studies have investigated the effects of forest harvesting on snowmelt processes during rainfall. However, recent concern about the influence of harvesting on slope stability, peak flows, and aquatic habitats necessitates the analysis of this problem. Because snowmelt and subsequent water yield are governed by processes which transfer energy to snowpacks, evaluation of the magnitudes of energy transferred to snowpacks during rainy conditions is essential. In this way, snowmelt rates can be linked to differences in microclimate. Detailed microclimatic studies of forested and clearcut sites during rain-on-snow periods will identify the differences in the dominant processes melting snowpacks and lead to an increased understanding of the effects of clearcutting on rain-on-snow hydrology.

OBJECTIVE

The major objective of this study is to define how clearcutting influences snow accumulation and subsequent melt during rainfall in the transient snow zone of the western Oregon Cascades. To achieve this objective, four key tasks involving a forest and clearcut plot are performed:

1. Differences in snow accumulation between the two plots are determined.
2. Differences in snowmelt during rainfall between the two plots are determined.
3. The energy processes acting to melt the snow during rainfall at each plot are quantified, converted to melt water depths (energy melt), and compared. The energy balance of each snowpack is then computed.
4. Snowmelt predicted by the energy balance method is compared to the measured snowmelt.

The information gained in this study will provide a better understanding of the microclimatic differences of snowpacks in forested and clearcut areas. Although only two plots are studied intensively, the information will be of significance to areas of similar climatic characteristics throughout the western Cascades of the Pacific Northwest. The information will also be useful for comparison with similar studies focusing on microclimatology of snowpacks.

LITERATURE REVIEW

SNOW ACCUMULATION AND MELT

The quantity of snow available for melt at a particular location is the result of the snow's accumulation and ablation history. Numerous studies have shown both greater snow accumulation and melt rates in open areas compared to areas under forest cover (Niederhof and Dunford, 1942; Kittredge, 1953; Anderson, 1956; Miner and Trappe, 1957; Anderson and Gleason, 1959; Rothacher, 1965; Packer, 1971; Gary, 1974; Leaf, 1975; Swanson and Hillman, 1977; Haupt, 1979a and b; Harr, 1981; Gary and Troendle, 1982; Christner and Harr, 1982; Beaudry and Golding, 1983; Megahan, 1983). However, Haupt (1972 and 1979b) found that greater water output from forest snowpacks often occurs due to high rates of canopy drip from melting snow in forest canopies.

Greater snow accumulation in open areas (or clearcuts) relative to forests is attributed to different causes in different regions. Redistribution of snow is an important process in the colder, drier regions of the West (Rocky Mountains) where snowflakes are light and dry. Snow intercepted by a forest canopy is stripped off the trees by wind and redeposited at varying distances. Openings will have greater snow accumulations than the surrounding forests due to snow contributions from windward forests while little snow is contributed by the openings to the leeward forests (Leaf, 1975).

Differential placement of snow by aerodynamic processes is probably the most important factor resulting in greater snow accumulation in forest openings. Anderson and Gleason (1959) in central California and Gary (1975) in southern Wyoming reported that eddy formation occurred at forest-opening interfaces due to the separation of airstreams over the openings. This allowed dissipation of wind energy over the openings and preferential deposition of snow in them.

The snow zones of Oregon and Washington and, in some years, northern Idaho and western Montana are influenced by warm, moist winters. Consequently, snowfalls generally consist of large, wet snowflakes that are easily intercepted and temporarily stored in dense, forest canopies. The percentage of snow intercepted by a forest canopy will be large until the interception storage capacity is satisfied. Satterlund and Haupt (1970) reported that one third of the total snowfall was intercepted and temporarily stored in the forest canopy at the Priest River Experimental Forest, Idaho during the winters of 1966-1968. Once intercepted, the snow may be blown off to the ground by heavy winds. In other instances, the wet snow will cling to the tree branches and needles. Melt processes can then work to reduce the quantity of this intercepted snow and it will subsequently slide or drip off the canopy. Evaporation losses are usually quite small compared to the melt losses of intercepted snow (Miller, 1966; Satterlund and Haupt, 1970). Snow in openings (or clearcuts) will not be subjected to these interception losses.

The effects of clearcutting on snowmelt during rainfall in the Pacific Northwest have only recently become a subject of concern to

land managers. As a result, the actual effects have been studied only recently. Although previous studies have analyzed snowpack and streamflow observations from forested and clearcut areas, results have been contradictory. By observing changes in snowpack water equivalents between 1934 and 1941 in the Sierra Nevada of California, Kittredge (1953) concluded that reduced snowmelt rates under forest cover may reduce flood crests during heavy rains. Anderson and Hobba (1959), analyzing peak flows of 14 western Oregon streams, concluded that clearcutting 2.6 km^2 of forest in the snowmelt zone increased peak flows by 2.9 m^3/sec during rain-on-snow conditions. Later, however, Anderson (1970) acknowledged that the influence of clearcutting on snowmelt during rainfall needed more study. Rothacher (1970), using paired watersheds in the H. J. Andrews Experimental Forest in western Oregon, found no significant increase in peak flow discharges in a clearcut watershed when compared to a forested watershed during rain-on-snow. Haupt (1972), in northern Idaho, found that when significant amounts of snow was stored in forest canopies, water output was greater from forest snowpacks than snowpacks in openings due to increased canopy drip during rain-on-snow conditions. More recently, Harr and McCorison (1979) found that snowmelt peak flows were 36 percent smaller and delayed 11.5 hours after clearcut logging of a small watershed in the H. J. Andrews Experimental Forest in western Oregon. It was hypothesized that intercepted snow in the forest canopies melted quickly due to high exposure to the moist, turbulent air. Christner and Harr (1982) described the apparent relationship between cumulative timber harvest

and higher peak flows.

Because results from past research studies appear contradictory, the increased concern about the influence of clearcut timber harvesting on snowmelt rates during rainfall has led to controversy. As an example, proposed limitations on clearcut timber harvesting in the transient snow zone of British Columbia to protect the fishery and forest resources have been questioned on their validity in reference to published research (Toews and Wilford, 1978; Willington and Chatterton, 1983). No past research conducted in the Pacific Northwest has examined differential mechanisms of snowmelt during rainfall between forested and clearcut plots. In addition, differential snowmelt rates in reference to differential snow accumulation may further complicate the issue. If, for example, high rates of snowmelt occur in conjunction with greater accumulation in clearcut areas, snowpack water outputs will greatly increase after clearcut logging. Snowmelt studied as a process of energy transfer will help answer the harvesting-snow hydrology question.

SNOWPACK ENERGY BALANCE

The First Law of Thermodynamics states that energy can neither be created or destroyed, but may change in form. For a natural, terrestrial system, it is apparent that the energy entering a system must equal the energy leaving a system unless there is a change in the energy storage of the system. As a result, every system has an

energy balance:

$$\text{Energy Input} = \text{Energy Output} \pm \text{Energy Storage Change} \qquad (1)$$

Although a balance always exists, the magnitudes of the energy components vary. Variability of the energy component magnitudes occur over time and space by large scale, macro, and micro climatic differences. For most natural systems, the energy storage term can be omitted from the energy balance if the energy input and output components are integrated over a long period of time (Oke, 1978).

A snowpack is a system for which the energy balance applies. Snowmelt is a thermodynamic process that results from the different energy inputs to the snowpack (Davar, 1970; USACE, 1956). The relative magnitudes of energy sources for snowmelt, like those of any natural system, vary over space and time, but the sources are the same everywhere. Thus, determination of the energy balance of a melting snowpack during rainfall is dependent on determining the individual energy components of the balance. The energy balance of a melting, isothermal snowpack is described by:

$$K^* + L^* + F + G_b + H + \lambda E + Q_m = 0 \qquad (2)$$

where
K^* = net shortwave radiation flux density
L^* = net longwave radiation flux density
F = heat transfer from rainwater
G_b = heat transfer from the ground
H = turbulent transfer of sensible heat
λE = turbulent transfer of latent heat
Q_m = heat equivalent of snowmelt

The energy fluxes directed into the snowpack are considered to be positive while those directed away from the snowpack are considered negative. Solving the above equation for the heat of snowmelt (Q_m) yields:

$$Q_m = K^* + L^* + H + \lambda E + G_b + F \qquad (3)$$

It is evident that snowmelt may be predicted by the energy balance method once the energy components of the balance are known.

The components of the energy balance for a melting snowpack are the result of the transfer of energy by the processes of radiation, conduction, and convection. All of the energy balance components can be expressed in terms of energy flux densities, or the energy transfers per unit time over a unit area.

Radiation is the process of energy transfer by the oscillation of electromagnetic fields. A medium is not necessary for radiant energy transfer. The radiant energy emitted by an object is related to the temperature and emissivity of that object. The transfer of radiant energy to a surface or object is related to the transmissivity, reflectivity, and absorptivity of that surface or object. It is the net transfer, or absorbtion, of radiant energy that will be used as the energy balance component in reference to snowpacks.

The net transfer of radiation acting to melt a snowpack consists of only a small portion of the electromagnetic spectrum. Shortwave (solar) energy consists of radiation between the wavelengths of

0.2 and 4.0 μm which encompasses the visible spectrum (0.4-0.7 μm). Longwave (terrestrial) radiation is that portion of the electromagnetic spectrum with wavelengths between 3.0 and 80.0 μm. Longwave radiation also includes the infrared portion of the electromagnetic spectrum at about 11.0 μm. Longwave radiation (as well as shortwave radiation) emitted by an object is directly proportional to the fourth power of that object's absolute temperature.

Conduction is the process whereby energy is transmitted by molecular collisions within a medium or from one medium to another. It is usually most effective in solids due to high molecular density. Conductive heat transfer requires an energy gradient and proceeds in the direction of lower energy levels. Heat transfer from the ground to the snow is a process of conductive heat transfer. When rain is falling onto a snowpack, the heat transferred from the raindrops to the snowpack due to the temperature gradient between the two mediums is also a process of conductive heat transfer.

Convection is the process of energy transfer accomplished by molecular displacement within a fluid medium. Energy transfer by convection requires an energy gradient and occurs in the direction of lower energy. The intensity of convection varies with the gradient magnitude and the displacement or mixing mechanism. During snowmelt, eddys transport energy or mass from the atmosphere to the snowpack. The turbulent motions of the eddys over snowpacks are instigated by winds (forced convection)(Gates, 1962; Holbo, 1973; Rosenberg, 1974). Not surprisingly, convective heat transfer to snowpacks

proceeds at high rates when windspeeds are high (USACE, 1956; Obled and Harder, 1978). The turbulent transfer of sensible heat involves the transfer of heat from the air to a body, such as snow. The turbulent transfer of latent heat involves the transfer of water molecules from the air to a body, such as snow. When water vapor condenses on a snowpack, the water vapor flux density is converted to energy through the latent heat of vaporization released during condensation.

DETERMINATION OF SNOWPACK ENERGY COMPONENTS

NET SHORTWAVE RADIATION

The portion of shortwave radiation acting to melt snow is that which is absorbed by the snowpack. Absorbed shortwave radiation may be determined by subtracting transmitted shortwave radiation and reflected shortwave radiation from incoming shortwave radiation. When snowmelt occurs during rainfall, the high degree of cloudiness reduces the incoming shortwave radiation by up to 85 percent (USACE, 1956; Reifsnyder and Lull, 1965). Although shortwave radiation can penetrate snow even during rainy conditions, the transmissivity of most snowpacks at 10 cm depth is generally less than 10 percent of the incident shortwave radiation. Low transmissivity coupled with low intensity shortwave radiation during rainfall allows transmitted shortwave radiation to be ignored (USACE, 1956; O'Neill and Gray, 1972). As a result, absorbed

shortwave radiation is determined by the difference between incoming and reflected shortwave energy:

$$K^* = K\downarrow - K\uparrow \tag{4}$$

where K^* is net shortwave radiation (W/m^2), $K\downarrow$ is incoming shortwave radiation (W/m^2), and $K\uparrow$ is outgoing shortwave radiation (W/m^2). Shortwave radiation is diffuse during rain-on-snow periods so slope and aspect corrections are not necessary as would be the case for direct beam shortwave radiation (Obled and Harder, 1978).

NET LONGWAVE RADIATION

The net longwave radiation acting to melt a snowpack is the difference between incoming longwave radiation received by the snowpack and outgoing longwave radiation emitted by the snowpack:

$$L^* = L\downarrow - L\uparrow \tag{5}$$

where L^* is the net longwave radiation (W/m^2), $L\downarrow$ is the incoming longwave radiation (W/m^2), and $L\uparrow$ is the outgoing longwave radiation (W/m^2). The view of the snowpack is the sky, forest canopy, or other terrain features to which the snowpack is exposed.

Snow, like all bodies, emits longwave radiation as a function of

its temperature according to the Stefan-Boltzmann Law:

$$L\uparrow = \varepsilon\sigma T_s^{\ 4} \tag{6}$$

where $L\uparrow$ is the longwave radiation emitted by the snowpack (W/m^2), ε is the emissivity of the snowpack, σ is the Stefan-Boltzmann constant (5.67×10^{-8} $W/m^2 \cdot {}^\circ K^4$), and T_s is the temperature of the snowpack (°C). However, snow is a near perfect black body with respect to longwave radiation (USACE, 1956). Therefore, it's emissivity is near unity so that:

$$L\uparrow = \sigma T_s^{\ 4} \tag{7}$$

Longwave radiation from the sky is dependent on the moisture content and temperature of the entire sky exposed to the snowpack. During rainy periods, cloud cover significantly affects the longwave exchange process. Like snow, thick cloud cover is essentially a black body with an emmissivity near unity (USACE, 1956; Davar, 1970; Monteith, 1973; Campbell, 1977; Male and Granger, 1981). The longwave radiation emitted by clouds can then be determined by:

$$L\downarrow = \sigma T_c^{\ 4} \tag{8}$$

where $L\downarrow$ is the incident longwave radiation from the clouds (W/m^2) and T_c is the temperature of the cloud base (°C). Base temperatures of low, thick clouds are commonly similar to the air

temperatures near the ground (USACE, 1956; Campbell, 1977). As a result, equation (8) becomes:

$$L\downarrow = \sigma T_a^{\ 4} \tag{9}$$

where T_a is the air temperature (°C) near the ground. However, during windless periods, the cloud base temperature may deviate from the air temperature. For example, at the wet adiabatic lapse rate of 0.6°C per 100 m, the error would be less than 3 percent when the cloud base is 300 m above the snow surface with no winds.

For a snowpack in a forest, longwave radiation emitted by the forest canopy must also be considered. A solid forest canopy, like clouds and snow, approximates a black body with an emissivity near unity (USACE, 1956; Baumgartner, 1967; Jeffrey, 1970). Typically during clear weather, the temperature of a forest canopy varies a great deal, but during rainy periods, the canopy can be considered to be at the prevailing air temperature near the ground (USACE, 1956; Gray, 1970; Jeffrey, 1970). Thus, longwave radiation, $L\downarrow$ (W/m^2), emitted by the forest canopy can also be expressed by equation (9). Because the longwave radiation emitted by thick clouds and forests can be considered equal during rainfall, the longwave radiation incident upon a snowpack under a forest canopy or in the open may be approximated by equation (9). Combining equations (5), (7), and (9) yields the net longwave radiation in the forest or open according to:

$$L^* = \sigma(T_a^{\ 4} - T_s^{\ 4}) \tag{10}$$

TURBULENT ENERGY EXCHANGE

The processes of turbulent transfer of sensible heat and latent heat are more difficult to model than radiant energy transfer. In general, the convective transfer of an atmospheric property is related to the gradient of that property:

$$X = K(dx/dZ) \tag{11}$$

where X is the flux density of that property (W/m^2), (dx/dZ) is the vertical concentration gradient of the property, and K is the exchange coefficient (m^2/sec). For sensible heat exchange, the atmospheric property is temperature. For latent heat exchange, the property is water vapor. Analogous equations for each property can be synthesized with each exchange coefficient presented with a suffix for specification:

$$H = \rho_a C_a K_H (dT_a/dZ) \tag{12}$$

$$\lambda E = \rho_a \lambda K_E (dq/dZ) \tag{13}$$

where

H = turbulent transfer of sensible heat (W/m^2)
λE = turbulent transfer of latent heat (W/m^2)
K_H = exchange coefficient for sensible heat (m^2/sec)
K_E = exchange coefficient for latent heat (m^2/sec)
ρ_a = air density (kg/m^3)
C_a = specific heat of air ($kJ/kg\ ^\circ C$)
λ = latent heat of vaporization (kJ/kg)
T_a = air temperature ($^\circ C$)
q = specific humidity (kg/kg)
Z = vertical distance (m)

It can be seen that if each gradient is positive, a positive exchange will occur between the air and a snowpack. The above equations were developed on the assumption that wind flows over a uniform surface of adequate fetch to assure that the boundary layer properties are equilibrated with the surface studied (Federer and Leonard, 1971; Rosenberg, 1974).

The exchange coefficient, K, between the convective flux and property gradient is a function of windspeed. Thus, increased turbulent transfer of sensible and latent heats occurs with increasing windspeeds. The estimation of the exchange coefficient is difficult, and assumptions must be made for its computation. As a result, many different methods of estimating sensible and latent heat fluxes to a snowpack have been developed and there is little agreement on the validity of most of them. It is not surprising that the most precise method to evaluate turbulent transfer over snowpacks, the eddy correlation method, requires extensive and expensive instrumentation which is not suited for remote measurements. However, a method developed by the United States Army Corps of Engineers (1956) is simple and inexpensive to use for sensible and latent heat estimation. This method incorporates microclimatic measurements at one level above a snowpack.

The U.S. Army Corps of Engineers (USACE, 1956) developed equations to estimate sensible and latent heat transfer from the air to the snowpack. These equations are semi-empirical in that they are based on physical, aerodynamic principles, but the exchange

coefficients are incorporated in a constant determined by multiple regression analyses. It is assumed that the vertical gradients of windspeed, air temperature, and humidity vary with height as a power law profile during conditions of atmospheric stability. Lapse conditions over snowpacks are commonly stable due to a cold layer of air adjacent to the snowpack beneath warmer layers of air. It is also assumed that windspeed is zero, air temperature is 0°C, and vapor pressure is 610.78 Pa immediately above a snowpack. Thus, measurements of windspeed, temperature, and vapor pressure taken only at one level above a snowpack can be incorporated directly into the estimating equations. The equations estimate snowmelt by sensible and latent heat fluxes in terms of meltwater per unit time:

$$M_H = 1.80 \times 10^{-2} \, (P_a/P_o)(Z_a \times Z_t)^{-1/6} \, (T_a - T_s)V \qquad (14)$$

$$M_E = 8.63 \times 10^{-4} \, (Z_a \times Z_d)^{-1/6} \, (e_a - e_s)V \qquad (15)$$

where

M_H = sensible heat melt (mm/hr)
M_E = latent heat melt (mm/hr)
P_a = local atmosperic pressure (Pa)
P_o = atmospheric pressure at sea level (Pa)
Z_a = height of windspeed measurement (m)
Z_t = height of air temperature measurement (m)
Z_d = height of humidity measurement (m)
T_a = air temperature (°C)
T_s = snow temperature (°C)
V = windspeed (m/sec)
e_a = vapor pressure of air (Pa)
e_s = vapor pressure of snow (Pa)

HEAT TRANSFER BY RAIN WATER

The heat transferred to a snowpack by rain is a function of the quantity and temperature of the rain. Because the rain temperature is above the temperature of a snowpack, the rain will cool to the snowpack temperature and give up heat to the snow. The heat will serve to melt an isothermal 0°C snowpack, but for colder snowpacks, the heat will raise the snow temperature toward 0°C. For a melting snowpack at 0°C, the heat transfer from the rain is given by:

$$F = \rho_w C_w T_p P \tag{16}$$

where

F = heat transfer by rainfall (kJ/m^2)
ρ_w = density of water (kg/m^3)
C_w = specific heat of water (kJ/kg °C)
T_p = rain temperature (°C)
P = amount of rainfall (m^3/m^2)

Dewpoint temperature may be used as an estimate of the rain temperature due to the near-saturated air conditions existing during rain (USACE, 1956; Anderson, 1968). Thus, equation (16) becomes:

$$F = \rho_w C_w T_d P \tag{17}$$

where T_d is the dewpoint temperature (°C).

HEAT TRANSFER FROM THE SOIL

The heat transfer to a snowpack from the underlying soil is a function of the thermal gradient in the upper soil layers. With snow covering unfrozen ground, the ground surface is cooled to 0°C creating a thermal gradient with heat directed upwards from the warmer and deeper soil layers. During rain-on-snow periods, the release of 0°C water from the melting snowpack into the soil will reduce the soil thermal gradient resulting in near negligible heat transfer to a snowpack (USACE, 1956; Oke, 1978).

ENERGY BALANCE COMPONENTS IN REFERENCE TO THE LITERATURE

Although snowmelt prediction is one important use of energy balance analyses, quantification of the ongoing energy transfer processes may provide a basis for evaluating differential snowmelt in varying microclimates. Microclimatic alteration by forest management will affect the energy regime of a location which, in turn, will affect snowmelt. Clearcutting, by removing the forest canopy, may influence the energy regime of a site sufficiently to affect snowmelt during rainfall. The two dimensional surface of a clearcut contrasts greatly to a forest protruding its biomass into the atmosphere.

The relative magnitudes of the various energy transfer processes acting to melt snow have varied considerably among the numerous studies that applied energy balance analyses to snowmelt problems. However, grouping the studies according to weather conditions and

microclimate (forest or open) helps to identify some patterns. Numerous studies have applied energy balance techniques to analyze snowmelt during clear weather. The results of these studies suggest that net radiation is the dominant energy source for snowmelt when the ground is fully covered by snow and the sky is clear (Boyer, 1954; Hoinkes, 1955; Adkins, 1958; Gold and Williams, 1961; Federer, 1968; Gray, 1970; DeWalle and Meiman, 1971; Federer and Leonard, 1971; de la Casiniere, 1974; Gray and O'Neill, 1974; Hendrie and Price, 1978; McKay, 1978; McKay and Thurtell, 1978; Granger and Male, 1978; Male and Granger, 1981). Net radiation available for melting snow is greater in open locations than under forest canopies due to greater intensities of shortwave radiation in the open. This is because forest canopies absorb up to 90 percent of the incoming shortwave radiation before it reaches a snowpack on the forest floor (Boyer, 1954; USACE, 1956; Jeffrey, 1970). Because the clear sky is a poor absorber and emitter of longwave radiation, snowpacks in open areas commonly emit more longwave radiation than they receive. As a result, the net longwave radiation of melting snowpacks in open areas is commonly negative. Although melting snowpacks in the open lose more longwave radiation to the clear atmosphere than forest snowpacks, the high shortwave radiation insolation of open snowpacks during clear days usually assures greater net radiation magnitudes (USACE, 1956; Federer, 1968; Gray, 1970; Federer and Leonard, 1971; Hendrie and Price, 1978). Thus, snow generally melts most rapidly in the open when net radiation strongly dominates the energy budget.

During periods of advection, the transfer of sensible heat to

snowpacks becomes an important melt component (USACE, 1956; McKay and Thurtell, 1978). Advection of sensible heat is especially important when a site is under the influence of another area having different microclimatic conditions. DeWalle and Meiman (1971) found that in a Colorado forest, advected sensible heat from air in contact with warm, exposed patches of forest floor caused high sensible heat snowmelt rates (45.2 percent of the total melt). Cox and Zuzel (1976) and Granger and Male (1978) attributed high sensible heat snowmelt rates to sensible heat advected from bare ground in open areas. High melt rates have also been attributed to sensible heat advected by warm, dry winds originating from different regions (Gray, 1970). Table 1 compares results of selected energy balance studies on snowmelt during predominantly clear weather. Each value is given as a percentage of the total energy input for the period displayed.

Although snowmelt during rainfall is prevalent in the Pacific Northwest, New Zealand, and other areas with maritime climates, there have been relatively few energy balance studies of this phenomenon. The thick clouds and windy conditions, which commonly occur during rainfall, control the energy processes that melt snow. The significance of shortwave radiation in clear weather melt is severely reduced during rainfall due to the high degree of absorbtion by the clouds (USACE, 1956; Reifsnyder and Lull, 1965). In contrast, longwave radiation emitted by the clouds is much greater than from clear skies, and the resulting longwave radiation budget for a melting snowpack is increased. Thick clouds, like forest canopies,

Table 1. Selected Results of the Percentage Contribution of Radiant and Turbulent Energy Transfers Over Snow During Predominantly Clear Weather Conditions. (Q_N is net radiation, H is sensible heat transfer, and λE is latent heat transfer. Negative values represent energy outputs expressed as percentages of the total energy inputs.)

Observer	Location	Observation Period	Percentage Contribution		
			Q_N	H	λE
Boyer (1954)	Oregon forest	July, 1952	65	20	15
Hoinkes (1955)	Eastern European Alps	September, 1951	84	-	-
		July-August, 1952	58	-	-
		September, 1953	65	-	-
Adkins (1958)	Salmon Glacier, British Columbia	August, 1957	74.7	15.4	9.9
Gold and Williams (1961)	Ottawa, Canada	March, 1959	74.6	25.4	-74.1
DeWalle and Meiman (1971)	Colorado forest	June, 1968	56.3	43.7	-3.1
de la Casiniere (1974)	Sierra de Guardarrama of Spain	April-May, 1970	100.0	-10.6	-42.1
	European Alps	July, 1963	84.5	15.5	-15.5
Gray and O'Neill (1974)	Canadian Prairie of Saskatchewan	March, 1972	93	7	-
Cox and Zuzel (1976)	Reynolds Creek, Idaho	Unknown	36	64	-48
Hendrie and Price (1978)	Chalk River Forest, Ontario	April, 1978	98.5	-	-
Granger and Male (1978)	Canadian Prairie of Saskatchewan	April, 1975	95.2	4.8	-19.5
		March, 1976	62.0	38.0	-4.2

act as black body radiators with base temperatures similar to the air temperatures near the ground (USACE, 1956; Davar, 1970; Campbell, 1977; Male and Granger, 1981). The similar longwave emittance characteristics of forest canopies and clouds coupled with reduced shortwave radiation during rainfall result in similar net radiation budgets in forest and open sites.

The warm, humid air advected over snowpacks during rainfall has a large effect on the turbulent energy processes that melt snow. During rainfall, air temperatures rise above 0°C, and the air can become nearly saturated with water vapor. The heat and moisture gradients that form over snowpacks, along with wind, transfer sensible and latent heats to the snowpacks. Thus, it is not surprising that the turbulent transfer of energy to snowpacks may dominate snowmelt along the mountain ranges of the Pacific Coast.

Energy transferred to snowpacks from rainfall is not a major source of snowmelt except during periods of heavy rain (more than 17 cm/day) and low winds (less than 2.4 m/sec) (USACE,1956). During these periods, the mechanism of turbulent transfer is overshadowed by the release of heat as the rain comes into contact with snow and cools to 0°C. Anderton and Chinn (1978) found heat transfer by precipitation to be significant during a major rainstorm at Ivory Glacier in New Zealand. During a rainstorm of 400 mm in November, 1974, heat from precipitation was estimated to melt 28 mm of snow (45 percent ot the total snowmelt).

The majority of energy balance analyses involving snowmelt during rainfall suggest that turbulent energy transfer (sensible and latent

heat transfers) is the dominant source of snowmelt (Table 2). In a speculative analysis, Harr (1981) used the U.S. Army Corps of Engineers snowmelt indices to synthesize snowmelt and its energy components during simulated rain-on-snow events. The events consisted of rainfall varying between 0 and 200 mm/day with air temperatures of 2-10°C and an average windspeed of 2.4 m/sec. During light to moderate rainfalls of 0-170 mm/day, total daily melt was approximately 40-55 mm/day when the air temperature was 10°C. When the air temperature was 2°C, total daily melt was approximately 10 mm/day. Turbulent energy transfer was the dominant source of melt contributing 35-60 percent of the total melt when the air temperature was 10°C and 30-45 percent when the air temperature was 2°C. Melt by latent heat exhange accounted for approximately 80 percent of the turbulent melt. Energy supplied by longwave radiation was shown to be an important source of melt during light to moderate rainfall contributing 28-35 percent when the air temperature was 10°C and 22-29 percent when the air temperature was 2°C. During periods of heavy rainfall above 170 mm/day, energy supplied by rain exceeded the energy supplied by turbulent exchange and accounted for more than 35 percent of the total daily melt when the air temperature was 10°C and more than 30 percent of the total daily melt when the air temperature was 2°C. Total daily snowmelt exceeded 55 mm/day during these periods.

Other studies utilizing energy balance analyses for actual rain-on-snow periods generally agree with the speculative ranking of energy fluxes presented by Harr (1981), but there are some minor

Table 2. Results of the Percentage Contribution of the Energy Transfers to Open Snowpacks During Rainfall. (Q_N is net radiation, H is sensible heat transfer, λE is latent heat transfer, F is heat transfer from rain, and P is amount of precipitation (mm).)

Observer	Location	Observation Period	Percentage Contribution					P
			Q_N	H	λE	$H+\lambda E$	F	
Fitzharris, et al. (1980)	Southern Alps of New Zealand	10/12/78-10/14/78	23	-	-	58	19	150
Prowse and Owens (1982)	Southern Alps of New Zealand	11/24/76	23	46	30	76	1	11.5
		11/25/76	10	48	40	88	2	6.8
		10/29/77	29	59	10	69	2	19.0
		10/29/80	4	68	20	88	8	22.0
Zuzel, et al. (1983)	Northeastern Oregon	1/12/80	11	57	31	88	1	10.7
Moore and Owens (1984)	Southern Alps of New Zealand	10/28/82-11/8/82	16	57	25	82	2	127

deviations (Table 2). The studies of Prowse and Owens (1982) and Zuzel et al., (1983) agree that turbulent energy melt is dominant during rainfall, but in contrast to the scenarios presented by Harr, sensible heat was greater than latent heat melt. Beaudry and Golding (1983) found that during rainy periods with little wind, the significance of the turbulent melt components was reduced while the roles of longwave radiation and rain melt were enhanced.

Although there is a lack of information on the actual effects of clearcut timber harvesting on the energy regime of a melting snowpack during rainfall, one can compare microclimatic characteristics of forest areas with open areas and deduce differences in snowmelt. It is known, for example, that during rainfall, incident shortwave radiation is a minor source of melt in both forest and open areas (USACE, 1956; Reifsnyder and Lull, 1965). Net longwave radiation may be a significant source of melt during rainy periods, but clouds and forest canopies emit similar magnitudes of longwave radiation (USACE, 1956; Davar, 1970; Campbell, 1977; Male and Granger, 1981). Thus, clearcut timber harvesting would probably not significantly affect snowmelt from shortwave or longwave radiation. However, during rainfall, sensible and latent heat exchange with snowpacks is a dominant source of melt which may be significantly affected by clearcut logging. Sensible and latent heat exchanges are, respectively, related to temperature and water vapor gradients over snow as well as to a turbulent transfer coefficient. Because the air is virtually saturated during rainfall, similar gradients of temperature and moisture exist over snowpacks in both forest and

clearcut areas. However, there is no doubt that winds are both deflected upwards by the forest barrier and reduced by the numerous obstacles (trees) in the forest. As a result, windspeeds in open areas, such as clearcuts, are greater than in forests (Federer and Leonard, 1971; Jeffrey, 1971). Holbo (1984) found that windspeeds may be four times greater in a clearcut than in a forest. The relation between windspeed and turbulent transfer of energy suggests that the turbulent transfer coefficients would be increased by clearcut timber harvesting and, as a result, sensible and latent heat transfers would be increased. Toews and Wilford (1978), using the U.S. Army Corps of Engineers (USACE, 1956) snowmelt indices, speculated that it is possible that snowmelt rates could be more than doubled after clearcut timber harvest due to increased sensible and latent heat exchanges by high windspeeds. During a major rainfall event, snowmelt by energy transfer from the rain would probably be similar in both forest and clearcut sites because both sites receive similar rainfall (Rothacher, 1963).

METHODS

STUDY AREA

The study area is located at an elevation of 900 m in the McRae Creek drainage of the H. J. Andrews Experimental Forest near Blue River, Oregon. This area is located on the western slope of the Cascade Range crest about 72 km east of Eugene, Oregon (Figure 1). This study area was chosen because adjacent clearcut and forest study plots were easily accessible, yet protected by a locked gate. Although greater snow accumulation occurs at higher elevations, easy accessibility was limited by vehicle capabilities over snow and adjacent clearcut and forested plots protected by a locked gate were not found. Additionally, a cabin was located less than 1 km from the study plots.

The average annual precipitation for this study site is approximately 2340 mm of which approximately 80 percent occurs during the winter as both rain and snow (Harr, et al., 1982). Winters are relatively mild with January temperatures ranging between -12°C and 12°C (Rothacher, Dyrness, and Fredriksen, 1967). As a result, snowmelt during the winter is common and often occurs during rainfall.

EXPERIMENTAL DESIGN

The basic premise of this study is that site microclimatic characteristics of forests and clearcuts influence the water output

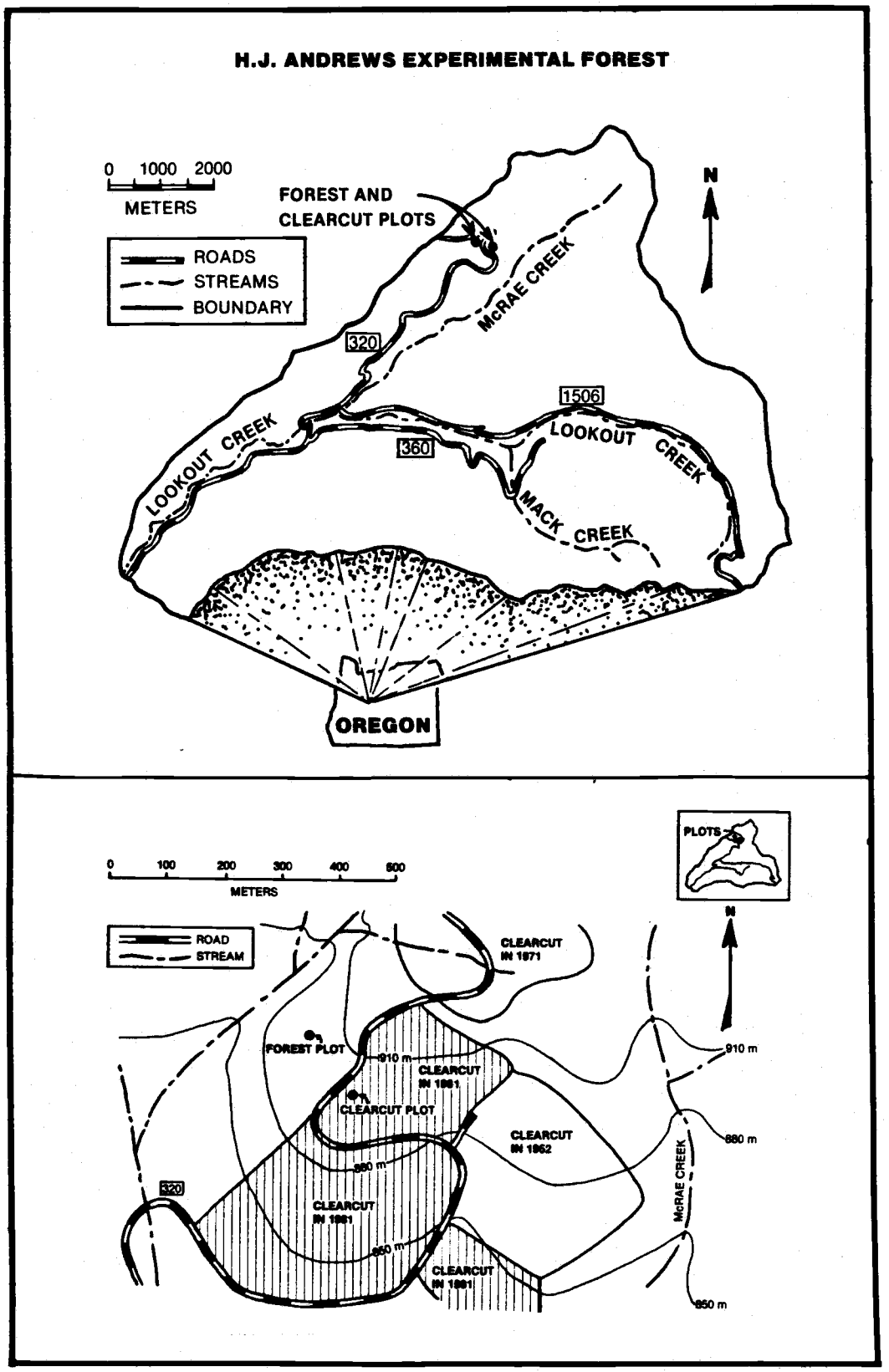

Figure 1. Location of Forest and Clearcut Study Plots in the H. J. Andrews Experimental Forest.

from snowpacks during rainfall. The specific hypothesis of this study is that, by clearcutting, snowpack water output during rainfall is increased by enhanced snowmelt of a deeper snowpack. Snowmelt is hypothesized to accelerate following clearcutting due to greater exposure of snowpacks in clearcut areas to wind. This results in increased sensible and latent heat transfer.

The case study utilized a pair of adjacent plots equipped with snowmelt lysimeters, raingages, and microclimatic sensors to determine and compare snowmelt rates and the energy processes that melt snow (Figures 2 and 3). One plot was located in a 22 ha clearcut logged in 1981 and broadcast burned in 1982. The clearcut plot had an unobstructed view to the south-southwest, the predominant direction of winter frontal winds. The forest edge was about 40 m to the northwest. The forest plot was located in an old-growth forest of Douglas-fir and western hemlock 30-60 m tall about 130 m from the clearcut plot and 150 m from the windward (south-southwest) edge. The canopy density of the forest plot averaged 86 percent and varied between 82 and 89 percent. Both plots were on nearly level ground, but surrounding slope gradients approached 80 percent.

Precipitation was measured by heated tipping bucket raingages mounted on the top of heated shelters. In addition, 16 small storage gages were installed in the forest and four gages were installed in the clearcut to account for spatial variation in rainfall.

Each plot contained eight snowmelt percolate pans which collect precipitation. These pans were scattered throughout the clearcut plot, but in the forest plot, they were systematically located under

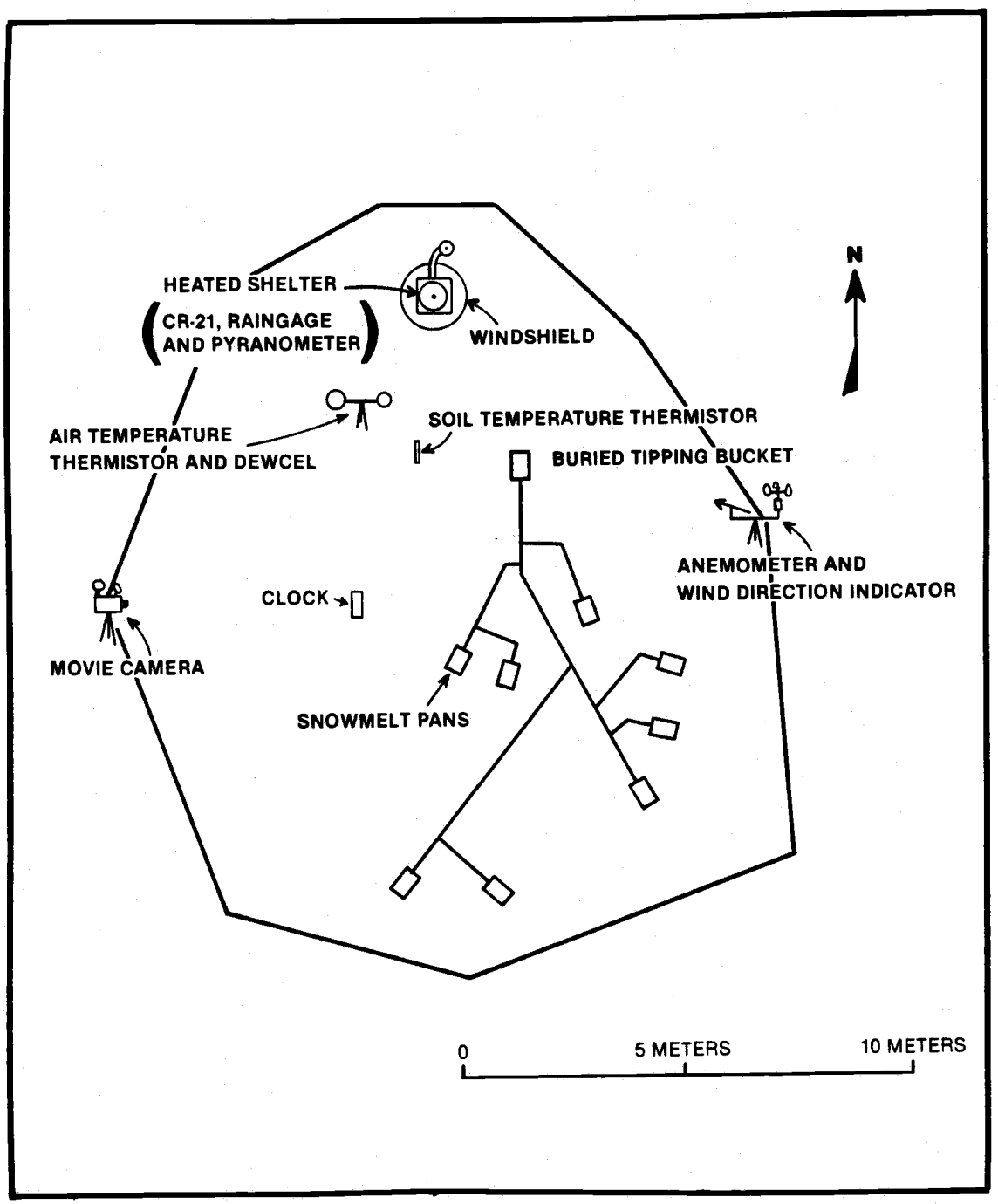

Figure 2. Instrumental Layout of the Clearcut Plot.

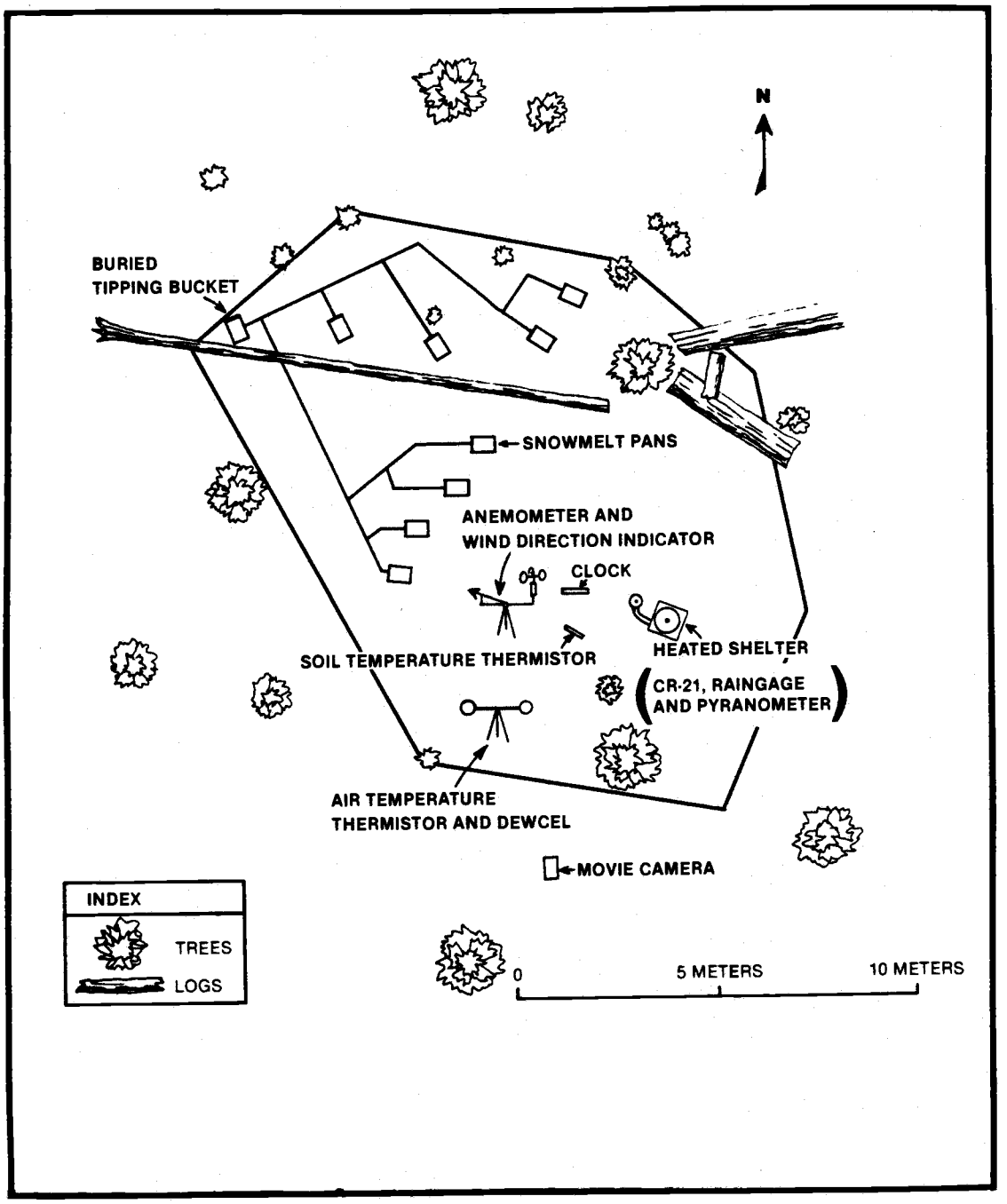

Figure 3. Instrumental Layout of the Forest Plot. (Trees shown represent the location of the boles.)

variable canopy covers to collect the variable precipitation falling in the forest. Each pan, a flat "vee", fiberglassed masonite trough with a projected surface area of 0.25 m^2, was installed flush with the ground surface to prevent atypical accumulation of snow. Polyvinylchloride (PVC) pipe routed rain and snowmelt water from the pans to buried tipping buckets for measurement. The pipe was buried to prevent clogging by ice. Calibration of the buried tipping buckets, like the heated raingages, occurred during the prior summers by adjusting the tipping bucket thresholds to fixed volumes. Collectively, the eight pans and the tipping bucket of each plot constituted a snowmelt lysimeter.

Time lapse photography was used to delineate periods of rainfall, snow accumulation, and snowmelt for periods when nobody was at the site. A super-8 mm movie camera equipped with halogen automobile headlights photographed a staff gage and clock at approximately 15 minute intervals. The time lapse movie record also supplemented the raingage and tipping bucket data by providing a visual basis for evaluating the progress of snowmelt during rainfall.

Information from the tipping bucket raingages, the snowmelt lysimeters, and time lapse photography was used to distinguish rainfall, snowfall, and snowmelt. During rainfall when no snowpack was present, data from the raingages and the snowmelt lysimeters were similar. When snow was accumulating, the raingages measured greater water volumes than the snowmelt lysimeters. When snow melted during rainfall, the snowmelt lysimeters measured greater water depths than the amount of precipitation measured by the raingages once the water

holding capacity of the snowpack was satisfied. Measured snowmelt rates were determined over extended time periods by comparing the snowmelt lysimeter data with the raingage data. (The term, "measured snowmelt," used later in the text refers to this definition.)

Microclimatic data was obtained from a variety of sensors in each plot. Incoming shortwave radiation was measured by a LI-COR Model LI-200S silicon pyranometer. This sensor was calibrated during cloudy conditions by comparing its output with that of a Kipp solarimeter. Outgoing shortwave radiation was assumed to be 85 percent of the incoming shortwave radiation throughout the study. This was confirmed by comparing data from upfacing and downfacing Kipp solarimeters during a number of cloudy periods when snow was on the ground.

Air temperature was measured at each plot by Campbell Scientific Model 101 thermistors installed 1.5 m above ground. The thermistors were mounted within radiation shields designed to minimize radiative heat transfer to the thermistor while allowing air movement within. Soil temperature was measured by the same type of thermistor at a depth of 2 cm.

Dewpoint temperatures were measured by lithium chloride dewcel-type hygrometers as described by Holbo (1981). These sensors were mounted in radiation shields installed 1.5 m above the ground. The dewcels were calibrated prior to field use each winter by comparing their outputs to that of a mirror hygrometer (E.G. and G. Model 880) under different known humidity levels. A regression relation was then determined. Dewpoint temperatures were used to

calculate the vapor pressure of the air according to:

$$e_a = 610.78\exp[(17.269T_d)/(237.3+T_d)] \quad (18)$$

where e_a is the vapor pressure of the air (Pa) and T_d is the dewpoint temperature of the air (°C).

Windspeed was measured by Weathertronics Model 2031 3-cup anemometers mounted 1.8 m above the ground. The anemometers were calibrated in a wind tunnel. Wind direction was measured by Weathertronics Model 2020 low-threshold wind vanes mounted 1.8 m above the ground surface.

Each plot contained a Campbell Scientific CR-21 micrologger and cassette recorder in the heated shelter. The climatic and snowmelt data obtained by the sensors in each plot was processed by the CR-21. The CR-21 scanned outputs from eight sensors every 10 seconds. Mean values were computed for solar radiation, air and dewpoint temperatures, wind speed and direction, and soil temperature. Precipitation and outflow from snowmelt lysimeters were totalized at specified time intervals. The processed data were then entered onto a cassette tape for storage.

The study plots were visited at least every three weeks for routine maintenance. During these visits, batteries, cassette tapes, movie film, and dessicant boxes were changed, and the microprocessors, sensors, and snowmelt lysimeters were checked.

When snow was present and rainfall was expected, the plots were visited to measure snowpack variables, check the instruments, and

observe snowmelt during rainfall. Additional measurements of snowpack characteristics were made to supplement the data processed by the CR-21.

The water equivalent of a snowpack refers to the depth of water resulting from melting a snowpack with no water loss. Snowpack water equivalent consists of both ice and liquid water. Because we are looking at the same mass in different states:

$$\rho_w d_w = \rho_s d_s \tag{19}$$

and

$$d_w = (\rho_s/\rho_w) d_s \tag{20}$$

where ρ_w is the density of water (kg/m^3), ρ_s is the density of snow, (kg/m^3), d_w is the depth of water (m), and d_s is the depth of snow (m). The depth and density of the snowpack are necessary for this measurement. Snow depth of each site was measured by a ruler and the snowpack density was measured by weighing a known volume of snow. Snowpack water equivalent measurements were made before rain-on-snow periods to determine the accumulation of snow. If a snowpack existed after a melt period, a measurement of snowpack water equivalent was also made after that period. In this way, snowmelt was determined by comparing the snowpack water equivalents before and after a rain-on-snow period.

The free water content of the snowpack refers to the percentage of the snowpack water equivalent that exists as liquid water. Because the snowpacks of the transient snow zone are commonly at 0°C,

a portion of the snowpack may exist as liquid water. This water can exist as gravitational water moving downward through the snowpack and capillary water held in the snow matrix by surface tension (Jones, 1983; Jones, Rango, and Howell, 1983). The free water content of the snowpack was determined by a calorimetric method similar to that described by Yoshida (1960). This relatively inexpensive and simple procedure used the concept of heat balance in a closed system: the heat lost by the warmer component is equal to the heat gained by the cooler component in the system. In this case, a known weight of snow at 0°C was mixed with hot water of a known weight and temperature in the calorimeter. When the system reached an equilibrium temperature, the heat required to melt the snow and raise the melt water to equilibrium temperature equalled the heat lost by the hot water and the calorimeter. The mass of ice, I (kg), contained in the wet snow was then determined by:

$$I = [4.2(T_1 - T_2)(W_1 + w) - T_2W_2]/333.6 \quad (21)$$

where T_1 is the initial temperature of hot water (°C), T_2 is the final equilibrium water temperature (°C), W_1 is the initial mass of hot water (kg), W_2 is the mass of the snow (kg), w is the water equivalent of the calorimeter (kg), and the latent heat of fusion is 333.6 kJ/kg. The free water content of the wet snow is then:

$$FWC = 100[(1 - (I/W_2)] \quad (22)$$

where FWC is the free water content of the wet snow (percent by

weight). Because the initial free water content before snowmelt periods cannot be considered as meltwater, it must be subtracted from the water equivalent of each snowpack when computing snowmelt from snow survey information or lysimeter information.

During measurements of snowpack density and free water content, the snowpack temperature was also measured. If the snowpack temperature was below 0°C, then the cold content (depth of water required to raise the snowpack temperature to 0°C) of the snowpack had to be accounted for in the snowmelt analyses.

All snowpack variables were measured at 2-5 locations at each site to account for spatial variations. This was especially important at the forest plot due to differential snow accumulation under different canopy covers.

During the winter field season, intensive measurements of microclimatic variables were made to check the validity of the assumptions made in the determination of the energy transfer processes that melt snow. Albedo was measured with upfacing and downfacing Kipp solarimeters, snow temperature was measured with a Campbell Scientific Model 101 thermistor, and the temperatures of the cloud base, forest canopy, and tree boles were measured with a Telatemp AG-42 infrared thermometer.

DETERMINATION OF SNOWPACK ENERGY BUDGETS

Determination of the energy budget of a snowpack melting during rainfall was dependent on computing the individual components of the energy budget. The energy components were computed by applying the necessary microclimatic variables to equations (4), (10), (14), (15), and (17). Because the computed energy budget components had different units, they were standardized to melt water depths by applying the latent heat of fusion and the appropriate unit conversions. Thus, net shortwave radiation (K*) was converted to shortwave radiation melt (K_M*), net longwave radiation (L*) was converted to longwave radiation melt (L_M*), and heat transfer by rain water (F) was converted to snowmelt resulting from rainfall (F_M). Sensible and latent heats were previously converted to melt water depths in equations (14) and (15). The energy processes acting to melt snow during rain could then be viewed as the depth of snow the processes melted. Total snowmelt, as a process of energy transfer, was predicted by the sum of its energy melt components. The measured melt water depth for each plot could then be compared to the depth predicted by the energy balance of the snowpack. Additionally, snowmelt predicted by snow survey information was compared to the measured and predicted melts.

RESULTS

Between the start of data collection in mid November of 1982 and April, 1984, 33 snow accumulation-melt sequences occurred. During the winter of 1982-1983, only in 7 of the 19 sequences did a significant amount of snow accumulate (depth of at least 50 mm) in the clearcut plot, and only during those sequences did any snow accumulate in the forest plot. During the winter of 1983-1984, significant snow accumulation occurred in 9 of the 14 snow accumulation-melt sequences.

OBSERVATIONS AND MEASUREMENTS OF FOREST CANOPY INFLUENCES

Interception of snow by the forest canopy greatly influenced snowpack characteristics in the forest plot. During snowfall, the forest canopy intercepted a large percentage of the snow. As the snow loaded the canopy, it was observed that the branches of the western hemlocks and the limber, terminal portions of the Douglas-fir branches bent into steeply sloping positions producing locally unstable situations. The steeply sloping branches subsequently released large masses of snow to the lower branches or the ground. The release of snow masses from the canopy was triggered by the loss of frictional bonds at the steep branch angles, the impact of snow falling on the branch from a higher branch, or partial melt of the intercepted snow wetting and loosening the frictional bonds between the snow and a branch. Once the snow was released, the branches

returned to their normal positions and snow continued to load them. While this process was occurring, snow also fell from the trees in small clumps and flakes. According to Miller (1964), the interception storage capacity depends on snow adhesion to the branches or needles, snow cohesion, branch and needle geometry and surface characteristics, flexibility of the branches, and meteorologic conditions. As a result of canopy interception, the snow accumulation on the forest floor was greatly reduced during snowfalls.

After a snowfall, the resulting snow masses on the forest canopy were highly exposed to the atmosphere. Partial melt occurred when the energy budget of these snow masses became positive. Miller (1967) suggested that the high exposure of intercepted snow combined with its high surface-to-volume ratio assured relatively large energy transfers which act to melt the intercepted snow during these periods. Observations of canopy melt revealed that drip fell from the trees accompanied by the release of masses of snow in a variety of sizes. Canopy drip and masses of snow would often originate from the upper canopy layers and drop down to the lower canopy layers in a cascading fashion. The intercepted snow of the lower canopy became wetter and was often shaken off the branches by the impact of the falling snow.

More canopy melt than surface melt was commonly observed because of the higher exposure of the intercepted snow to energy inputs. The resulting accumulation of snow on the forest floor was significantly less than the snow accumulation in the clearcut plot. Table 3 shows

Table 3. Snowpack Characteristics of the Clearcut and Forest Plots during the Winters of 1982-1983 and 1983-1984.

Date	Clearcut				Forest			
	Depth (mm)	Water Equivalent (mm)	Density (%)	Free Water Content (%)	Depth (mm)	Water Equivalent (mm)	Density (%)	Free Water Content (%)
11/30/82	100	--	--	--	50	--	--	--
12/19/82	220	35.0	15.9	8.1	54	21.0	39.1	15.8
12/22/82	168	32.3	19.2	9.5	patchy	--	--	--
2/10/83	125	40.5	32.4	16.8	patchy	--	--	--
11/27/83	135	31.2	23.1	13.6	patchy	--	--	--
12/02/83	184	36.7	19.9	6.6	48	15.5	32.0	11.5
12/07/83	500	116.0	23.2	--	123	41.7	33.8	--
12/09/83	215	74.8	34.8	13.4	68	22.6	33.1	27.1
12/12/83	200	63.2	31.6	--	43	15.6	36.5	14.9
12/13/83	160	59.6	37.3	18.0	32	12.0	36.8	--
12/27/83	141	39.1	27.7	0.0	94	30.0	32.0	0.0
12/31/83	30	12.8	42.7	12.0	no snow	--	--	--
2/11/84	242	36.1	14.9	5.5	42	16.5	39.3	23.4
2/12/84	67	18.0	27.3	24.1	patchy	--	--	--
2/19/84	64	21.3	33.6	11.0	no snow	--	--	--
2/23/84	93	12.7	13.7	13.7	20	10.7	54.1	26.7
2/27/84	253	67.4	26.6	11.1	90	30.3	33.7	12.5
3/18/84	56	18.1	32.2	21.7	6	2.8	--	--
4/11/84	192	--	--	--	73	--	--	--

snowpack depth and other characteristics for dates that snow surveys were taken. During the two year study, the water equivalents of forest snowpacks were an average of 29 mm, but up to 74 mm less than snowpacks of the clearcut plot. This was most pronounced during series of snowfalls with intervening periods of above-freezing temperatures. Snow intercepted by the canopy would melt or fall off the canopy during the periods between snowfalls. At the same time, the snowpack in the clearcut melted slowly apparently because of its lower exposure to energy inputs. After canopy melt, the canopy was again available to intercept more snow during a subsequent snowstorm. The period between November 24 and December 7, 1983 is a vivid example of the preceding sequence. A series of five snowfalls occurred during this period with canopy melt occurring between each storm. The evolution of the snowpacks in the forest and clearcut during this period can be seen in Table 3. The accumulation of snow in the forest was 377 mm less than the clearcut during this period while the water equivalent of the forest snowpack was 74 mm less.

The studies of Niederhof and Dunford (1942), Kittredge (1953), Anderson (1956), Rothacher (1965), Gary (1974), Leaf (1975), Swanson and Hillman (1977), Haupt (1979a and b), Gary and Troendle (1982), Megahan (1983), and others similarly found that more snow accumulated in open areas than in forests. A review of these studies revealed that the water equivalent of snowpacks in open areas was 46 to 170 mm greater than forest snowpacks. The contrast between clearcut and forest snowpack accumulations was greater in the literature than in this study. The reason for this difference is because this study was

located in the transient snow zone while the studies referred to were located in permanent snow zones primarily out of the Pacific Northwest. Because permanent snowpacks accumulate snow throughout the winter, differences in snowpack accumulation become additive through the winter until melt commences. However, in the transient snow zone, the differences in snowpack accumulation are cancelled as the snowpacks dissappear during the common melt periods.

The forest canopy not only played a strong role in reducing the accumulation and water equivalent of the forest snowpack, but it also influenced the density and wetness of the accumulated snow. Snow survey measurements showed that snowpacks beneath the forest canopy were usually denser and had higher free water contents than snowpacks in the clearcut. The impact of snow masses falling from the canopy certainly increased the density of both the falling masses and the snow already on the ground. Canopy drip and saturated snow masses dropped to the forest floor saturating the snowpack in the forest before the snowpack in the clearcut was saturated. Additional water input would flush through the snow into the soil. Measurements of density and free water content of forest and clearcut snowpacks showed the higher density and free water content of the forest snowpacks (Table 3). Density measurements showed that the density of forest snowpacks averaged 12.4 percent greater (-1.7-40.4 percent) than clearcut snowpacks. Kittredge (1953) found that the densities of forest snowpacks were 1-7 percent greater than snowpacks in open areas. The greater differences between forest and clearcut snowpack densities in this study can probably be accounted for by the shallow

and often patchy snowpack studied. These snowpacks are more sensitive to canopy drip and the impacts of falling masses of snow than the deeper forest snowpacks of the permanent snow zone which Kittredge studied. Measurements in both plots showed that the free water contents of the forest snowpacks were greater than the clearcut snowpacks by an average of 9.8 percent (1.4-17.9 percent). Although no studies were available for comparison of free water contents, Smith (1974) acknowledged that snowpacks beneath forest canopies were often saturated as a consequence of canopy drip.

During rain-on-snow periods, the forest canopy modified the microclimate of the forest floor. Recorded data and observations made during snow surveys showed that the forest consistently had lower air and dewpoint temperatures, lower windspeeds, and less shortwave radiation than the clearcut. The canopy sheltered the snowpack on the forest floor from large energy inputs which contributed to snowmelt. As a result, energy inputs to the snowpacks were consistently lower in the forest than the clearcut. However, water outflow resulting from snowmelt and rainfall were not always less in the forest than the clearcut despite the lower water equivalents and energy inputs. If snow was on the forest canopy, it would melt quickly during rainfall and drip water to the snowpack below. Additionally, large clumps of saturated snow falling from the canopy released water to the surface snowpack upon impact. Because of the added water inputs from canopy melt during rainfall, water output from forest snowpacks was consistently greater than that from clearcut snowpacks during these periods. Additionally, drip zones

were observed under the canopy where canopy melt and rain were concentrated.

The influences of each plot on the accumulation and melt of snow during different climatic conditions are presented in Table 4. Although discrete temperatures, free water contents, and densities are shown, it should be recognized that they are only used as levels of reference.

ENERGY BALANCE OF MELTING SNOWPACKS DURING RAINFALL

Significant snowmelt during rainfall occurred in seven instances since data collection began; two of the events occurred during the winter of 1982-1983 and five occurred during the winter of 1983-1984. However, the two rain-on-snow events which occurred during the winter of 1982-1983 were not examined because of instrument failures. Each of the five rain-on-snow events in the winter of 1983-1984 constituted discrete periods for analysis.

ERROR OF SITE MEASUREMENTS

Since many of the instruments which measured microclimatic variables in each plot were subject to instrument errors, an analytical method was necessary to evaluate the errors of the derived energy budget terms. A technique presented by Scarborough (1966) was used because of its effectiveness in previous studies (Holbo, 1973 and Vanderwaal, 1983) and its simplicity. An explanation of the

Table 4. Influences of Clearcut and Forest Plots on Snow Accumulation and Snowmelt During Given Climatic Conditions.

Climatic Condition	Clearcut	Forest
Snowing Air temperature < -1.0°C	Accumulation of dry, powdery snow. Snow drifting common when windy. No melt.	Dry, powdery snow intercepted by forest canopy and blown off by gusty winds. Dry, powdery snow on forest floor. Less snow accumulation than clearcut. No melt.
Snowing Air temperature = -1.0 to 1.0°C	Accumulation of moderately wet to wet, cohesive snow. Snowmelt common at warmer temperatures.	At cold extreme: Cohesive snow accumulates on forest canopy. Snow falls from canopy as large clumps. Light canopy drip. Snowpack accumulation less than clearcut. Light snowmelt common. At warm extremes: Snow intercepted by canopy commonly melts and drips off canopy. Largest accumulation of snow under open spaces of the canopy. Snowmelt common.

Table 4. Continued

Climatic Condition	Clearcut	Forest
Cloudy and dry Snow in canopy Air temperature = 1 to 5°C	Snowmelt water saturates snowpack. Free water content = 12 to 25% Density = 25 to 35% Subsequent release of melt water from snowpack.	Heavy canopy drip and large clumps of snow dropping from the canopy to the underlying snowpack quickly saturate it and increase its density. As a result, lysimeter outflow is greater in the forest. Free water content = 20 to 30% Density = 30 to 50% Snowmelt common.
Rain when snow in canopy. Air temperature 0.5°C	Rain stored in snowpack until saturation. Free water content = 12 to 25% Density = 25 to 35% Snowmelt occurring. Release of melt water from snowpack once saturated.	Rain on intercepted snow causing: canopy drip snow to fall as large, saturated clumps. Rain on wet and saturated snowpack. Free water content = 20 to 30% Density = 30 to 50% Lysimeter outflow greater in forest (rain + canopy melt + snowmelt)

Table 4. Continued

Climatic Condition	Clearcut	Forest
Light rain (<3 mm/hr) No snow in canopy. Air temperature > 0.5°C	Rain stored in snowpack until saturation. Once the snowpack is saturated, lysimeter outflow is light to moderate (0.0 to 4.0 mm/hr).	Rain and canopy drip fall on saturated snowpack with less water equivalent than clearcut. Lysimeter outflow is light to heavy (0.0 to 6.0 mm/hr) depending on: Concentration of rainfall into drip zones by the canopy. Patchiness of the snowpack.
Heavy rain (>5 mm/hr) No snow in canopy. Air temperature > 0.5°C	Rain quickly saturates snowpack. High lysimeter outflow when warm and windy (0.0 to 4.0 mm/hr) Greater lysimeter outflow than forest snowpack.	Heavy canopy drip. Lower lysimeter outflow than clearcut due to: Lower energy inputs Lower snowpack water equivalent

method is presented and the errors in the energy balance components are calculated in Appendix A. The relative probable errors for each of the derived energy balance components are presented in Table 5.

The results from the error analysis (Table 5 and Appendix A) show that the relative probable errors were often large. However, it must be noted that it was common to have instrument errors approaching or exceeding the actual measurements taken during rain-on-snow periods. This can be explained by the fact that the microclimatic variables measured often had very low magnitudes. Even if the instrument errors were low, they could easily approach or exceed the microclimatic variables. For example, during periods when the dewpoint temperature was actually 0°C, latent heat melt (M_E) and snowmelt resulting from rain (F_M) were both actually 0.0 mm/hr. However because of instrument errors, the dewpoint temperature may have been measured as 0.3°C. The resulting calculated latent heat melt and rain melt were infinitely larger than the actual melts of 0.0 mm/hr. Thus, it is not surprising that the largest relative probable errors of L_M*, M_H, M_E, and F_M were associated with periods of low melt. No other reviewed study that assessed snowpack energy balances included any type of formal error analysis.

Table 5. Relative Probable Errors and Probable Errors of Snowmelt as a Result of the Energy Balance Terms. (K_M* is snowmelt resulting from shortwave radiation (mm/hr), L_M* is snowmelt resulting from longwave radiation (mm/hr), M_H is sensible heat melt (mm/hr), M_E is latent heat melt (mm/hr), and F_M is snowmelt resulting from rainfall (mm/hr).)

Source	Relative Probable Errors (%)	Probable Errors (mm/hr)
K_M*	28	0.001-0.139
L_M*	15-73	0.045-0.077
M_H	8-25	0.006-0.021
M_E	28-∞	0.036-0.161
F_M	23-∞	0.007-0.097

ANALYSIS OF INDIVIDUAL RAIN-ON-SNOW EVENTS

Event 1: December 9-10, 1983

A series of five snowfalls between November 24 and December 7, 1983 followed by a period of light melt preceded the rain-on-snow event of December 9-10, 1983. The observation period began when rain began to fall at 1400 on December 9 and ended at 2400 on December 10. All calculations and comparisons were made for that 34-hour period. Each component of the energy balance was computed on an hourly basis and then time-integrated for each snowpack's energy balance during the event.

The snow depth at 1700 on December 9 averaged 215 mm in the clearcut and 68 mm in the forest. Density of the clearcut snowpack averaged 34.8 percent resulting in a water equivalent of 74.8 mm. The forest snowpack's density averaged 33.1 percent which yields a water equivalent of 22.6 mm. The clearcut snowpack was also "drier" than the forest snowpack; free water content in the clearcut averaged about 13.4 percent compared to 27.1 percent in the forest. During the 34-hour melt period, 33.3 mm of rain fell in the clearcut. Precipitation in the forest could not be measured during the entire period because the heated tipping bucket raingage was not functioning properly. As a result, the precipitation was estimated at 31.2 mm by applying an interception factor of 0.94 to the clearcut precipitation (see Appendix A). Precipitation intensity was highest during the afternoon and evening of December 9 and the early morning hours of

December 10, but it was also variable during that period, ranging from 0.3 to 4.8 mm/hr (Figure 4). Precipitation intensity in the forest plot was not plotted because it was synthesized rather than measured.

Lysimeter outflow, consisting of snowmelt water, rain, and water stored in the snowpack, showed a pattern similar to that of precipitation intensity in both plots (Figure 4). This was not surprising because rainfall made up 74 percent of the clearcut's lysimeter outflow and 63 percent of the forest's lysimeter outflow. Lysimeter outflow was slightly greater in the clearcut at the beginning of the event, but between 2100 and 2300, when lysimeter outflow for both plots was greatest, lysimeter outflow in the forest was greater than the clearcut by about 1.5 mm/hr. Lysimeter outflow in the clearcut totaled 45.0 mm, of which 33.3 mm was rain and 1.5 mm was free water in the snowpack. In the forest, lysimeter outflow totaled 49.5 mm, of which 31.2 mm was rain (synthesized) and 5.0 mm was free water in the snowpack.

Once rain began, the air temperature of the clearcut plot cooled rapidly to about 4.0°C, remained fairly constant between 2.5 and 4.0°C, and then cooled again to near 0°C (Figure 5). The air temperature of the forest plot followed the same trend as the clearcut, but it was generally lower than the clearcut by about 0.5-1.5°C. Dewpoint temperatures were generally constant with a downturn at 1600 on December 10. They ranged between -0.9 and 2.8°C in the clearcut and -1.2 and 1.6°C in the forest. Net shortwave radiation was much higher in the clearcut with a maximum of

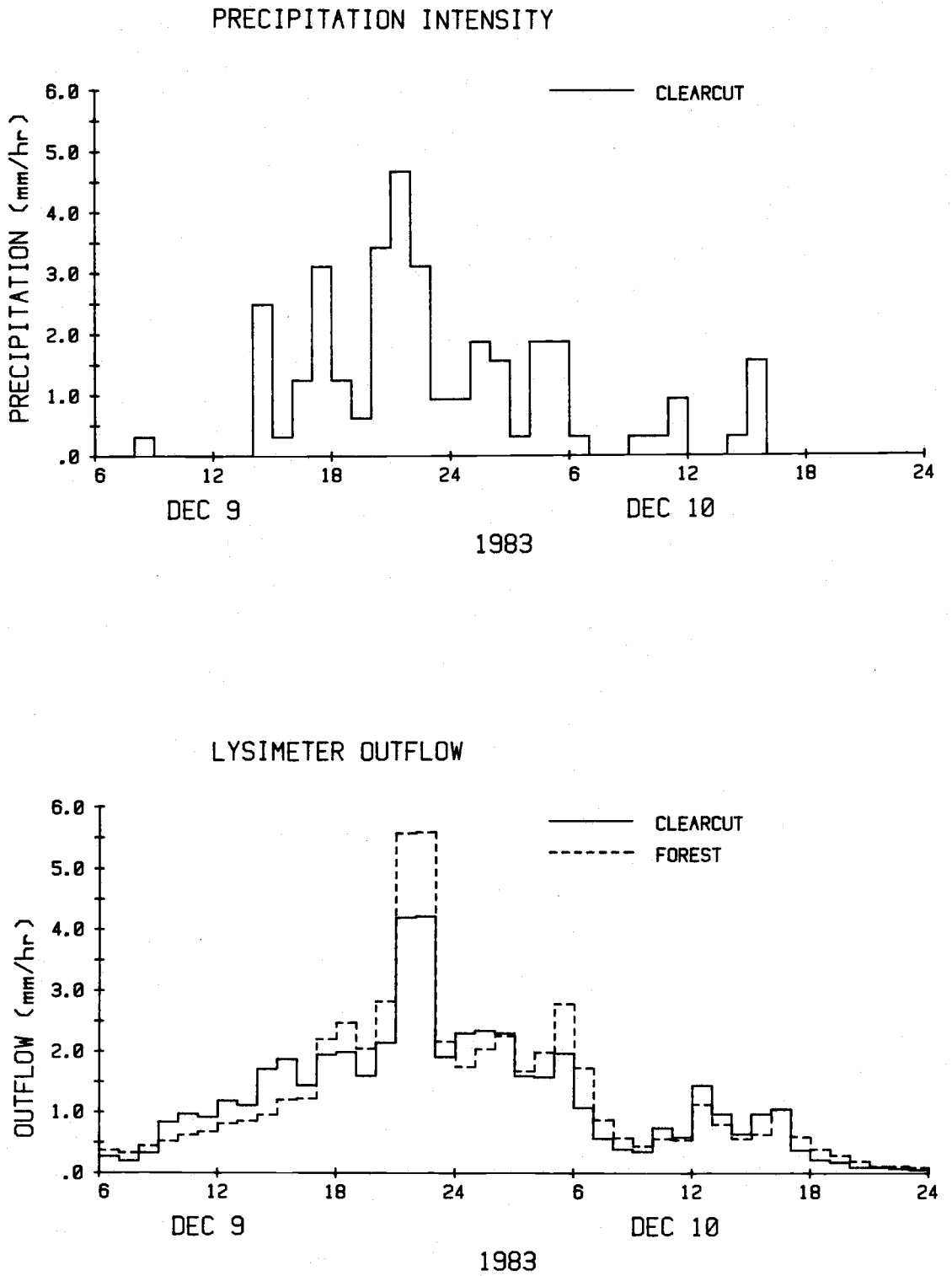

Figure 4. Precipitation Intensity and Lysimeter Outflow, Event 1: December 9-10, 1983.

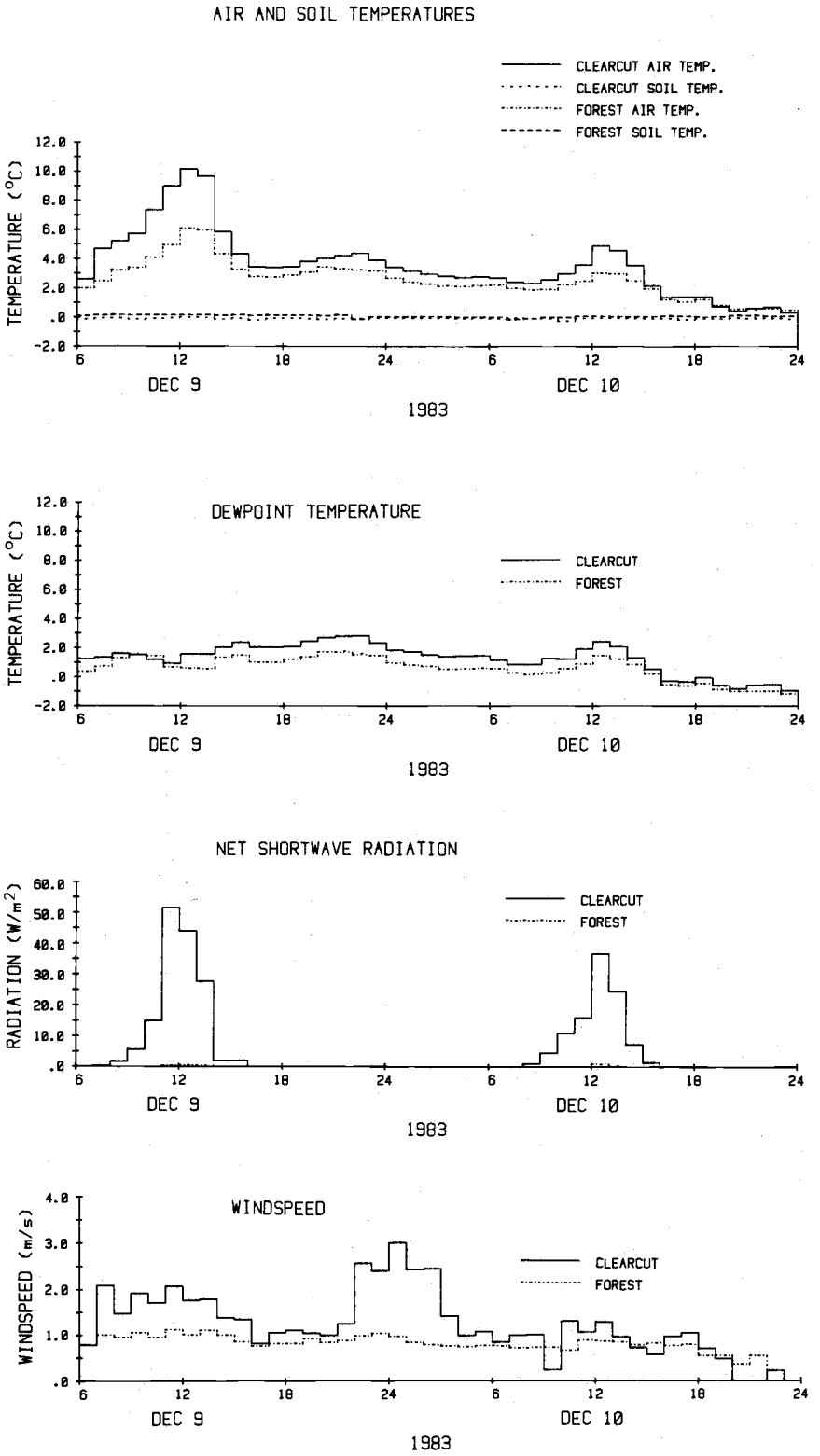

Figure 5. Measured Microclimatic Variables, Event 1: December 9-10, 1983.

36.7 W/m^2 compared to 0.9 W/m^2 in the forest. Mean hourly windspeeds in the clearcut were moderate for most of the entire 34-hour period, ranging from 0.0 to 3.0 m/s. Gusts were as high as 7.5 m/s. The forest plot had lower mean hourly windspeeds ranging from 0.0 to 1.0 m/s with gusts up to 2.2 m/s.

The trends of the energy balance components (in units of energy melt) are shown in Figures 6 and 7. (It should be noted that rainfall in the forest was synthesized instead of measured. Although snowmelt resulting from rainfall was computed for the forest plot, its trend was not graphed.) It is evident that the energy melts were consistently lower in the forest. This is not surprising because the microclimatic data indicated that net shortwave radiation, air temperature, dewpoint temperature, and windspeeds were all lower in the forest. The graphs of sensible and latent heat melts are examples of the preceding point. Windspeeds in the clearcut increased to more than 2.0 m/s between 2200 and 0300 on December 9. Although these windspeeds could hardly be considered "high winds," sensible heat melt rose to 0.10-0.16 mm/hr and latent heat melt rose to 0.13-0.26 mm/hr. Windspeeds did not significantly increase in the forest and, as a consequence, the turbulent heat melts (sensible and latent heat melts) did not increase.

Table 6 shows each snowpack's energy balance for the melt event. For this event and hereafter, "predicted melt" refers to snowmelt estimated by the energy balance model and "measured melt" refers to snowmelt estimated by subtracting rainfall and snowpack free water from lysimeter outflow. It is evident that longwave radiation was

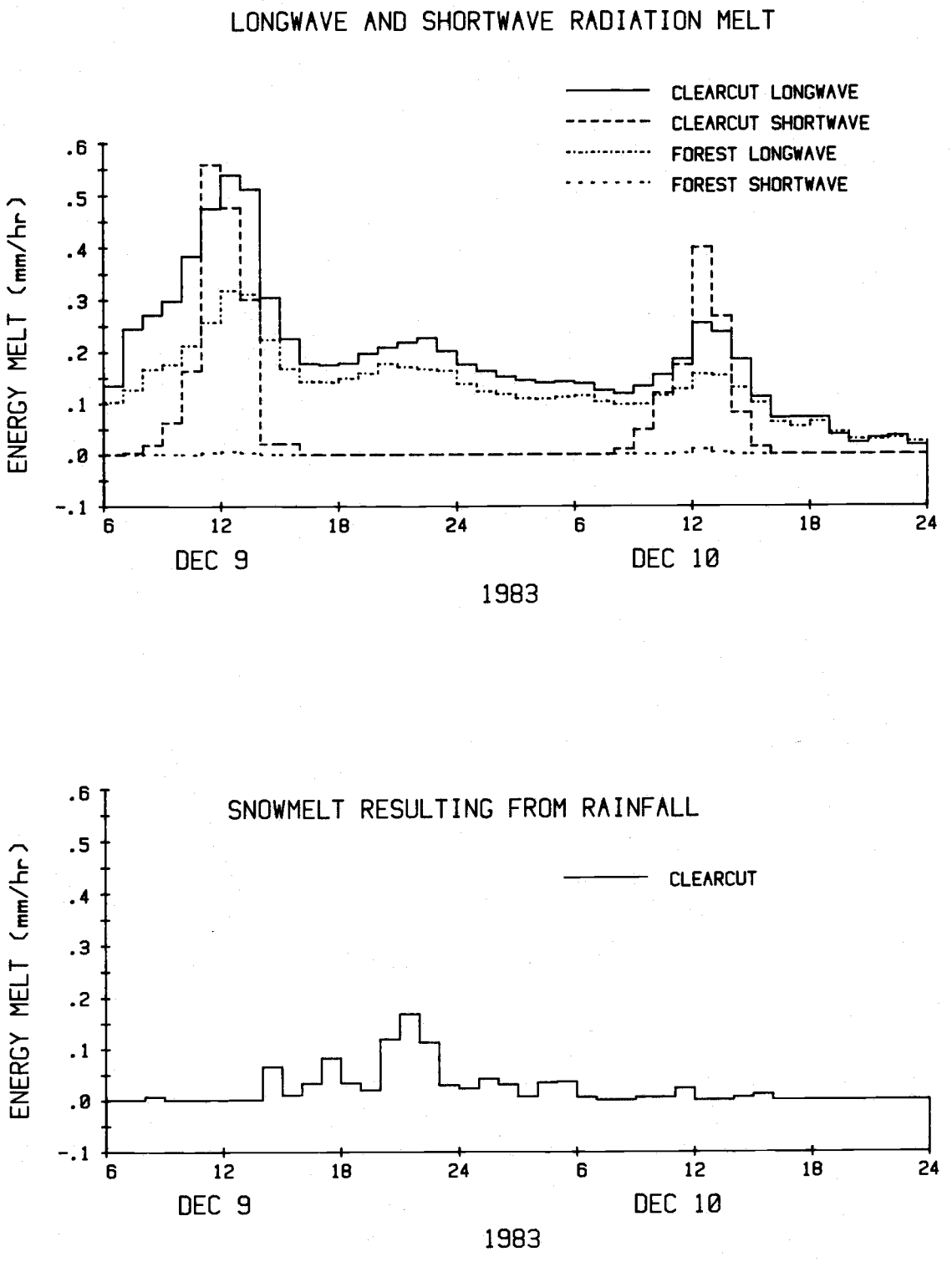

Figure 6. Time Trends of Longwave Radiation Melt, Shortwave Radiation Melt, and Snowmelt Resulting from Rainfall, Event 1: December 9-10, 1983.

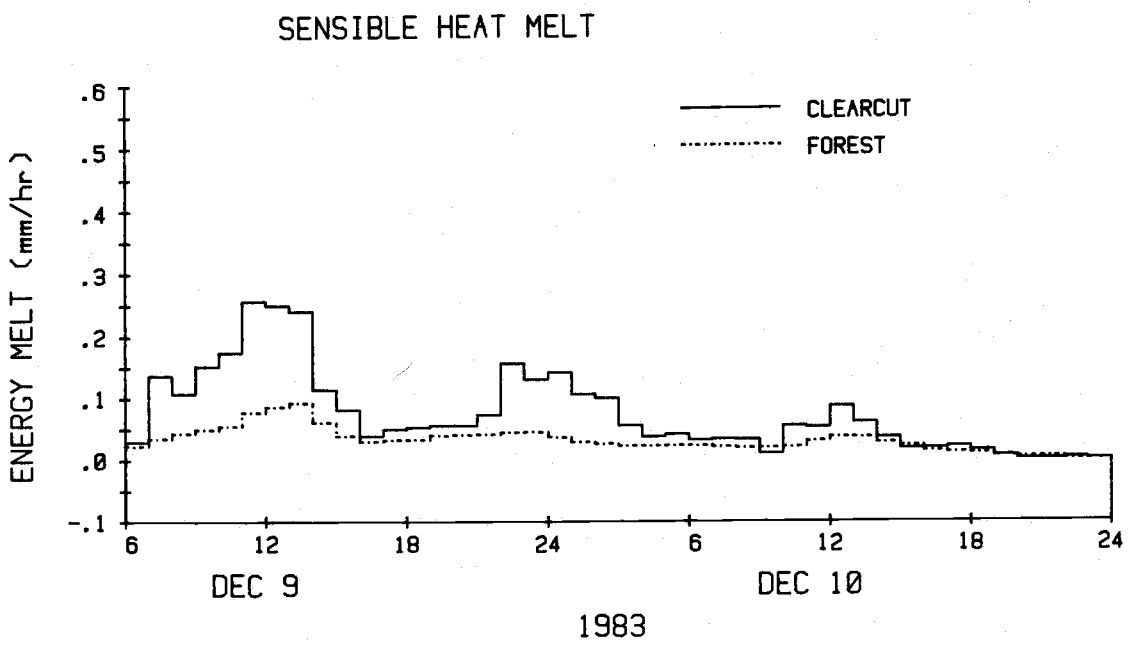

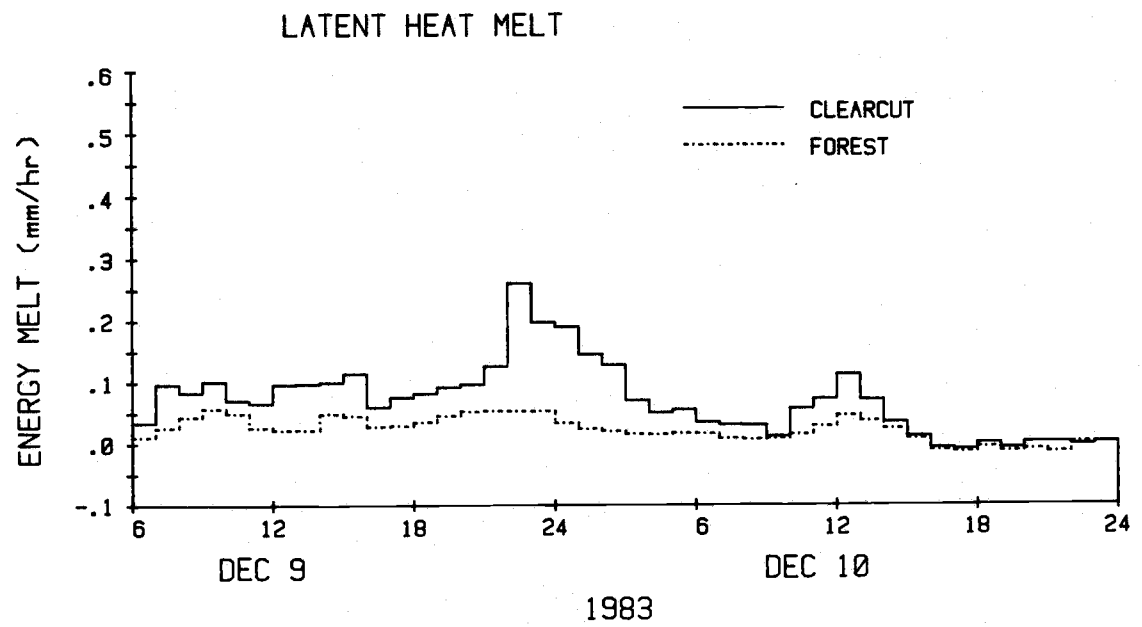

Figure 7. Time Trends of Sensible and Latent Heat Melts, Event 1: December 9-10, 1983.

Table 6. Comparison of Melt Predicted by the Energy Balance Model and Measured Melt for Clearcut and Forest Plots During Event 1. December 9, 1983 at 1400 to December 10, 1983 at 2400.

Source	Clearcut			Forest		
	Predicted (mm)	Predicted (%)	Measured (mm)	Predicted (mm)	Predicted (%)	Measured (mm)
Shortwave Radiation	1.1	10.1		0.0	0.0	
Longwave Radiation	5.0	45.8		3.9	66.1	
Sensible Heat	1.7	15.6		0.8	13.5	
Latent Heat	2.2	20.2		0.7	11.9	
Rain	0.9	8.3		0.5	8.5	
Total	10.9	100.0	10.1	5.9	100.0	13.4

Table 7. Snowpack Characteristics and Melt Determined by Snow Survey Information for Event 1.

Snowpack Characteristics	Clearcut 12/9/83 at 1400*	Clearcut 12/10/83 at 2400**	Forest 12/9/83 at 1400***	Forest 12/10/83 at 2400****
Water Equivalent (mm)	76.0	61.7	24.3	16.1
Density (%)	34.8	--	33.1	--
Free Water Content (%)	13.4	13.4	27.1	27.1
Ice (mm)	65.8	53.4	17.7	11.7
Melt (mm)	12.4		6.0	

* Snow survey taken December 9, 1983 at 1700. The water equivalent was adjusted to December 9 at 1400 by adding the intervening melt, assuming density and free water content were constant.

** Snow survey taken December 12, 1983 at 1700. The water equivalent was adjusted to December 10 at 2400 by adding the intervening melt. Free water content was assumed to be constant throughout the event.

*** Snow survey taken December 9, 1983 at 1500. The water equivalent was adjusted to December 9, 1983 at 1400 by adding the intervening melt

**** Snow survey taken December 12, 1983 at 1530. The water equivalent was adjusted to December 10, 1983 at 2400 by adding the intervening melt. Free water content was assumed to be constant throughout the event.

the dominant source of melt for both snowpacks, contributing 45.8 percent of the total predicted melt in the clearcut and 66.1 percent in the forest. Windspeeds were not high enough to overcome the dominance of longwave melt and, as a result, turbulent heat exchange (combined sensible and latent heats) was the second ranking source of melt. Combined sensible and latent heat melts, hereafter called turbulent heat melt, accounted for 35.8 percent of the total predicted melt in the clearcut and only 25.4 percent in the forest. The reduction of windspeeds by the forest coupled with lower air and dewpoint temperatures in the forest significantly reduced the role of the turbulent melt components in the forest. Because precipitation intensity was generally light to moderate, snowmelt induced by rainfall was of secondary importance. Shortwave radiation was predictably low because the dense clouds and forest canopy reduced the incoming shortwave radiation.

Snowmelt predicted by the energy balance model agreed with the measured melt in the clearcut plot, but significantly underestimated melt in the forest plot. Predicted melt of 10.9 mm in the clearcut compared well with the measured melt of 10.1 mm. Forest snowmelt was predicted to be 5.9 mm, but the measured melt was 13.4 mm. Thus, although predicted melt was significantly greater in the clearcut plot, measured melt was greater in the forest plot.

Snow surveys conducted at the initial stages of the event and after the event were also used to estimate melt during the event (Table 7). The latter snow survey was conducted approximately 40 hours after the event was over. As a result, the water

equivalents measured from the latter survey were adjusted to December 10 at 2400 by adding the melt which occurred during the 40-hour period between the end of the study period and the snow survey. Because an ice crust formed during the late night and early morning periods of December 10 and 11, the free water content measurements of the latter survey were assumed to be unreliable estimates of the actual free water content at the end of the study period. Because no additional free water content information was available, it was assumed that the free water content (expressed as a percentage of the water equivalent) at the beginning of the event would roughly approximate the free water content at the end of the event for both snowpacks. The snow survey estimates of snowmelt for both plots agreed well with snowmelt predicted by the energy balance model. Although the snow survey estimate of snowmelt in the clearcut agreed well with the measured melt, the melt estimate for the forest plot underestimated the measured melt. The energy balance model and the snow survey data both indicated that snowmelt was 5-6 mm greater in the clearcut than the forest. However, measured melt in the forest was about 3 mm greater than the clearcut.

Because the snow survey melt estimate in the forest agreed well with the energy balance model's prediction of snowmelt, there is evidence that the measured snowmelt may be in error. Not only was precipitation synthesized from the clearcut precipitation data, but drip zones under the canopy were observed on subsequent dates. Thus, it is posssible that the amount of precipitation synthesized for the forest plot underestimated the actual rain falling on the snowmelt

pans. This explanation would also account for the higher lysimeter outflows in the forest during some periods of the event. Unfortunately, this possible explanation is impossible to verify with the data collected during this event.

Event 2: December 12-14, 1983

The rain-on-snow event of December 12-14, 1983 was separated from event 1 by only 30 hours. The time between events was characterized by cloudy weather with short, drizzly periods and short freezes during the early morning hours of December 11 and 12. A 66-hour period starting at 0600 on the morning of December 12 and ending at 2400 on December 14 was designated for analysis.

Initial snowpack characteristics for both plots were measured by snow surveys conducted between 1530 and 1700 on December 12. Snowpack depth averaged 200 mm in the clearcut and 43 mm in the forest. Density averaged to 31.6 percent in the clearcut and 36.5 percent in the forest yielding snowpack water equivalents of 63.2 mm in the clearcut and 15.6 mm in the forest. Small patches of bare ground were apparent in the forest plot by the end of the analysis. The free water content averaged 14.9 percent in the forest. The free water content in the clearcut was not measured on December 12, but the December 13 snow survey indicated an average free water content of 18.0 percent.

Although rainfall lasted for almost the entire 66-hour period, its intensity was variable, ranging from 0.0 to 4.7 mm/hr

(Figure 8). Rainfall totaled 89.5 mm in the clearcut. However, as in event 1, rainfall had to be estimated at 83.9 mm in the forest because the heated tipping bucket raingage was not operating properly. Air temperatures and dewpoint temperatures were generally slightly warmer than in event 1 for both plots until temperatures rose significantly during the day of December 14 (Figure 9) Air temperatures ranged between -0.1 and 6.7°C in the clearcut and 0.0 and 6.0°C in the forest. Dewpoint temperatures followed the same trends as air temperatures, but were generally 1.0-1.5°C cooler. Net shortwave radiation was virtually zero at all times except for a few hours in the middle of each day in the clearcut plot. Both plots had light to moderate gusty winds with mean hourly windspeeds up to 1.6 m/s in the clearcut and 1.0 m/s in the forest. Wind gusts in the clearcut reached 5.0 m/s, but in the forest, they reached only 2.0 m/s.

Lysimeter outflow in both plots varied from 0.0 mm/hr at the beginning of the study period to 5.4 mm/hr at 1600 on December 14 (Figure 8). As in event 1, lysimeter outflow was greater in the forest during most of the event. In the clearcut, it totaled 129.3 mm, of which 89.5 mm was rainfall and 7.1 mm was free water in the snowpack. In the forest, lysimeter outflow totaled 139.0 mm, of which 83.9 mm was estimated rainfall and 8.2 mm was free water.

The energy balances of the clearcut and forest snowpacks are shown in Table 8. Longwave radiation was computed to be the dominant source of melt, contributing 11.3 mm (51.8 percent) to the total melt of the clearcut snowpack and 9.2 mm (66.2 percent) to the total melt

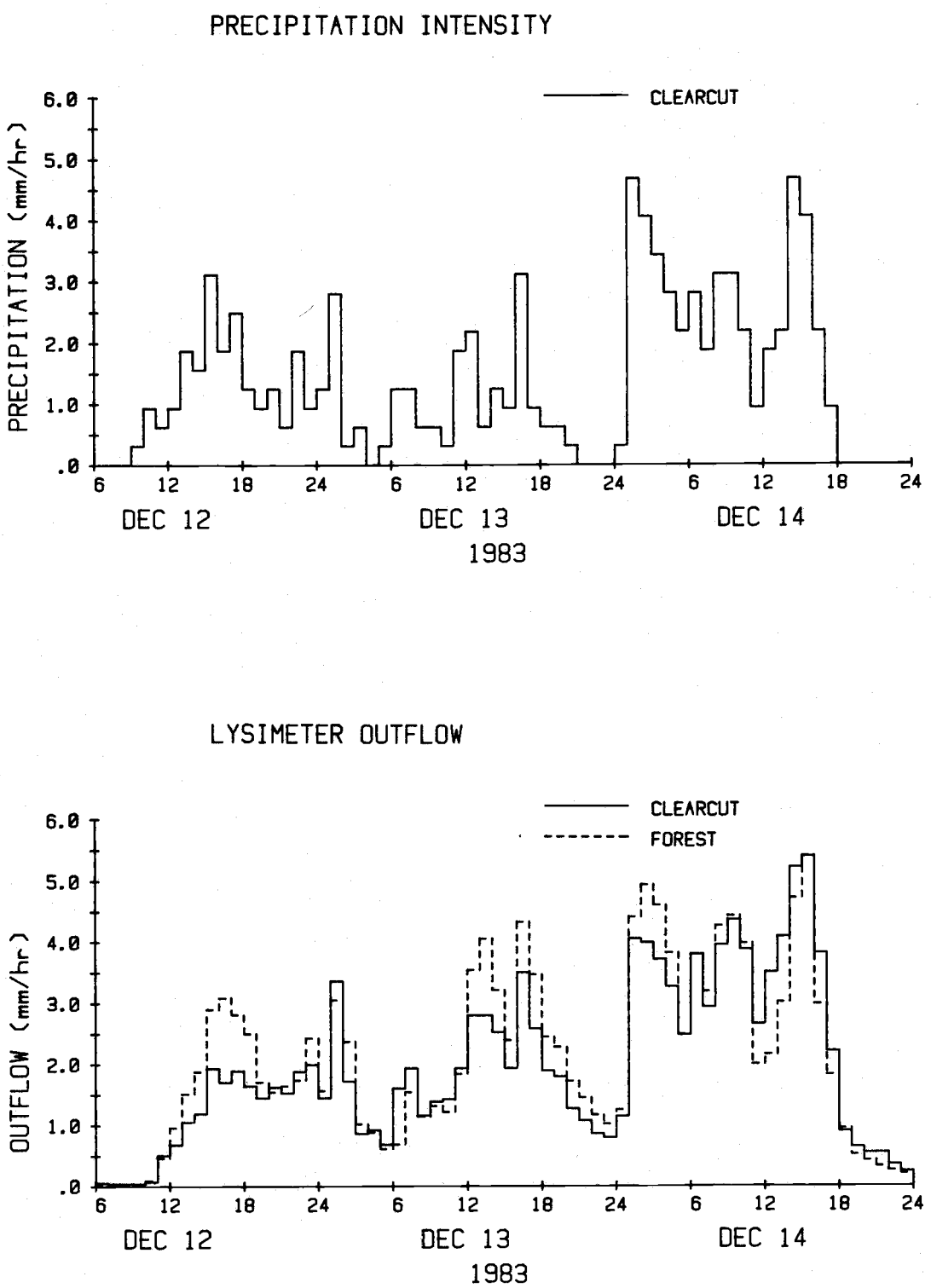

Figure 8. Precipitation Intensity and Lysimeter Outflow, Event 2: December 12-14, 1983.

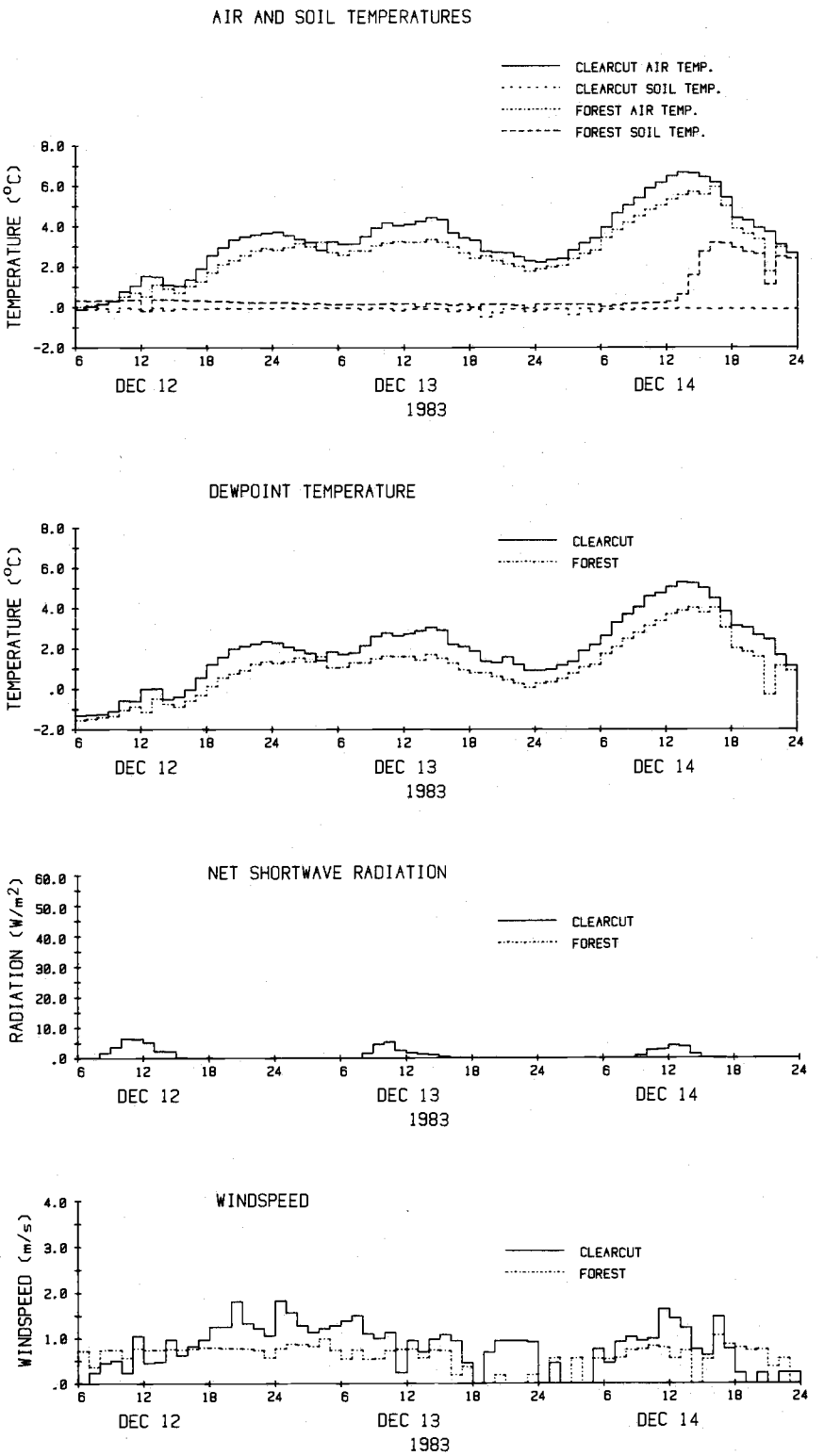

Figure 9. Measured Microclimatic Variables, Event 2: December 12-14, 1983.

Table 8. Comparison of Melt Predicted by the Energy Balance Model and Measured Melt for Clearcut and Forest Plots During Event 2. December 12, 1983 at 0600 to December 14, 1983 at 2400.

Source	Clearcut			Forest		
	Predicted (mm)	Predicted (%)	Measured (mm)	Predicted (mm)	Predicted (%)	Measured (mm)
Shortwave Radiation	0.7	3.2		0.0	0.0	
Longwave Radiation	11.3	51.8		9.2	66.2	
Sensible Heat	2.7	12.4		1.5	10.8	
Latent Heat	4.3	19.7		1.6	11.5	
Rain	2.8	12.9		1.6	11.5	
Total	21.8	100.0	32.3	13.9	100.0	46.9

Table 9. Snowpack Characteristics and Melt Determined by Snow Survey Information for Event 2.

Snowpack Characteristics	Clearcut 12/12/83 at 0600*	Clearcut 12/14/83 at 2400***	Forest 12/12/83 at 0600****
Water Equivalent (mm)	59.2	21.9	14.8
Density (%)	31.6	31.6	36.5
Free Water Content (%)	18.0**	18.0	14.9
Ice (mm)	48.5	18.0	12.6
Melt (mm)	30.5		12.6

* Snow survey taken December 12, 1983 at 1700. The water equivalent was adjusted to December 12 at 0600 by adding the intervening melt, assuming constant density and free water content.
** Free water content of clearcut snowpack was determined on December 13, 1983 at 0930.
*** Snow survey taken December 22, 1983 at 1100. The water equivalent was adjusted to December 14, 1983 at 2400 by adding the intervening melt and subtracting the water added to the snowpack during that period. Density and free water content were assumed to be constant throughout the event.
**** Snow survey taken December 12, 1983 at 1530. The water equivalent was adjusted to December 12, 1983 at 0600 by adding the intervening melt, assuming constant density and free water content.

of the forest snowpack. The combined turbulent transfers of sensible and latent heats (turbulent heat) were also important sources of snowmelt, contributing 7.0 mm (32.1 percent) to the total snowmelt of the clearcut plot and 3.1 mm (22.3 percent) to the total snowmelt of the forest plot. The lower windspeeds, air temperatures, and dewpoint temperatures of the forest were the primary causes of the lower turbulent heat melt in the forest. The 3.9 mm reduction of turbulent heat melt in the forest is a large contributor to the reduced predicted melt in the forest. Latent heat melt was the major source of turbulent heat melt in the clearcut (61 percent of the total turbulent heat melt), but in the forest, latent and sensible heats were nearly equal sources of turbulent heat melt. Snowmelt attributed to rainfall accounted for 2.8 mm (12.9 percent) of the total predicted snowmelt in the clearcut and 1.6 mm (11.5 percent) in the forest. Shortwave radiation was a minor source of snowmelt, especially in the forest. The computed energy balance indicated that all of the energy transfer processes contributing to snowmelt were lower in the forest.

Trends of snowmelt separated into its components are shown in Figures 10 and 11. Not surprisingly, the lower air and dewpoint temperatures, shortwave radiation, and windspeeds in the forest resulted in lower energy melts in the forest. The significant rise in air and dewpoint temperatures along with high rainfall intensities during the morning of December 14 caused a significant increase in snowmelt and lysimeter outflow. Predicted snowmelt increased markedly during this period. Longwave radiation melt and snowmelt

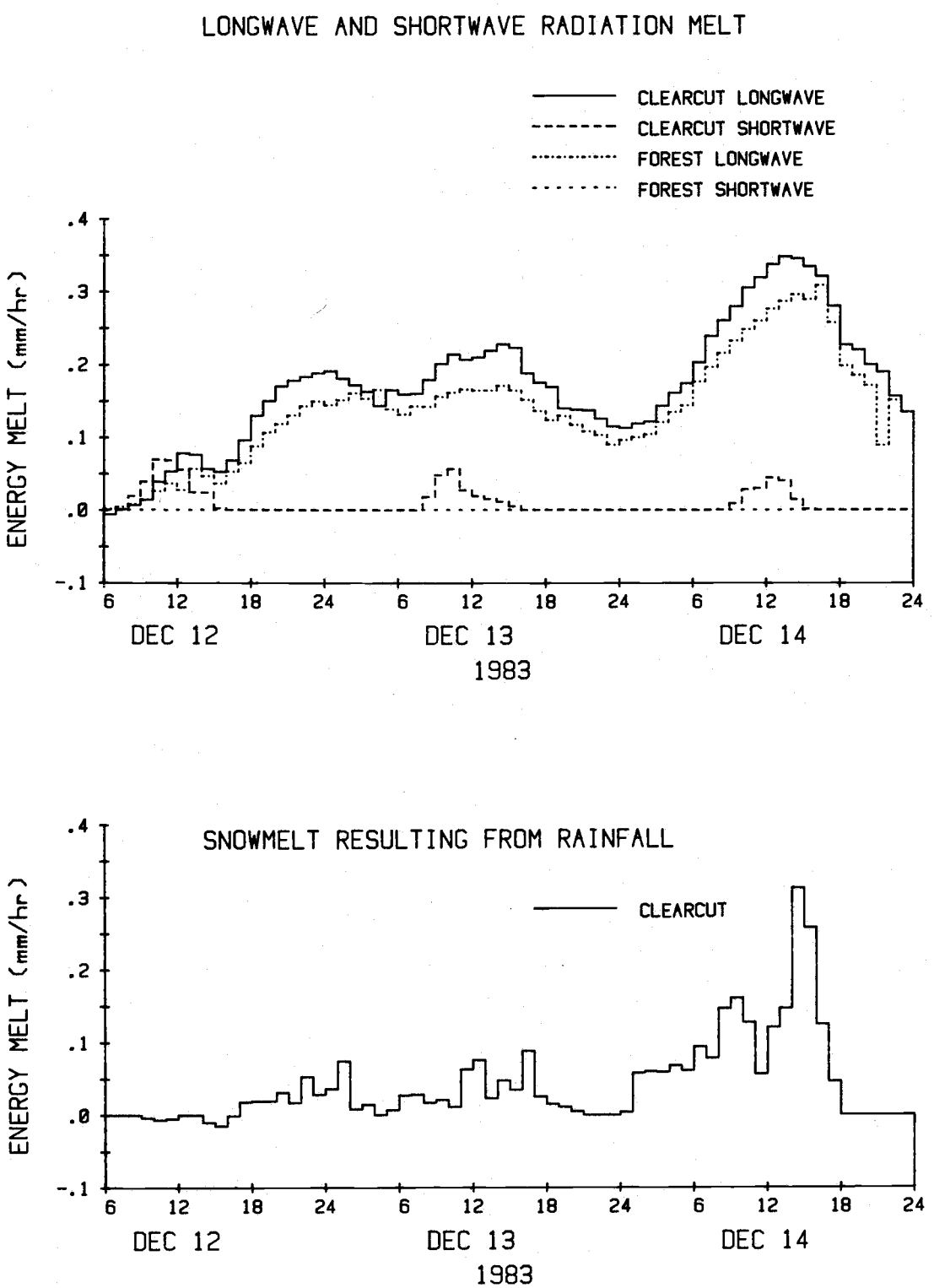

Figure 10. Time Trends of Longwave Radiation Melt, Shortwave Radiation Melt, and Snowmelt Resulting from Rainfall, Event 2: December 12-14, 1983.

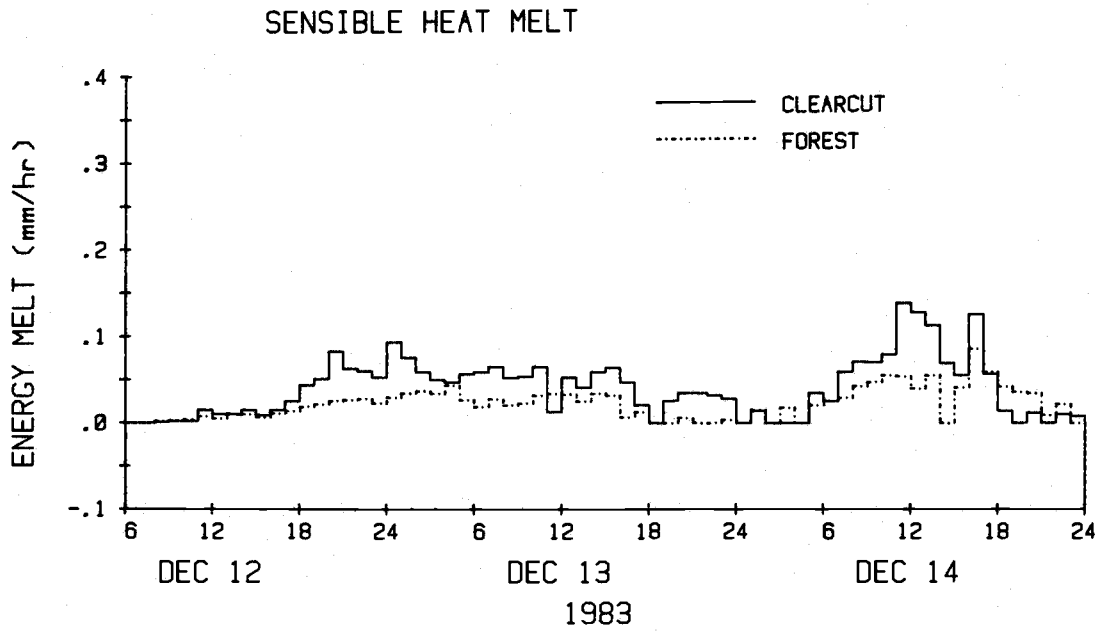

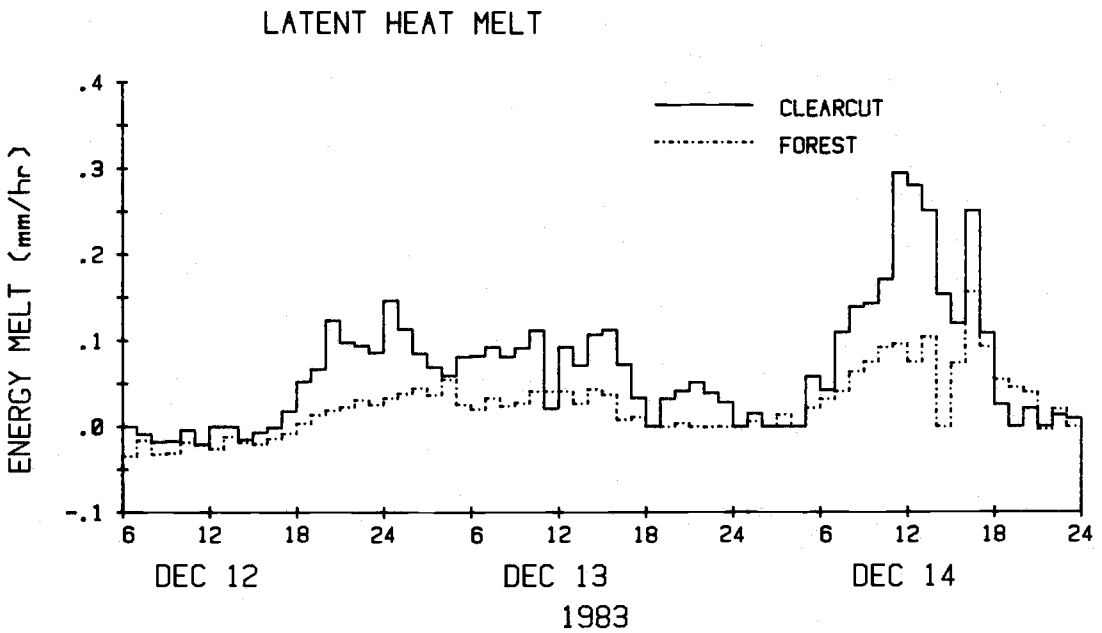

Figure 11. Time Trends of Sensible and Latent Heat Melts, Event 2: December 12-14, 1983.

resulting from rain were dominant during this period because of the heavy rainfall with high temperature and low winds.

Although predicted snowmelt was greater in the clearcut than the forest, measured melt was significantly greater in the forest (Table 8). In the clearcut plot, predicted melt was within 67 percent of the measured melt. These results agree reasonably well considering the magnitudes of the possible errors. However, as in event 1, predicted melt for the forest snowpack significantly underestimated measured melt.

There is ample evidence that the measured melt of 46.9 mm in the forest plot is in error. The snow survey of December 12 indicated that the water equivalent of the forest snowpack was only 15.6 mm. Thus, there was 31.3 mm of unaccountable snowmelt. As in event 1, there is the possibility that precipitation was underestimated in the forest plot because it had to be indexed from the clearcut plot. Additionally, the concentration of precipitation into drip zones beneath the forest canopy may be a possible explanation. If drip was concentrated over a snowmelt pan, lysimeter ouflow would be increased, and increased lysimeter outflow coupled with underestimated precipitation would lead to an increased computed measured melt.

In the clearcut, snowmelt could be only crudely estimated by snow survey information because a snow survey was not conducted until December 22 (Table 9). The clearcut snowpack's water equivalent on December 22 was adjusted back to December 14 by adding the intervening snowmelt and subtracting the intervening added water to

the water equivalent of the December 22 snowpack. The estimate of melt by snow survey was 30.5 mm which agreed reasonably well with the measured snowmelt, but overestimated the predicted snowmelt. Snowmelt in the forest could be predicted by the initial December 12 snow survey because time lapse movies indicated that there were only patches of snow left in the forest plot at the end of the study period. Although there were still some patches of snow in the forest plot, many of the snowmelt pans were empty. Thus, the amount of ice in the December 12 snowpack, 12.6 mm, served as a reasonable snowmelt estimate. This snowmelt estimate agrees well with the predicted snowmelt, but is far less than the measured snowmelt.

Event 3: December 28-31, 1983

A period of extremely cold weather preceded the rain-on-snow event of December 28-31, 1983. Air temperatures remained below freezing for most of the period between December 19 and December 28 and reached -16.5°C on December 23. Snow fell four times in this period. Because the fresh snow was uncommonly dry and powdery with a density of about 10 percent, the snowpacks of both plots were unusual. In the clearcut plot, snow was layered with a dense ice crust immediately on top of the ground surface and an intermediate crust covered with 50 mm of fresh, powdery snow. High, gusty winds up to 15.7 m/s occurred between December 21 and December 25. As a result, the depth of the clearcut snowpack was non-uniform, ranging from 25 mm to 152 mm on December 27. Because of the non-uniformity

of the clearcut snowpack, the snow survey of December 27 was increased to 12 sampling points. Average water equivalent of the clearcut snowpack was 39.1 mm with an average density of 27.7 percent. The snowpack's temperature averaged -0.5°C on December 26 and, consequently, had no free water. The cold content (depth of water required to raise the snowpack's temperature to 0°C) of the clearcut snowpack was 0.1 mm.

The forest snowpack was unusual because it was evenly distributed on the forest floor in contrast to the usually wide range of depths. The water equivalent of the forest snowpack was 30.0 mm with a density of 32.0 percent. The snow was dry, light, and powdery, and snow intercepted by the canopy could not adhere to branches and needles. Gusty winds easily blew the December 20 and 24 snowfalls off the canopy, and the light powder was evenly distributed over the forest floor. Interception losses were negligible since December 19 resulting in similar snowpack water equivalents in both plots. Like the clearcut snowpack, there was no free water because the average snowpack temperature on December 26 was -0.3°C resulting in a cold content of 0.05 mm.

The presence of snow in the forest canopy at the initiation of the rain-on-snow event (resulting from the snowfalls of December 27 and 28) had interesting implications. Precipitation became rain at approximately 0100 on December 29. When the rain fell on the intercepted snow, the snow began to melt and drop to the forest floor as both canopy drip and clumps of wet snow. Between 0100 and 1000 on December 29, lysimeter outflow was much higher in the forest than in

the clearcut (Figure 12). Because the proportions of rain, drip, and snow are unknown for the period between 0100 and 1000, energy balance analyses began at 1000 on December 29 and ended on December 31 at 0300.

The microclimatic data indicate that air and dewpoint temperatures, net shortwave radiation, and windspeeds were all lower in the forest than in the clearcut during this rain-on-snow event (Figure 13). Air temperatures ranged from 0.9 to 6.4°C in the clearcut and 0.6 to 5.0°C in the forest. Dewpoint temperatures ranged from -0.6 to 4.9°C in the clearcut and -1.0 to 3.0°C in the forest. Highest temperatures occurred during the afternoon and evening of December 29. Net shortwave radiation peaked at 22.4 W/m^2 in the clearcut and 0.4 W/m^2 in the forest. Windspeeds were generally light to moderate. Mean hourly windspeed in the clearcut reached 1.6 m/s, but gusts reached 4.9 m/s. Mean hourly windspeeds in the forest reached 0.9 m/s with gusts up to 1.9 m/s.

Although the heated tipping bucket raingage was not operating correctly in the forest, storage gages were placed near the snowmelt pans to measure cumulative precipitation. The storage gages accumulated 70.8 mm of precipitation between December 27 and December 31. This amount was then compared with the precipitation in the clearcut for the same period to estimate hourly precipitation in the forest plot. Because hourly precipitation was not directly measured, it was not graphed in Figure 12. For the study period, rainfall totaled 49.7 mm in the clearcut and 46.2 mm in the forest. The highest hourly rainfall intensity was 5.0 mm/hr at 2400 on December 29.

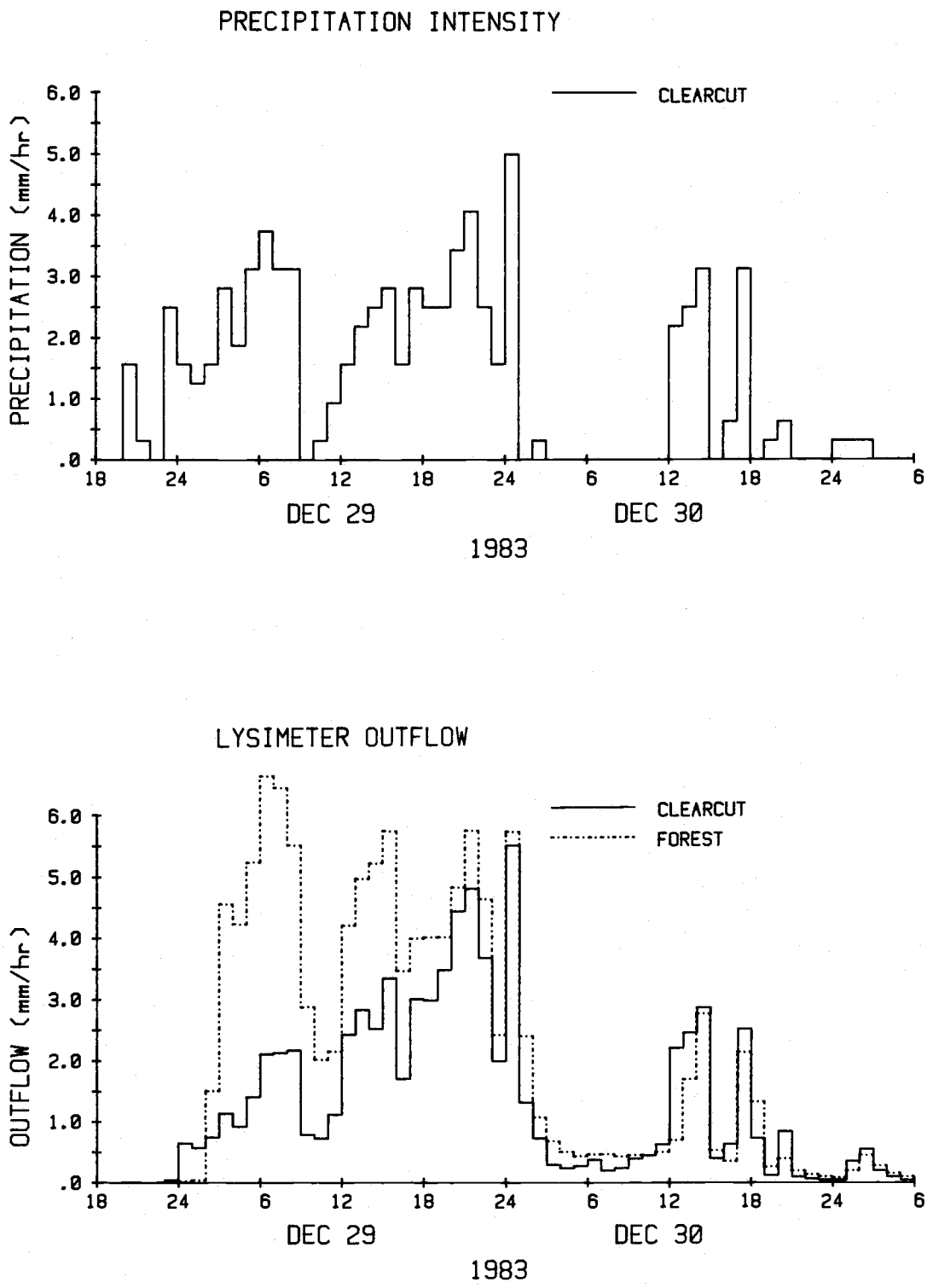

Figure 12. Precipitation Intensity and Lysimeter Outflow, Event 3: December 28-31, 1983.

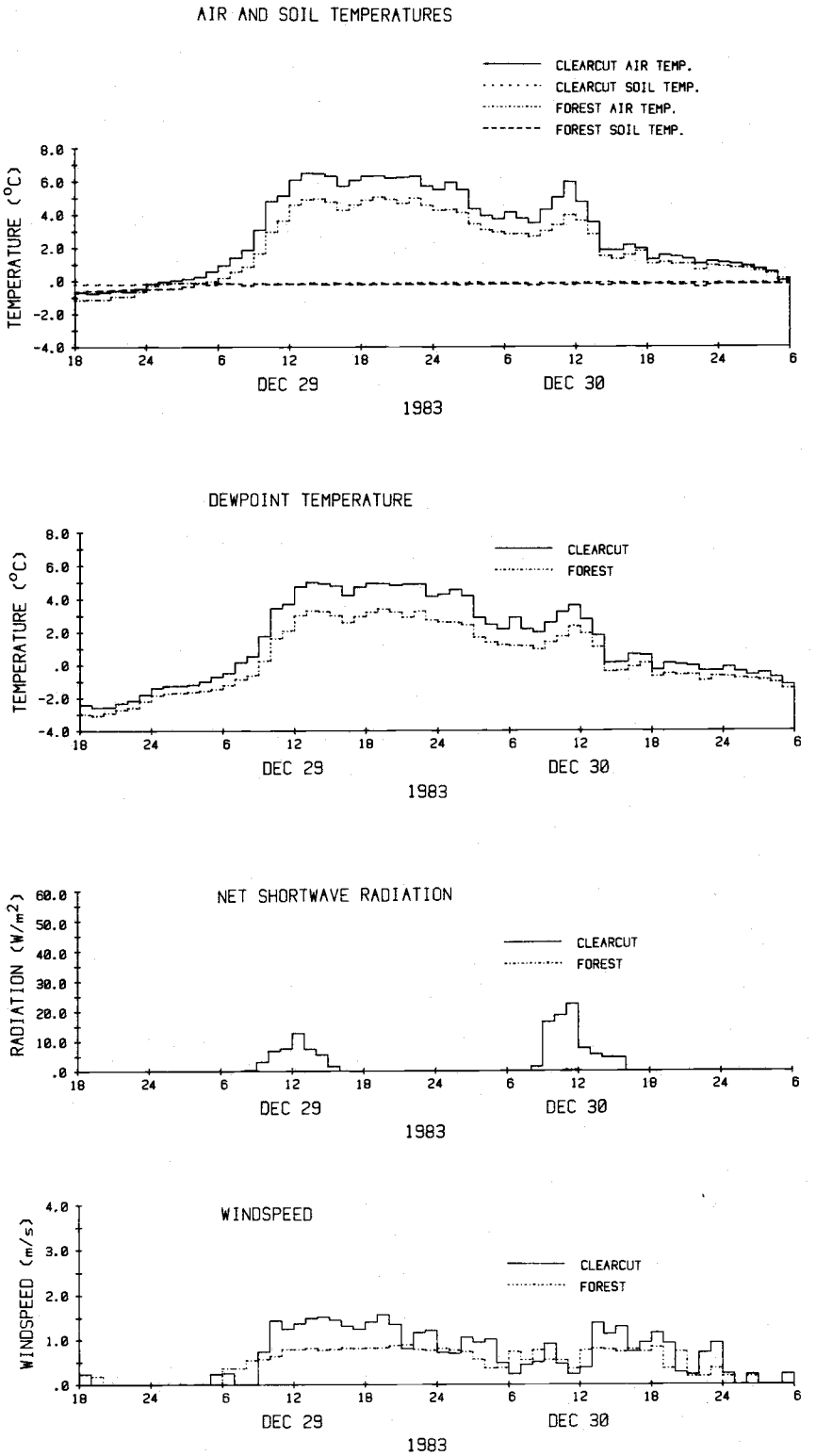

Figure 13. Measured Microclimatic Variables, Event 3: December 28-31, 1983.

Lysimeter outflow was greater in the forest than the clearcut until 1000 on December 30 (Figure 12). At that time, the forest snowpack became patchy and many of the snowmelt pans were empty. As previously mentioned, the first spike of lysimeter outflow (between 0200 and 1000 on December 29) was the result of wet snow and rain dripping from the canopy to the snowpack below. The snow was very wet and the outflow peak was enhanced. In the clearcut, lysimeter outflow totaled 63.4 mm, of which 49.7 mm was rain and 1.6 mm was free water in the snowpack. Forest lysimeter outflow totaled 81.6 mm, of which 46.2 mm was estimated rain and 8.1 mm was free water in the snowpack. (It was assumed that free water content was approximately 23 percent on the basis of past measurements of saturated snow.) However, if the period of canopy drip is considered (December 29 between 0100 and 1000), total lysimeter outflow of the forest plot was 117.0 mm compared to 74.0 mm in the clearcut plot. Greater snowmelt in the canopy compared to melt at the ground surface increased the lysimeter outflow differential between the forest and clearcut plots.

The energy balance of both snowpacks predicted 77 percent greater snowmelt in the clearcut than in the forest (Table 10). Snowmelt predicted in the clearcut was 18.6 mm while forest snowmelt was 10.5 mm. According to the energy balance, longwave radiation was dominant in both plots, accounting for 45.7 percent of the total predicted melt in the clearcut (8.5 mm) and 61.0 percent of the total predicted melt in the forest (6.4 mm). Lower temperatures in the forest caused a slight reduction in longwave radiation melt.

Table 10. Comparison of Melt Predicted by the Energy Balance Model and Measured Melt for Clearcut and Forest Plots During Event 3. December 29, 1983 at 1000 to December 31, 1983 at 0300.

Source	Clearcut			Forest		
	Predicted (mm)	Predicted (%)	Measured (mm)	Predicted (mm)	Predicted (%)	Measured (mm)
Shortwave Radiation	1.3	7.0		0.0	0.0	
Longwave Radiation	8.5	45.7		6.4	61.0	
Sensible Heat	2.3	12.4		1.2	11.4	
Latent Heat	4.2	22.5		1.6	15.2	
Rain	2.3	12.4		1.3	12.4	
Total	18.6	100.0	12.0	10.5	100.0	28.3

Table 11. Snowpack Characteristics and Melt Determined by Snow Survey Information for Event 3.

Forest Snowpack Characteristics	Clearcut 12/27/83 at 1530	Clearcut 12/31/83 at 0300*	Clearcut 12/27/83 at 1400
Water Equivalent (mm)	39.1	13.9	30.0
Density (%)	27.7	42.7	32.0
Free Water Content (%)	0.0	12.0	0.0
Ice (mm)	39.1	12.2	30.0
Melt (mm)		26.9	30.0

* Snow survey taken December 31, 1983 at 1200. Water equivalent was adjusted to December 31 at 0300 by adding the intervening melt, assuming density and free water content were constant.

Turbulent heat melt in the clearcut was over twice the turbulent heat melt in the forest. The reduced forest winds significantly decreased sensible and latent heats in that plot. Although turbulent exchange was not the dominant source of snowmelt, the large difference of turbulent exchange between the plots accounted for a large portion of the predicted snowmelt differential. Snowmelt as a result of rain and shortwave radiation melt were both lower in the forest than the clearcut. Trends of the energy melt components are shown in Figures 14 and 15.

Snowmelt predicted by the energy balance model slightly overestimated measured snowmelt in the clearcut and significantly underestimated measured snowmelt in the forest (Table 10). In the clearcut, the overestimation of 6.6 mm was probably the result of ice layers in the snowpack. Gerdel (1954) showed that melt water does not necessarily percolate vertically to the ground in a layered snowpack. He showed that melt water flowed vertically to an ice layer and then flowed on top of the ice layer until a zone of weakness was reached. At that point, the melt water funneled through the layer. If the ice layers of the clearcut snowpack routed water out of the snowmelt pans, the measured melt would be underestimated. The energy balance model underestimated snowmelt in the forest by 17.8 mm. As in the previous two events discussed, measured snowmelt may have been overestimated because of canopy drip zones. Additionally, the amount of rain collected by the storage gages may be higher or lower than the actual rain because the intercepted snow in the canopy may have fallen into the gages and splashed some water

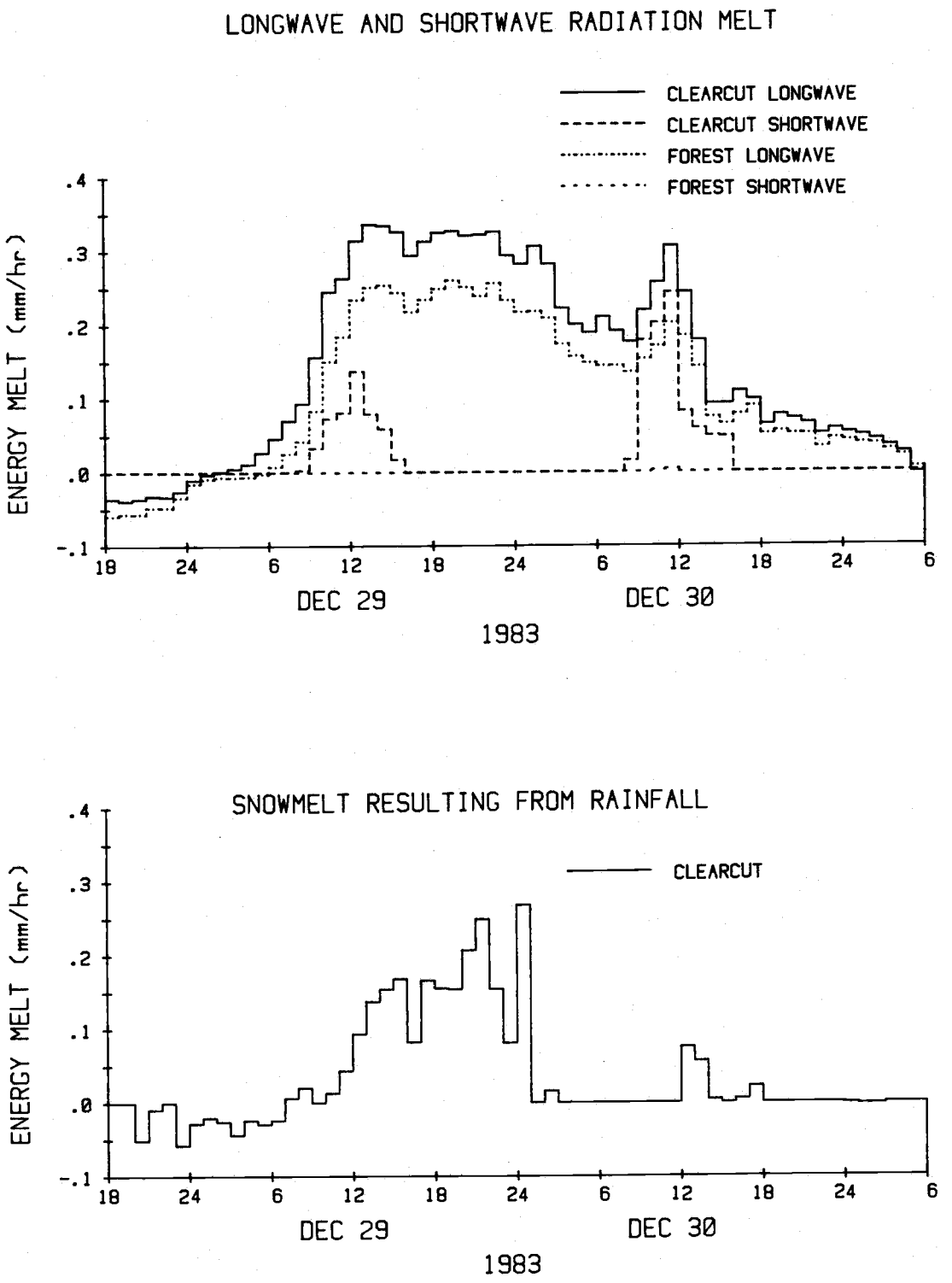

Figure 14. Time Trends of Longwave Radiation Melt, Shortwave Radiation Melt, and Snowmelt Resulting from Rainfall, Event 3: December 28-31, 1983.

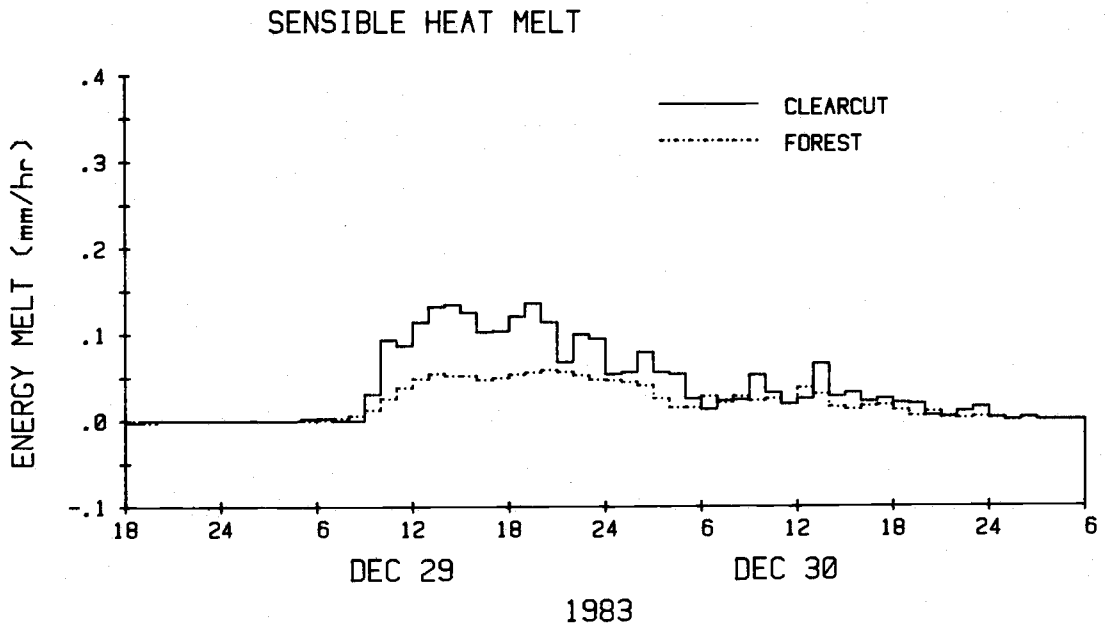

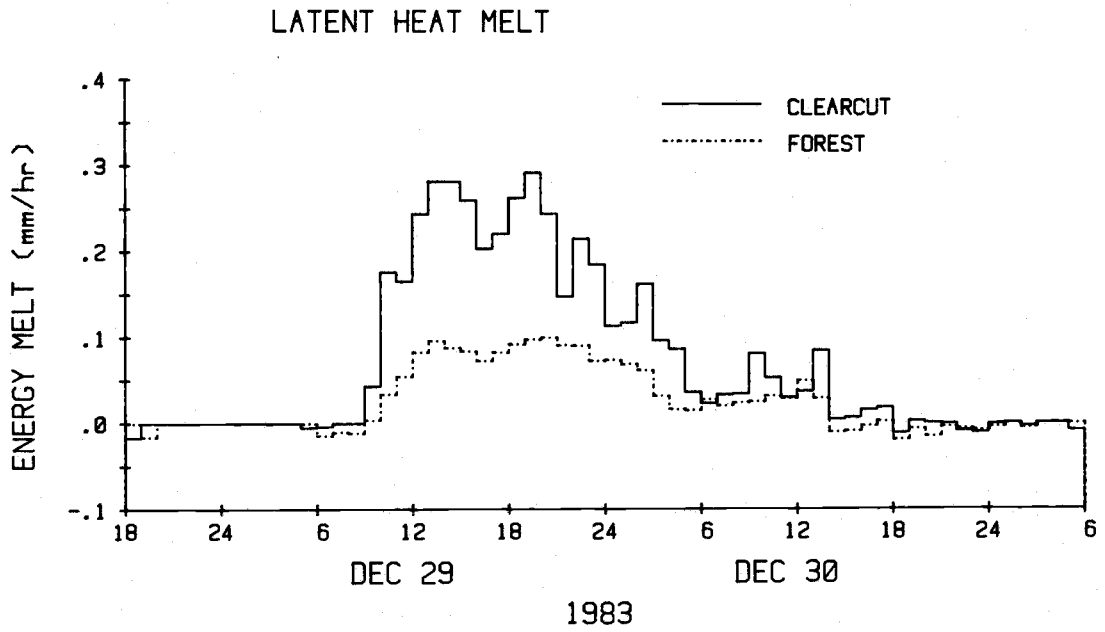

Figure 15. Time Trends of Sensible and Latent Heat Melts, Event 3: December 28-31, 1983.

out. However, the snow survey of December 27 indicated that the forest snowpack's water equivalent was 30.0 mm. This was similar to the measured melt of 27.3 mm. If the snow survey was correct, then the measured snowmelt was estimated correctly.

However, the accuracy of the snow surveys in both plots is questionable because a snow tube was used to determine the depths, water equivalents, and densities of both snowpacks. This was because of the presence of hard ice layers in the clearcut snowpack. The snow tube barely filled when the shallow snowpacks of both plots were sampled. As a result, the spring scale could not accurately weigh the small volume of snow sampled. In addition, the snow tube shattered the ice layers and compressed the snow of the snowpacks. Moreover, melt water and clumps of snow fell from the canopy between the snow survey and the beginning of the study period further decreasing the reliability of the forest snow survey. Because the depths of water and snow dropping from the canopy were not known, the water equivalent of the forest snowpack on December 27, 1983 could not be adjusted to the beginning of the study period. Thus, for this rain-on-snow event, the snow survey information taken two days before the rain-on-snow event, was unreliable to estimate melt because of both poor sampling techniques and water equivalent changes occurring during the period between the snow survey and the study period.

Despite the unreliability of the snow surveys for snowmelt estimation, the information is presented in Table 11 for comparative purposes. The snow surveys estimated melt to be 26.9 mm in the clearcut and 30.0 mm in the forest. Because the forest snowpack was

patchy by the end of the event, the snow survey of December 27 was considered adequate to estimate snowmelt. The 30.0 mm estimate of forest snowmelt agreed well with the measured melt, but was much greater than the predicted melt. In the clearcut snowpack, a snow survey was conducted on December 31 to estimate the water equivalent of the snowpack after the event. The 27.8 mm estimated snowmelt of the clearcut snowpack was greater than both the predicted and measured melts.

Event 4: February 11-13, 1984

Between February 8 and February 11, 1984, 36.1 mm water equivalent of wet snow fell at the clearcut plot followed by two days of rainfall totaling 163.2 mm. Not only was this the largest rainfall event of 1982-1984, but long term rainfall records of Watershed 2 in the H. J. Andrews Experimental Forest (on file at the Forestry Sciences Laboratory) indicate that this was close to the annual event (2.33-year return period). The initial 36.1 mm snowpack water equivalent in the clearcut completely melted by 0300 on February 13. The initial forest snowpack of 16.5 mm (snow was unmeasured in the forest canopy) completely melted by 1900 on February 12. Local stream runoff was high and peaked between 0900 and 1000 on February 13. Watershed 2, a watershed located 10.8 km from the study area in the H. J. Andrews Experimental Forest, had a peak flow of 10.0 liters/s-ha. According to Harr (1981), this peak flow had a return period of about four years. The peak flow of

8.0 liters/s-ha at Watershed 8, located 1.6 km from the study area, had a return period of three years according to records at the Forestry Sciences Laboratory. Snowmelt contributed heavily to the 3-4-year peak flows that resulted from the annual rainfall event.

Snowfall during the early morning hours of February 11 changed to light rain at about 0900. The influence of the forest canopy on precipitation intensity and lysimeter outflow can be seen in Figure 16. During the snowfall period before 0900, most of the snow falling over the forest was trapped by the branches of the forest canopy and could not be measured as precipitation. However, the clearcut raingage could measure the snowfall. Thus, more precipitation was measured in the clearcut. After the snow turned to rain, precipitation measured in the forest consisted of rain, melt from the intercepted snow, and wet clumps of snow dropping from the canopy. Thus, water stored in the canopy during the previous snowfall was measured with the rain and resulted in greater apparent precipitation in the forest plot. Lysimeter outflow was greater in the forest once rain began because of the enhanced precipitation resulting from intercepted snow dropping as meltwater or wet clumps.

Because it was difficult to differentiate rain and snow in the forest during the first portion of the event, the energy balance analysis began at 2300 on February 11 for both plots. At that time, there was no intercepted snow left on the canopy. Time lapse photographs showed that snow did not dissappear from the clearcut plot until 0300 on February 13, but had dissappeared from the forest plot by 1900 on February 12. These times were designated as the end

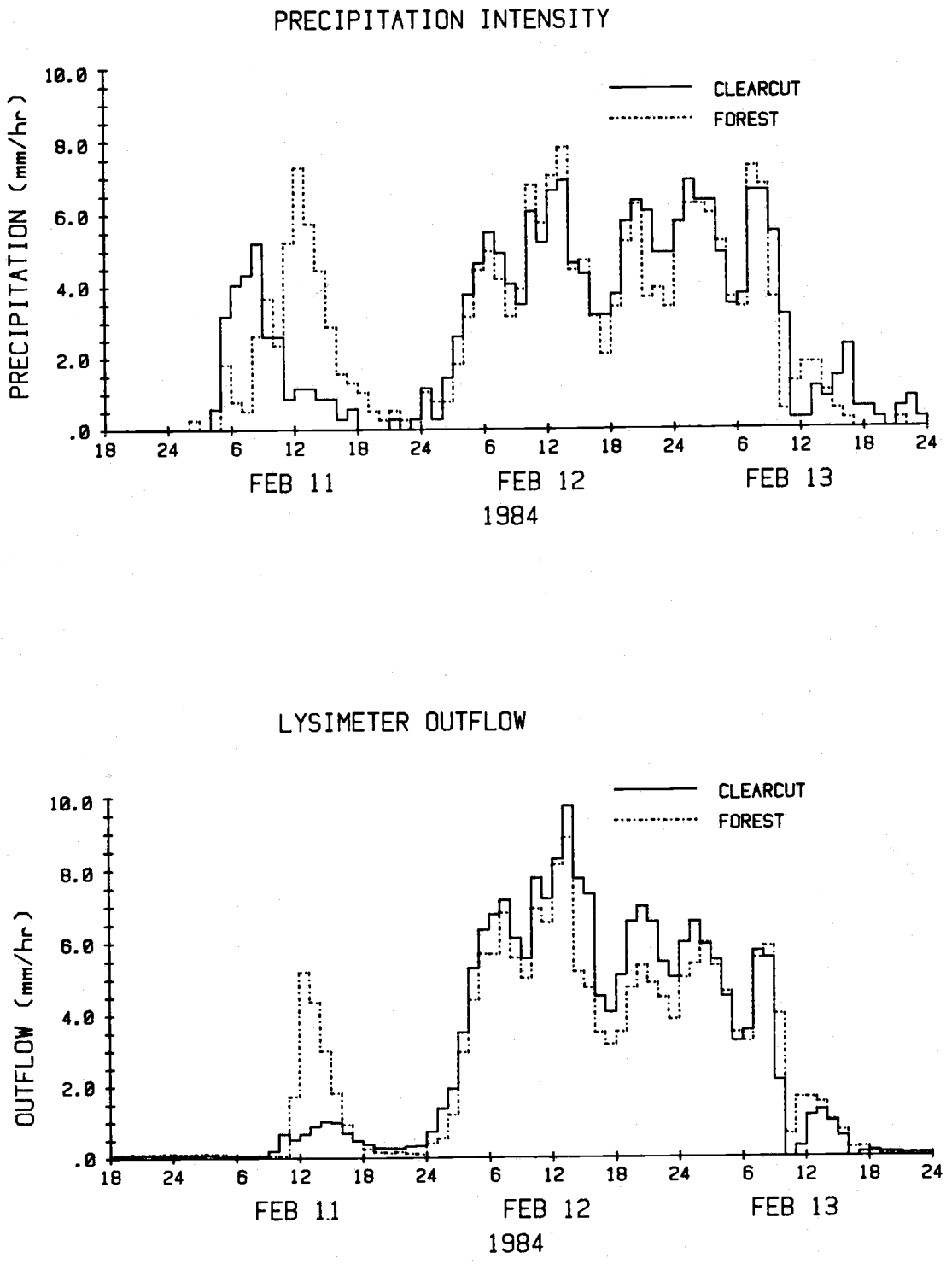

Figure 16. Precipitation Intensity and Lysimeter Outflow, Event 4: February 10-13, 1984.

of the energy balance analysis for each plot.

Initial snowpack characteristics were measured by snow surveys conducted on February 11 between 0800 and 1230. Average snow accumulation at that time was 242 mm in the clearcut and 42 mm in the forest. Density of the clearcut snowpack was 14.9 percent, and its water equivalent was 36.1 mm. The forest snowpack had a density of 39.3 percent and water equivalent of 16.5 mm. Free water content was 5.5 percent in the clearcut snowpack and 3.4 percent in the forest snowpack.

During the period between 0900 and 2300 on February 11, all of the intercepted snow fell from the forest canopy as melt water or wet clumps. Although much snow melted in the canopy because of its high exposure to energy inputs, clearcut snowmelt was relatively low. This is apparent in Figure 16 which shows greater lysimeter outflow in the forest plot than the clearcut plot during this period. Consequently, when the moderate rains began after midnight, a significant amount of the previous snowfall had already melted in the forest.

During the 28-hour clearcut study period, 121.9 mm of rain fell on the clearcut plot. Moderate rainfall rates exceeded 4.0 mm/hr for over 60 percent of the study period and peaked at 6.9 mm/hr. The heated tipping bucket raingage in the forest, which was operating properly during this event, measured 113.2 mm of rain for the same 28-hour period. For the 20-hour designated study period, however, rainfall totaled only 72.8 mm. Precipitation intensity, which was generally lower in the forest, exceeded 4.0 mm/hr for only 45 percent

of the period, and peaked at 7.8 mm/hr.

The forest plot consistently had lower air and dewpoint temperatures, net shortwave radiation, and windspeeds during the energy balance analysis (Figure 17). Between 2300 on February 11 and 1600 on February 12, clearcut air temperature slowly increased from 2.6 to 7.0°C. Temperatures then quickly dropped to about 3.5-4.5°C for the remainder of the analysis. The clearcut air temperature exceeded 4.0°C for 68 percent of the study period. Forest air temperatures increased from 2.0 to 6.2°C and then quickly dropped to 4.4°C. The forest air temperature exceeded 4.0°C for only 55 percent of the study period. Dewpoint temperatures closely followed air temperatures, but were generally about 1.5-2.0°C lower. Clearcut dewpoint temperatures were above 2.0°C for 71 percent of the study period and forest dewpoint temperatures were above 2.0°C for 65 percent of the study period. Soil temperatures displayed interesting trends during the analysis. Clearcut soil temperature ranged between 0.1°C and 0.5°C until February 12 at 2400 when it quickly increased to 2.7°C. In the forest, a similar abrupt increase occurred, but at 0700 on February 11. Soil temperature increases in both plots are attributed to complete snowmelt over the soil temperature thermistors followed by slow warming of the bare ground. Net shortwave radiation was low for both plots as a consequence of the dense cloud cover. At 1200 on February 11, net shorwave radiation peaked at 6.6 W/m^2 in the clearcut. Net shortwave radiation in the forest barely rose above 0.0 W/m^2 on February 11 and 13. Mean hourly windspeeds were low in both plots except for two

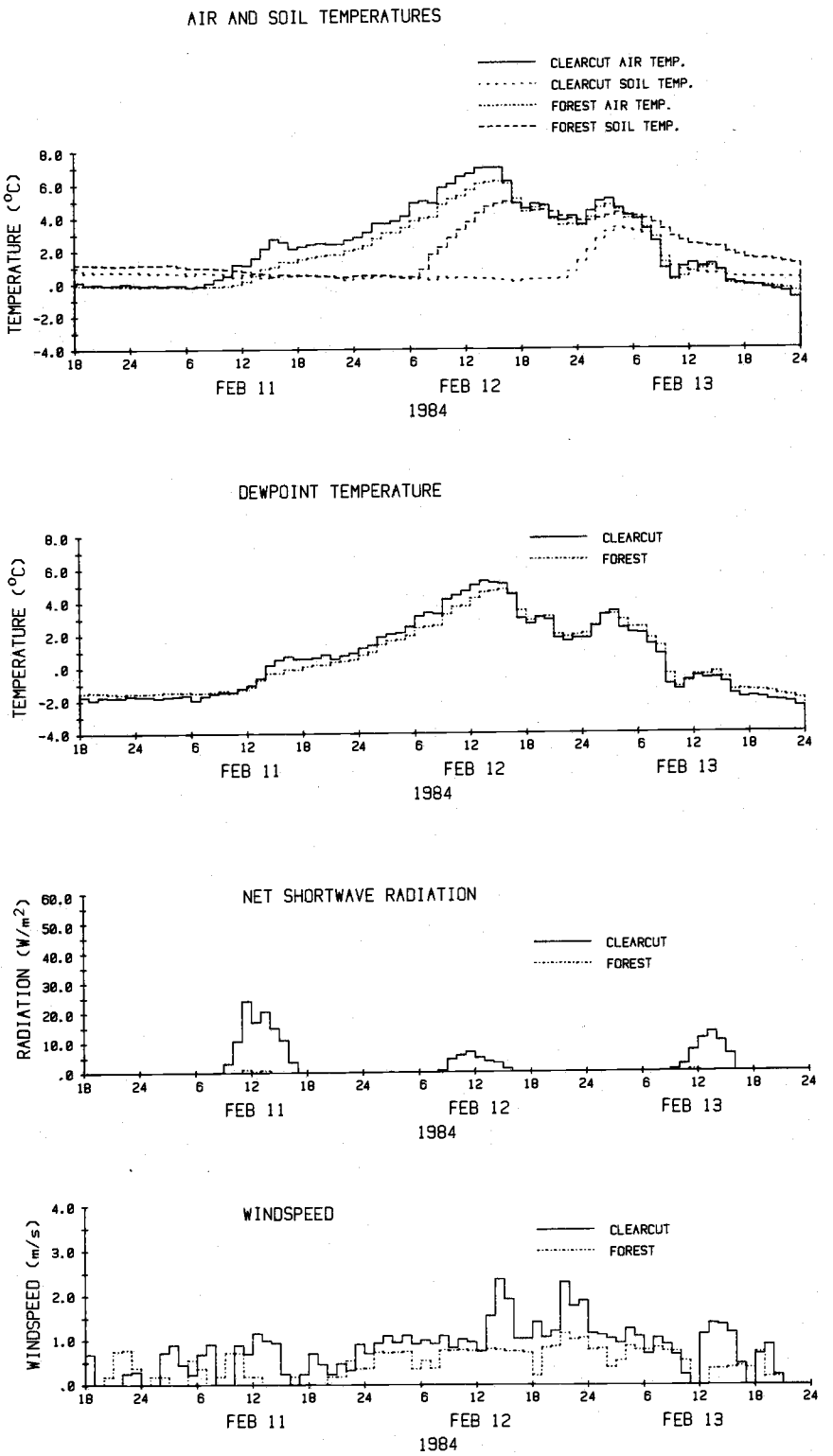

Figure 17. Measured Microclimatic Variables, Event 4: February 10-13, 1984.

periods when the mean hourly windspeeds were above 2.0 m/s in the clearcut plot.

It is evident from Figure 16 that once the energy balance analysis began (at 2300 on February 11, 1984), lysimeter outflow was greater in the clearcut than the forest. Although the energy balance analysis of the forest ended at 1900 on February 11, a comparison of cumulative lysimeter outflows for both plots between 2300 on February 11 and 0300 on February 13 (when the snow of both plots dissappeared) shows that lysimeter outflow was 27.3 mm greater in the clearcut (Figure 18). The increased outflow of the clearcut is attributed to the quick melt of the intercepted snow in the forest during the previous period. Thus, the forest contributed less melt water to lysimeter outflow during the study period. Cumulative lysimeter outflow totaled 155.0 mm in the clearcut and 127.7 mm in the forest. The clearcut plot had greater lysimeter outflow throughout this period. However, if the period of canopy drip is included in the analysis (between 0800 and 2300 on February 11), cumulative lysimeter outflow totaled 162.6 mm in the clearcut plot and 145.9 mm in the forest plot. Because lysimeter outflow was greater in the forest when canopy drip was occurring, the cumulative lysimeter outflow differential between the clearcut and forest plots was lower when the period of canopy drip was included. As a result, lysimeter outflow from the forest was 10.6 mm greater than the clearcut before the heavier rainfall and runoff occurred (starting at about 0100 on February 12). Thus, by the time the study period commenced, less snow was available in the forest to contribute to runoff.

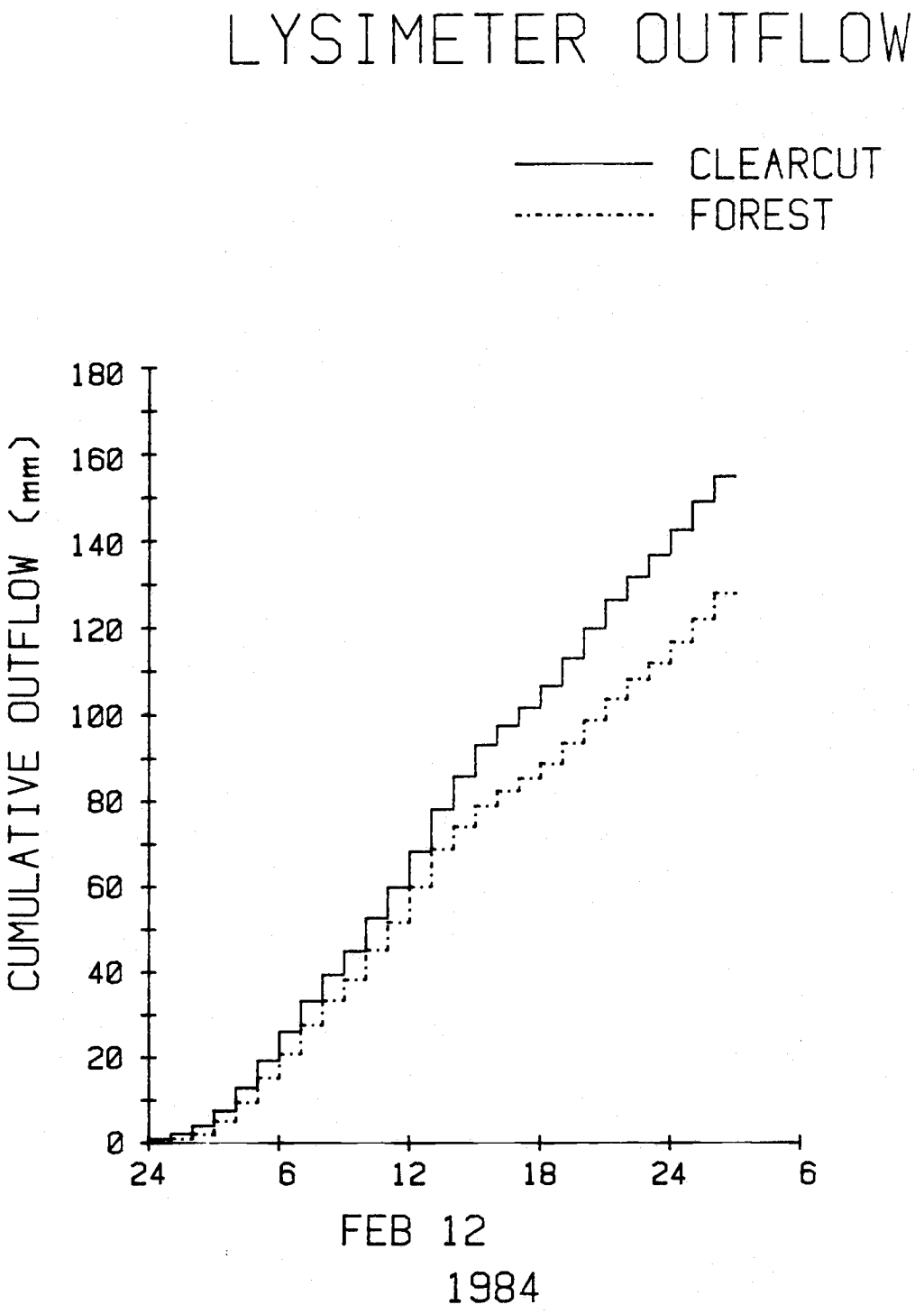

Figure 18. Cumulative Lysimeter Outflow During the February 12-13, 1984 Rain-on-Snow Study Period.

It is apparent in the energy balances of the clearcut and forest snowpacks that longwave radiation was the dominant source of snowmelt, contributing 37.9 percent of the total melt in the clearcut and 45.4 percent of the total melt in the forest (Table 12). Compared to the events previously discussed, longwave radiation played a slightly weaker role in contributing to total snowmelt. The trend of longwave radiation melt shows slightly higher melt rates in the clearcut until February 12 at 1600 (Figure 19). After that time, the longwave radiation melts of both plots were similar. Turbulent heat (consisting of sensible and latent heats) as a source of melt contributed 33.5 percent of the total melt in the clearcut compared to 22.6 percent in the forest. The plots of sensible and latent heat melts show that for the majority of the study period, snowmelt was slightly lower in the forest (Figure 20). However, between 1300 and 1600 on February 12, the clearcut exhibited a large increase in both sensible and latent heat melts while the forest turbulent heat melts remained fairly constant. In the clearcut at 1500, latent heat melt peaked at 0.5 mm/hr and sensible heat peaked at 0.2 mm/hr. At the same time in the forest plot, latent and sensible heats were approximately 0.1 mm/hr. Although all of the energy balance components except net shortwave radiation peaked during this period, only the turbulent energy components showed a marked contrast between the clearcut and forest plots. The microclimatic variable which accounts for the difference is the wind. Mean hourly windspeeds in the clearcut peaked at 2.4 m/s with one gust of 7.6 m/s. The mean hourly windspeed of the forest was only 0.8 m/s with a gust of

Table 12. Comparison of Melt Predicted by the Energy Balance Model and Measured Melt for Clearcut and Forest Plots During Event 4. February 11, 1984 at 2300 to February 13, 1984 at 0300 for Clearcut plot or February 11, 1984 at 2300 to February 12, 1984 at 1900 for Forest.

Source	Clearcut			Forest		
	Predicted (mm)	Predicted (%)	Measured (mm)	Predicted (mm)	Predicted (%)	Measured (mm)
Shortwave Radiation	0.3	1.7		0.0	0.0	
Longwave Radiation	6.9	37.9		4.4	45.4	
Sensible Heat	2.3	12.6		0.8	8.2	
Latent Heat	3.8	20.9		1.4	14.4	
Rain	4.9	26.9		3.1	32.0	
Total	18.2	100.0	25.1	9.7	100.0	11.9

Table 13. Snowpack Characteristics and Melt Determined by Snow Survey Information for Event 4.

Snowpack Characteristics	Clearcut 2/11/84 at 2300*	Forest 2/11/84 at 2300***
Water Equivalent (mm)	34.8	22.2
Density (%)	27.3**	49.3
Free Water Content (%)	24.1**	23.4
Ice (mm)	26.4	17.0
Melt (mm)	26.4	17.0

* Snow survey taken February 11, 1984 at 1200. Water equivalent adjusted to February 11, 1984 at 2300 by adding the intervening melt.
** Density and free water content were determined on February 12, 1984 at 1300 and were assumed to be constant throughout the event.
*** Snow survey taken February 11, 1984 at 1400. Water equivalent adjusted to February 11, 1984 at 2300 by adding the water that was added to the snowpack during the intervening period.

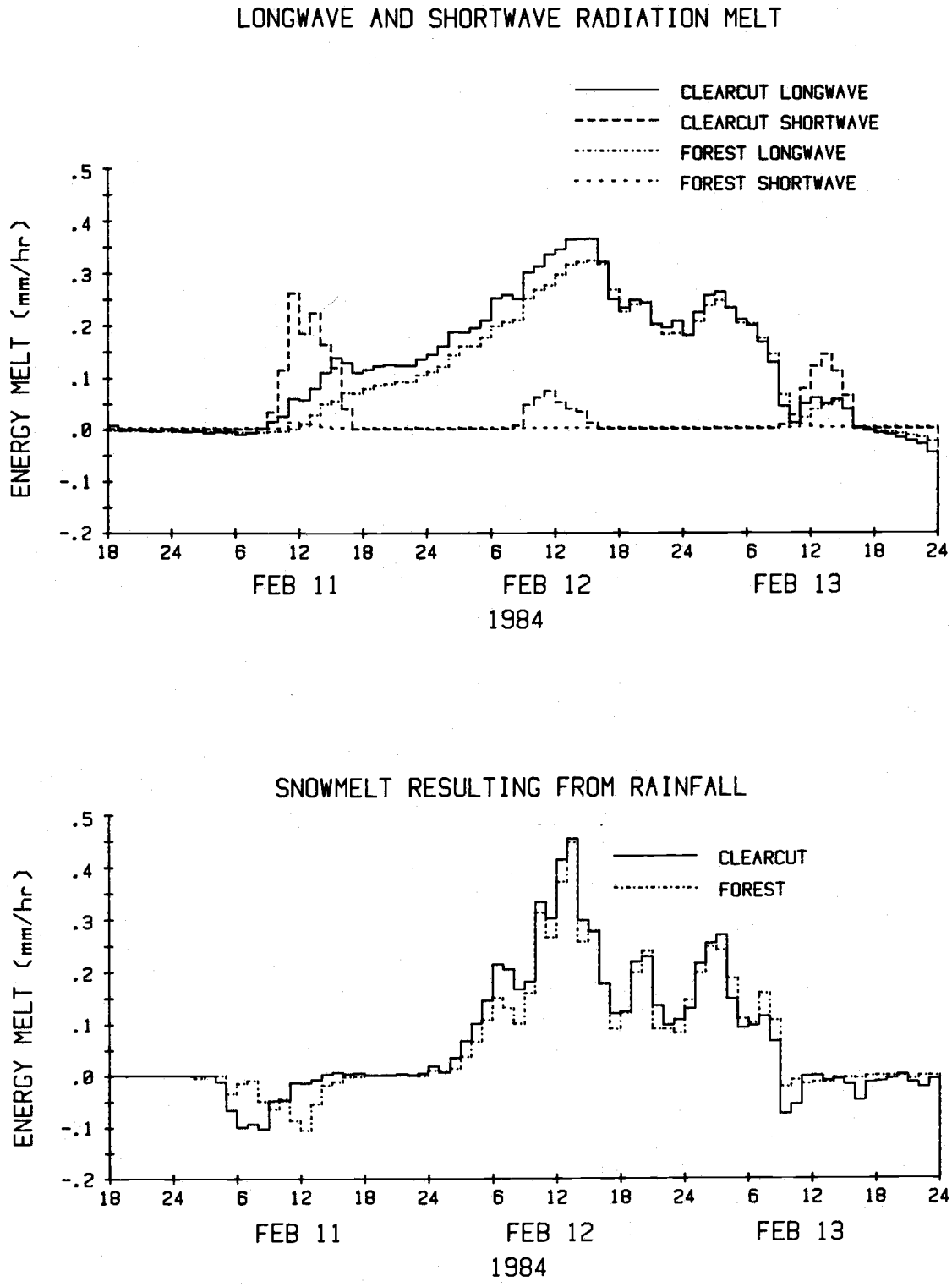

Figure 19. Time Trends of Longwave Radiation Melt, Shortwave Radiation Melt, and Snowmelt Resulting from Rainfall, Event 4: February 10-13, 1984.

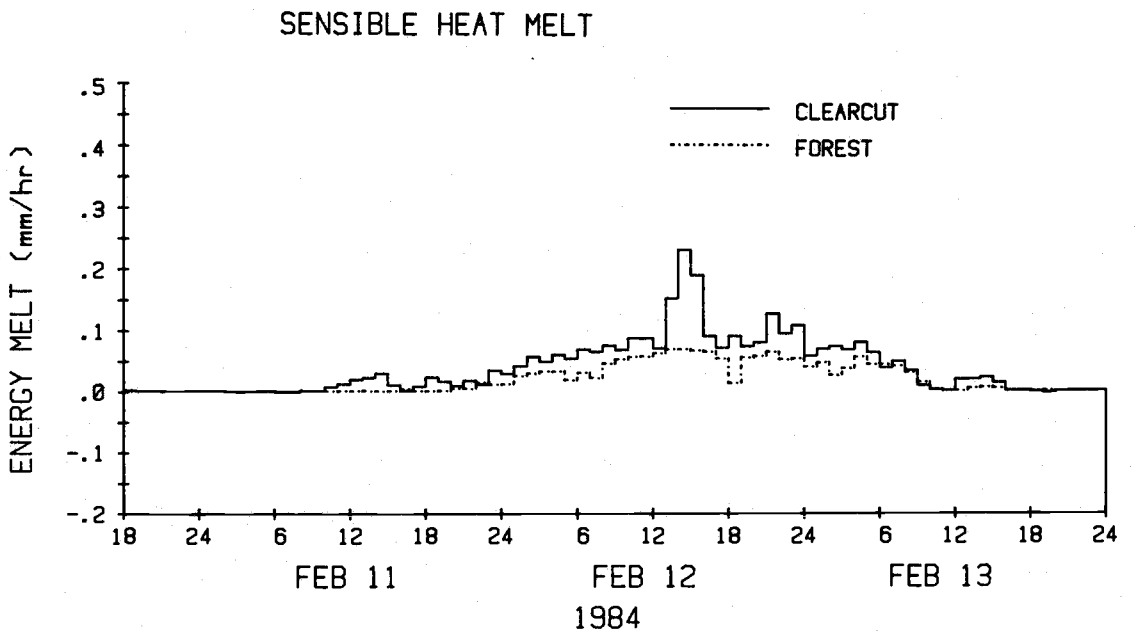

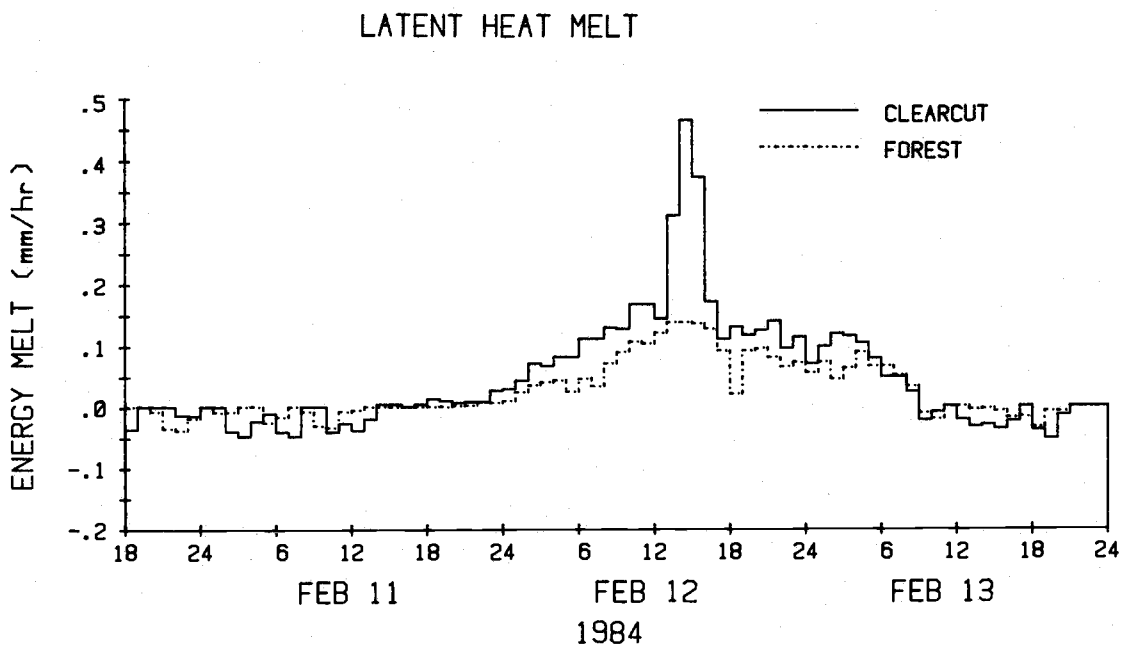

Figure 20. Time Trends of Sensible and Latent Heat Melts, Event 4: February 10-13, 1984.

1.9 m/s. Snowmelt resulting from rain was a large melt component in this event because of the relatively high amounts of rainfall and accounted for 26.9 percent of the predicted snowmelt in the clearcut and 32.0 percent of the predicted snowmelt in the forest. The clearcut and forest plots had similar trends and magnitudes of this melt component (Figure 19).

Snowmelt predicted by the energy balance model agreed reasonably well with the measured melt of both plots (Table 12). Both predicted and measured melts in the clearcut were approximately double the forest melts. The energy balance analysis was not entirely valid during this rain-on-snow event because it required a continuous snowpack on the ground. Small patches of bare ground became apparent in the forest at 0700 and in the clearcut at 1500 on February 12. The patches of bare ground gradually grew until the end of the analysis when all of the snow dissappeared.

The effects of the patches of bare ground were complex. With patchy snow on the ground surface, less snow was available for melt. Also, the patches of bare ground quickly warmed above 0.0°C as it became exposed to the various energy inputs from the atmosphere. As the ground warmed, it could then conduct heat laterally to the snowpack edges to increase melt. Additionally, the edges of the snowpacks were exposed to the energy inputs of sensible and latent heats, longwave radiation, and shortwave radiation. It has been shown by DeWalle and Meiman (1971) that sensible heat transfer from patches of bare ground to snowpacks may be significant. With the ground warmer than the snowpack, a pocket of warmer air over the bare

ground could be transported to a patch of snow by advection thereby increasing the sensible heat transfer to adjacent snow patches. Thus, the increased energy inputs to a non-continuous snowpack assure faster melt of a smaller volume of snow. The value of the energy balance analyses in this situation is that the components of the energy balance were quantified for a hypothetically continuous snowpack. As a result, it is known that greater water output from the clearcut was a result of greater snowpack water equivalent at the beginning of the analysis period and greater energy inputs in the clearcut plot.

The estimates of melt by snow survey information are shown in Table 13. Because the snowpacks of both plots completely melted, only an initial snow survey was necessary to determine melt by snowpack measurements. A snow survey in the clearcut plot was conducted on February 12 at 1200. The results of this survey were adjusted back to February 11 at 2300 by adding the intervening melt to the measured water equivalent and by assuming there was no change in density or free water content. The 26.4 mm of snowmelt estimated by the adjusted snow survey agreed well with the measured melt, but was greater than the predicted melt. No survey was conducted on February 12 in the forest because there was little snow left to sample. Consequently, the snow survey information of February 11 at 1230 was adjusted to 2300 by adding the intervening water that was added to the snowpack by snow and melt water dropping from the canopy to the water equivalent. It was assumed that density and free water content did not change during the intervening period. The resulting

melt of 17.0 mm agreed well with the actual melt and was slightly higher than the predicted melt.

Event 5: March 18-19, 1984

Although the rain-on-snow event of March 18-19, 1984 was minor compared to the previous events discussed, it served as a further example of the important role the forest canopy played in influencing snow accumulation and subsequent snowmelt. The forest canopy intercepted a large portion of the snow falling during the nights of March 15 and March 16. The intercepted snow lost water by the ongoing melt processes while little melt occurred on the forest floor or in the clearcut plot. As a consequence of the interception losses, the clearcut snowpack had 15.3 mm greater water equivalent than the forest snowpack during the initial stages of the rain-on-snow event. Snow surveys of both plots were conducted between 1100 and 1400 on March 18. The water equivalent of the clearcut snowpack was 18.1 mm while the forest snowpack's water equivalent was only 2.8 mm. Density of the clearcut snowpack averaged 32.2 percent and its free water content averaged 21.7 percent. Because the snowpack in the forest was patchy and could not be easily sampled, its density was judged to be 50.0 percent on the basis of its weight and hardness. The free water content of the forest snowpack was assumed to be 23.0 percent on the basis of past measurements with snow of similar characteristics.

Rain began falling at 0500 on March 18 and continued intermittently until 1400 on March 19 (Figure 21). Rainfall was generally light during this period with maximum rainfall intensities reaching only 2.3 mm/hr. The total rainfall during this analysis was 32.0 mm in the clearcut. Unfortunately, the heated tipping bucket raingage in the forest again was not operating properly during this period. However, storage gages were in place throughout the forest and measured 32.0 mm of rainfall during this period. The period for energy balance analysis began at 0500 on March 18 and ended when the snowpacks of each plot dissappeared. In the clearcut, the snowpack dissappeared at 1300 on March 19 and in the forest, the snowpack completely dissappeared at 2100 on March 18. These times were designated as the end of the energy balance analysis for each plot.

As in the previous events, air and dewpoint temperatures were 0.1-2.0°C lower in the forest throughout the event (Figure 22). Air temperature of the clearcut remained below 5.0°C until the end of the event, but subsequently increased to almost 10.0°C. The clearcut dewpoint temperatures generally followed the same trend, but remained below air temperatures by 1.5-2.0°C. The forest air temperature remained below 3.0°C during the energy balance analysis period while the dewpoint temperatures never exceeded 2.0°C during the same period. Soil temperature was generally 0.2-0.5°C in the clearcut plot until 0900 on March 19 at which time, it quickly increased to 12.5°C as snow completely melted above the soil temperature thermistor. Soil temperature of the forest plot remained above 1.0°C for the duration of the energy balance analysis because the snow was completely melted above the soil thermistor at the beginning of the

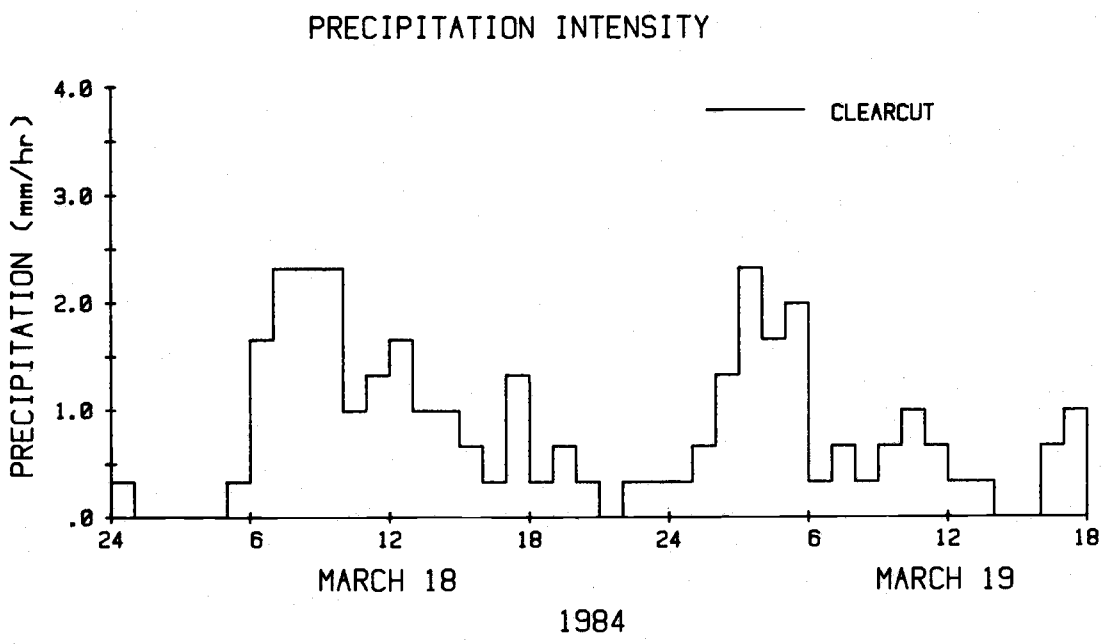

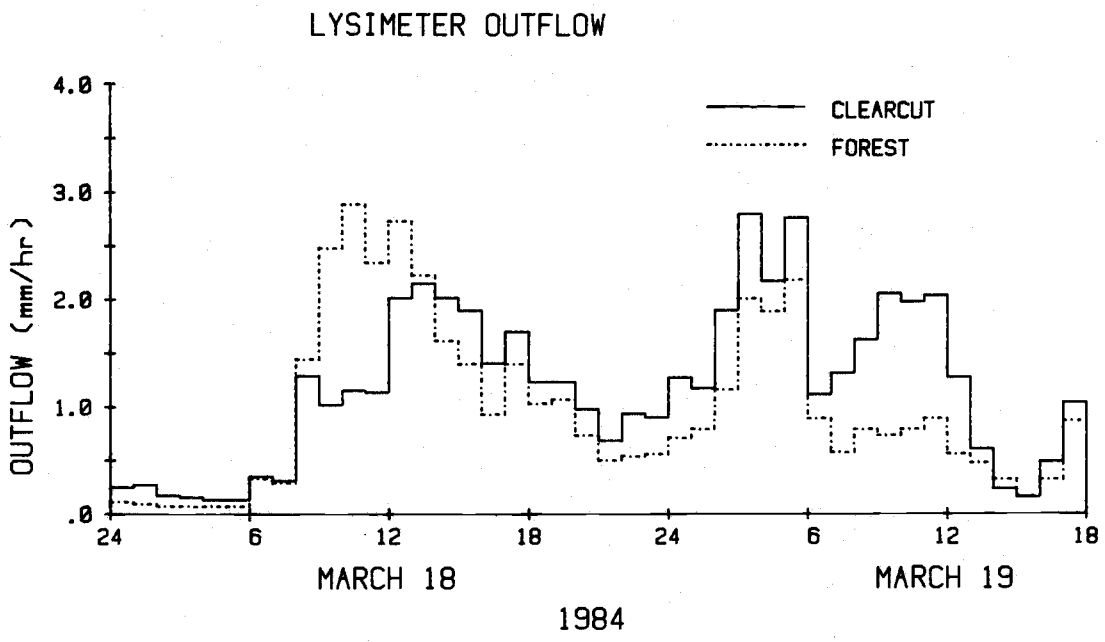

Figure 21. Precipitation Intensity and Lysimeter Outflow, Event 5: March 18-19, 1984.

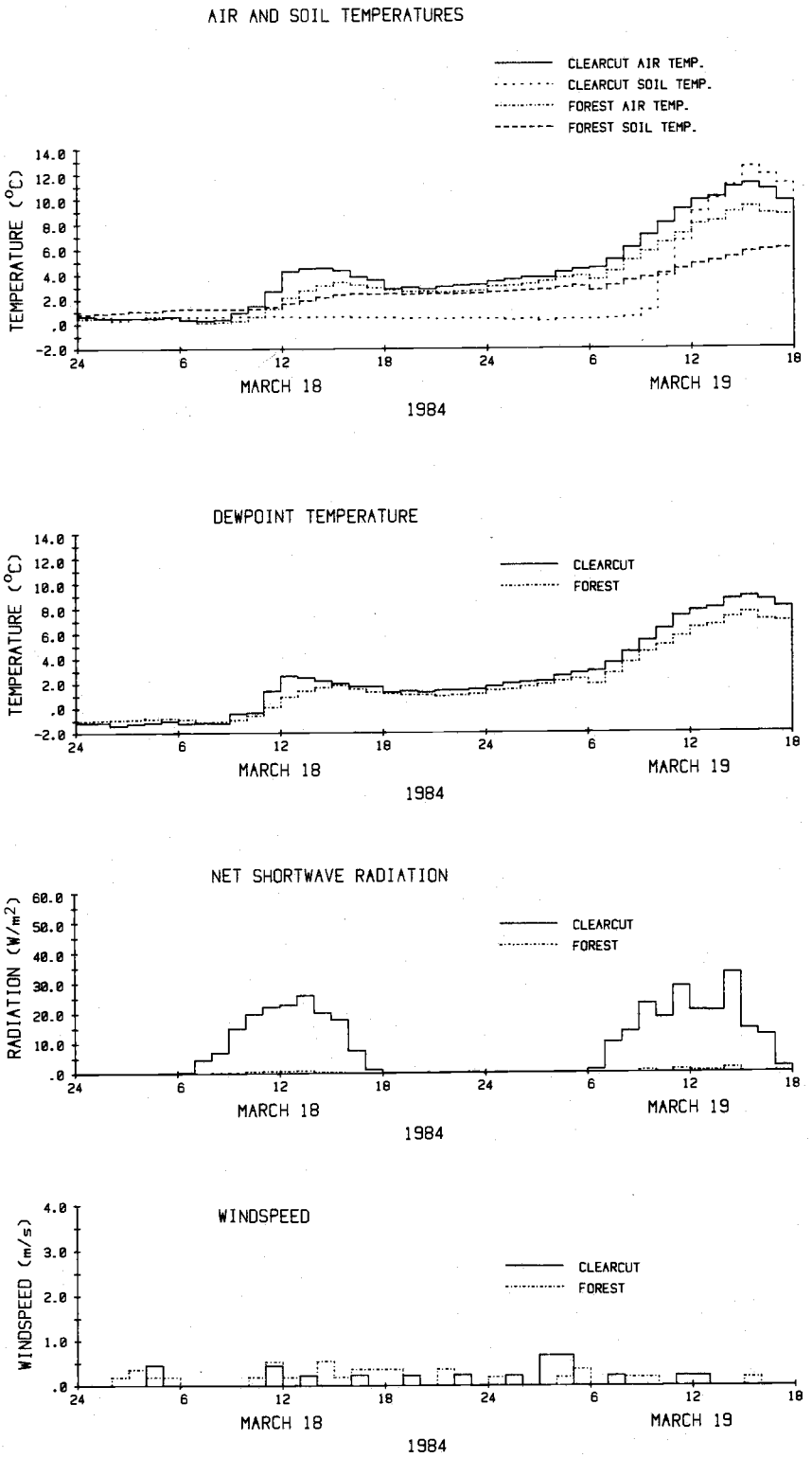

Figure 22. Measured Microclimatic Variables, Event 5: March 18-19, 1984.

analysis. Net shortwave radiation reached a maximum of 33.0 W/m^2 in the clearcut and 0.8 W/m^2 in the forest. Winds were consistently light throughout the event reaching maximums of 0.7 m/s in the clearcut and 0.6 m/s in the forest.

Greater initial depth and water equivalent in the clearcut snowpack relative to those of the forest snowpack had important consequences for lysimeter outflow (Figure 21). During the initial stages of the event, lysimeter outflow was greater in the forest plot than the clearcut plot. At that time, clearcut lysimeter outflow was lower than precipitation by about 1.0-2.0 mm/hr. Thus, some of the water supplied by precipitation was being stored in the clearcut snowpack because the snowpack's water storage capacity was not fulfilled. However, the shallow, wet snowpack of the forest was saturated with water when the rain commenced and, therefore, quickly released the incoming rain water and its melt water. Greater lysimeter outflow from the clearcut snowpack occurred once the clearcut snowpack became saturated at about 1400. By the time snow completely dissappeared from both plots (March 19 at 0300), total lysimeter outflow from the clearcut plot was 7.2 mm greater than the lysimeter outflow from the forest plot.

Snowmelt predicted by the energy balance model agreed well with the measured melt of both plots (Table 14). Longwave radiation, the dominant source of snowmelt for both plots, accounted for 59.6 percent of the total predicted melt in the clearcut and 87.5 percent of the total predicted melt in the forest. Although longwave radiation melt was not high until 0600 on March 19, the low windspeeds, light rain, and cool air and dewpoint temperatures

Table 14. Comparison of Melt Predicted by the Energy Balance Model and Measured Melt for Clearcut and Forest Plots During Event 5. March 18, 1984 at 0500 to March 19, 1984 at 1300 for Clearcut plot or March 18, 1984 at 0500 to March 18, 1984 at 2100 for Forest plot.

Source	Clearcut			Forest		
	Predicted (mm)	Predicted (%)	Measured (mm)	Predicted (mm)	Predicted (%)	Measured (mm)
Shortwave Radiation	3.0	28.8		0.0	0.0	
Longwave Radiation	6.2	59.6		1.4	87.5	
Sensible Heat	0.2	1.9		0.1	6.3	
Latent Heat	0.4	3.9		0.1	6.2	
Rain	0.6	5.8		0.0	0.0	
Total	10.4	100.0	11.3	1.6	100.0	2.9

Table 15. Snowpack Characteristics and Melt Determined by Snow Survey Information for Event 5.

Snowpack Characteristics	Clearcut 3/18/84 at 0500*	Forest 3/18/84 at 0500**
Water Equivalent (mm)	12.4	2.6
Density (%)	32.2	50.0***
Free Water Content (%)	21.7	23.0****
Ice (mm)	9.7	2.0
Melt (mm)	9.7	2.0

* Snow survey taken March 18, 1984 at 1200. The water equivalent was adjusted to March 18, 1984 at 0500 by adding the intervening melt. Free water content and density were assumed to be constant.
** Snow survey taken March 18, 1984 at 1400. The water equivalent was adjusted to March 18, 1984 at 0500 by adding the intervening melt. Free water content and density ware assumed to be constant.
*** Snowpack density was estimated to be 50.0 percent on the basis of its weight and hardness.
**** Snowpack free water content was estimated to be 23.0 percent on the basis of past measurements of snow with similar characteristics.

resulted in low energy transfers for most of the remaining components in both plots. During this event, shortwave radiation melt accounted for 28.8 percent of the total predicted melt in the clearcut plot. The trends of the energy balance components are shown in Figures 23 and 24.

Although predicted snowmelt in the forest agreed well with the measured melt, the accuracy of the energy balance model is questionable during this event. Because the forest snowpack was patchy during the energy balance analysis, additional energy transfers not adequately measured were acting to melt the snowpack. The additional energy inputs probably included heat input from the bare soil surrounding the snow patches and increased sensible heat inputs from the air overlying the bare soil. Thus, one would expect that if these heat inputs to the snow patches were adequately measured, predicted snowmelt would agree better with the measured melt. Similarly, the clearcut snowpack was patchy by the morning of March 19. The snowmelt prediction may also have been improved if the additional energy inputs caused by the bare soil surface could have been quantified.

Snowmelt estimated from snow survey information agreed well with measured and predicted snowmelt for both plots (Tables 14 and 15). As discussed previously, the average density and free water content of the forest snowpack had to be estimated because the shallow and patchy snowpack was difficult to sample. The results of both snow surveys were adjusted back to 0500 on March 18 by adding the intervening melt and assuming the density and free water content did not significantly change during the adjustment duration.

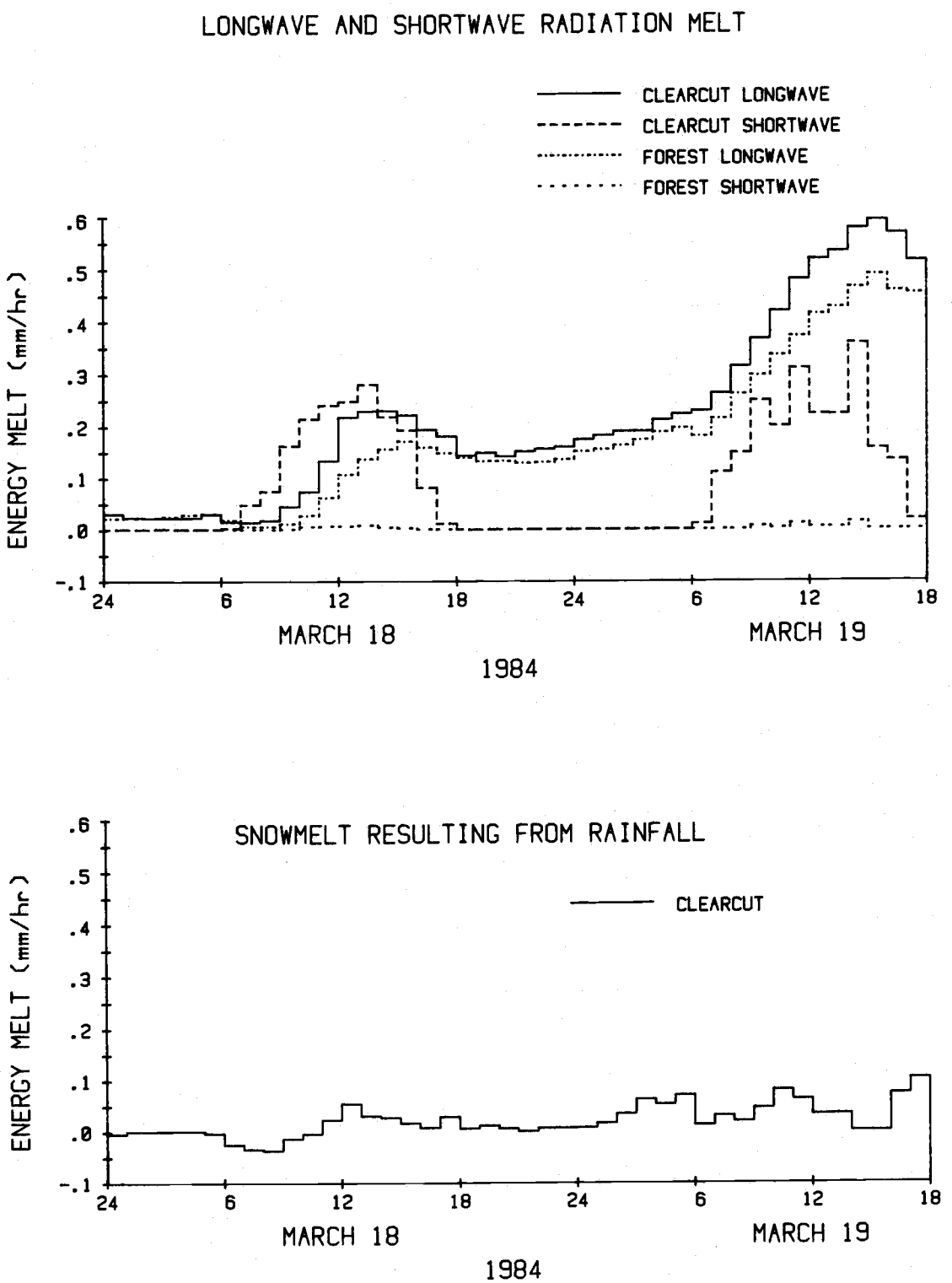

Figure 23. Time Trends of Longwave Radiation Melt, Shortwave Radiation Melt, and Snowmelt Resulting from Rainfall, Event 5: March 18-19, 1984.

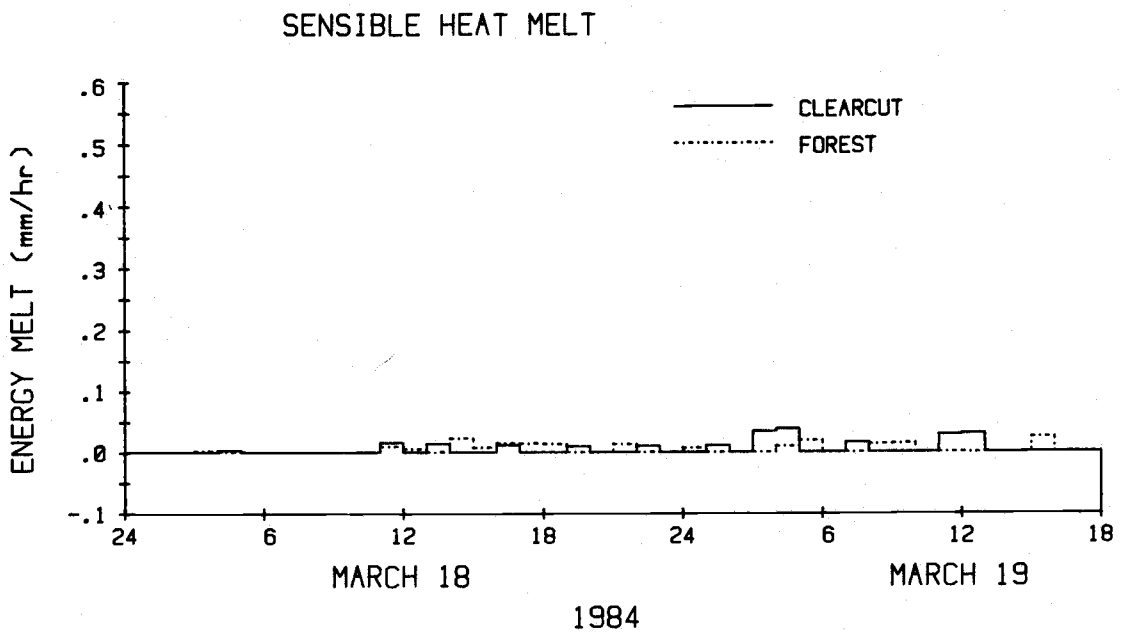

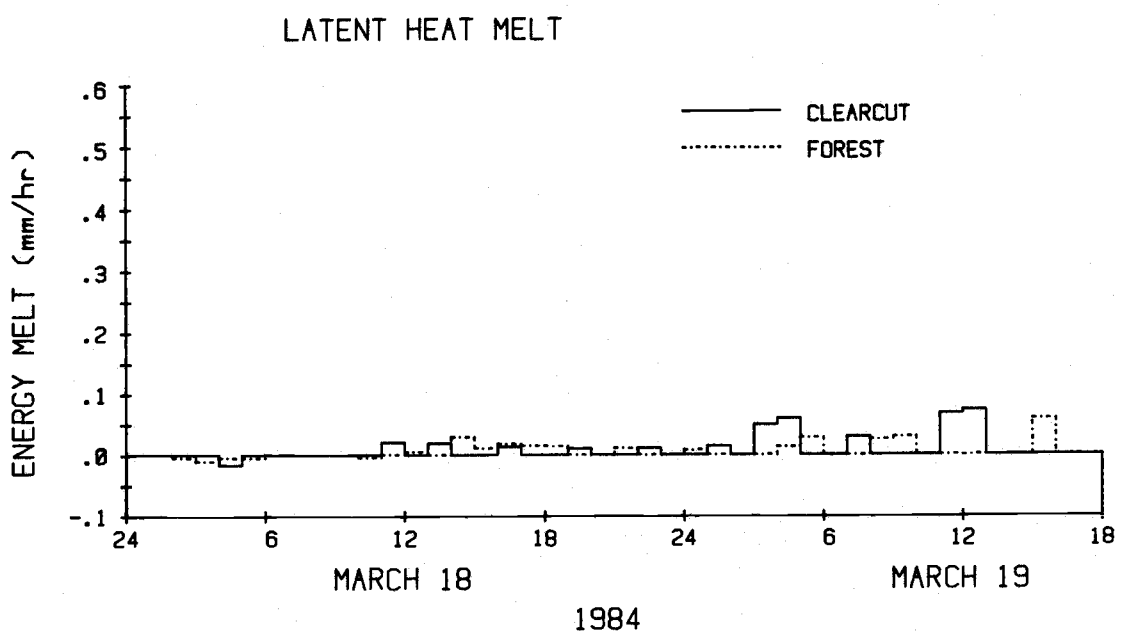

Figure 24, Time Trends of Sensible and Latent Heat Melts, Event 5: March 18-19, 1984.

DISCUSSION

A comparison of snowmelt predicted by the energy balance model with measured snowmelt and snowmelt determined by snow survey information is presented in Table 16. Table 17 is a summary of the snowmelt components attributed to the various processes of energy transfer for each rain-on-snow event.

It is evident in Table 16 that melt predicted by the energy balance model agrees reasonably well with measured snowmelt and melt determined by snow surveys for the clearcut plot. The largest errors occurred during event 2 where there was a 10.5 mm difference between predicted and measured snowmelt and event 3 where there was a 8.3 mm difference between predicted melt and melt determined by snow surveys. As discussed previously, the presence of ice layers in the clearcut snowpack during event 3 most likely accounted for a large portion of the error for that event. Other possible sources of error include:

1. Instrument errors and assumptions made in measuring the microclimatic variables. These errors and their magnitudes are discussed in Appendix A.
2. Calculation of sensible and latent heat melts by the USACE (1956) snowmelt equations. Because these equations incorporate a power law wind profile, their use at a clearcut site in mountainous terrain with large roughness elements and topographic variations may be questionable. The relationship of windspeed with height in this terrain may be more complex than a simple power law.

Table 16. Comparison of Melt Predicted by the Energy Balance Model, Measured Melt, and Melt Determined by Snow Survey (C = clearcut plot and F = forest plot).

Event	Date	Plot	Predicted Snowmelt (mm)	Measured Snowmelt (mm)	Snow Survey (mm)
1	12/9-10/83	C	10.9	10.1	12.4
		F	5.9	13.4	6.0
2	12/12-14/83	C	21.8	32.3	30.5
		F	13.9	46.9	12.6
3	12/28-31/83	C	18.6	12.0	26.9
		F	10.5	28.3	30.0
4	2/11-13/84	C	18.2	25.1	26.4
		F	9.7	11.9	17.0
5	3/18-19/84	C	10.4	11.3	9.7
		F	1.6	2.9	2.0

Table 17. Absolute and Relative Contributions to Total Snowmelt of Energy Balance Components (K_M* = snowmelt by net shortwave radiation; L_M* = snowmelt by net longwave radiation; M_H = snowmelt by sensible heat transfer; M_E = snowmelt by latent heat transfer; $M_H + M_E$ = snowmelt by total turbulent heat transfer; F_M = snowmelt by rain heat).

Event, Date, and Plot	K_M*		L_M*		M_H		M_E		$M_H + M_E$		F_M		Total Predicted Snowmelt
	(mm)	(%)	(mm)	(%)	(mm)	(%)	(mm)	(%)	(mm)	(%)	(mm)	(%)	(mm)
1 12/9-10/83													
Clearcut	1.1	10.1	5.0	45.8	1.7	15.6	2.2	20.2	3.9	35.8	0.9	8.3	10.9
Forest	0.0	0.0	3.9	66.1	0.8	13.5	0.7	11.9	1.5	25.4	0.5	8.5	5.9
2 12/12-14/83													
Clearcut	0.7	3.2	11.3	51.8	2.7	12.4	4.3	19.7	7.0	32.1	2.8	12.9	21.8
Forest	0.0	0.0	9.2	66.2	1.5	10.8	1.6	11.5	3.1	22.3	1.6	11.5	13.9
3 12/28-31/83													
Clearcut	1.3	7.0	8.5	45.7	2.3	12.4	4.2	22.5	6.5	34.9	2.3	12.4	18.6
Forest	0.0	0.0	6.4	61.0	1.2	11.4	1.6	15.2	2.8	26.6	1.3	12.4	10.5
4 2/11-13/84													
Clearcut	0.3	1.7	6.9	37.9	2.3	12.6	3.8	20.9	6.1	33.5	4.9	26.9	18.2
Forest	0.0	0.0	4.4	45.4	0.8	8.2	1.4	14.4	2.2	22.6	3.1	32.0	9.7
5 3/18-19/84													
Clearcut	3.0	28.8	6.2	59.6	0.2	1.9	0.4	3.9	0.6	5.8	0.6	5.8	10.4
Forest	0.0	0.0	1.4	87.5	0.1	6.3	0.1	6.2	0.2	12.5	0.0	0.0	1.6

In the forest, snowmelt predicted by the energy balance model agreed reasonably well with measured melt and melt determined by snow surveys for events 4 and 5. However, predicted melt was lower than measured melt for events 1, 2, and 3 while for event 3, it also underestimated melt determined by snow survey information. Snow survey information for the forest plot provides insight into the large differences between predicted and measured melt for events 1 and 2. For event 1 in the forest plot, snowmelt determined by the snow surveys of December 9 and 12 was 6.0 mm. This agreed well with the 5.9 mm of melt predicted by the energy balance model. For event 2, the forest snow survey information of December 12 indicated that both estimated melt and the depth of water held as ice in the forest snowpack were 12.6 mm. This melt and ice depth agreed with the predicted melt, but was much lower than the measured melt. Because the snow survey information from both events 1 and 2 agreed with the predicted melt from these events, it is reasonable to postulate that the measured melt was overestimated.

The overestimation of measured melt in the forest plot was possibly the result of underestimating precipitation. Precipitation during events 1 and 2 had to be synthesized from the clearcut precipitation data because the heated raingage did not operate properly and the storage gages were not yet installed. The reliability of the synthesized precipitation may be questionable due to variable interception and the presence of canopy drip zones. As previously discussed, many of the snowmelt pans were susceptible to occasional concentrated drip from the forest canopy during rainfall.

If the drip falling on some of the pans was greater than gross rainfall, then more water would be measured as lysimeter outflow resulting in greater measured melt. Rothacher (1963) found that throughfall in the forest was as high as 123.4 percent of gross precipitation when raingages were located under drip from branches of the canopy. If canopy drip zones also occurred during event 3, then measured melt for that event would have been overestimated as well. As discussed previously, the snow survey conducted before event 3 may have been erroneous because snow tube measurements were used in the analysis. Thus, it is possible that measured melt and melt determined by the snow survey were both overestimated for event 3. Other possible errors for all of the events in the forest include:

1. Instrumental errors and assumptions made in measuring microclimatic variables discussed in Appendix A.
2. Calculation of sensible and latent heat melts by the USACE (1956) snowmelt indices which assume a power law wind profile. Federer and Leonard (1971) found that beneath a forest canopy, the mechanical turbulence produced over a large range in heights by trees cause non-uniform wind profiles.
3. Wind measured by one anemometer in the forest may be non-representative because of the numerous obstacles to air flow.
4. Patchy snowpacks in events 4 and 5 were not accounted for by the energy balance model.

Thus, the nature of the forest made it difficult to predict reliably the snowmelt by sensible and latent heats while faulty measurement of precipitation possibly caused errors in measuring snowmelt by lysimeter outflow. As a result, snowmelt estimated in the clearcut by the three methods presented in Table 16 is more reliable than the snowmelt estimates in the forest.

Predicted melt, measured melt, and melt determined by snow survey methods all agreed reasonably well for the clearcut and forest plots during event 4. This event was the most important rain-on-snow event studied because of the relatively large amount of rainfall and the strong response of the local streams to the rain and snowmelt water. Thus, results from this event are most likely similar to the larger rain-on-snow events (events that cause peak streamflows with return periods greater than 5 years) that occur in the transient snow zone of the western Cascade Range of Oregon.

Although measured snowmelt was greater in the forest than the clearcut during events 1, 2, and 3, measured snowmelt in the forest, as previously discussed, may be unreliable during those events because of its discrepancy with snow survey information. However, snowmelt predicted by the energy balance model for all of the rain-on-snow events studied was 57 to 543 percent greater in the clearcut than the forest. Furthermore, it is apparent from Table 17 that every energy transfer process contributed to greater snowmelt in the clearcut than in the forest plot.

Net longwave radiation was the major energy component for both plots during all of the rain-on-snow events, contributing between

38 and 87 percent of total predicted snowmelt. The dominance of longwave radiation as a source of snowmelt can be attributed to:

1. Thick cloud cover and forest canopy having temperatures near air temperature.
2. Generally low windspeeds (maximum houly windspeed of 3.0 m/s) whereby turbulent exchange remained less important than net longwave radiation.

Longwave radiation melt was 22-56 percent greater in the clearcut than in the forest because of slightly warmer air temperatures. The strong dominance of net radiation (net shortwave radiation added to net longwave radiation) agrees with the results on Boyer (1954), Hoinkes (1955), Adkins (1958), Gold and Williams (1961), DeWalle and Meiman (1971), de la Casiniere (1974), Gray and O'Neill (1974), Cox and Zuzel (1976), Hendrie and Price (1978), Granger and Male (1978), and others (see Table 1). However, because these other studies were conducted in mostly clear weather, net shortwave radiation was the predominant energy source. In this study, net shortwave radiation during rainfall was usually a minor source of energy.

The fluxes of sensible and latent heat were also significant sources of snowmelt during events 1-4. Sensible heat was estimated to have contributed an average of 13.2 percent to the total predicted melt in the clearcut and 10.9 percent in the forest. Latent heat contributed an average of 20.8 percent to the total predicted melt in the clearcut and 13.2 percent in the forest. Latent heat melt averaged about 57 percent of the total turbulent heat melt while sensible heat melt accounted for 43 percent. However, latent heat

melt was less than sensible heat melt in the forest plot during events 1 and 5. During these events, dewpoint temperatures were lower than air temperatures by a greater difference than in events 2, 3, and 4. In contrast, USACE (1956) found that latent heat melt accounted for about 78 percent of the total turbulent heat melt during cloudy and rainy weather conditions. It is likely that dewpoint temperatures were closer to air temperatures (higher specific humidity) during the USACE (1956) studies. The studies of Prowse and Owens (1982), Zuzel et al. (1983), and Moore and Owens (1984) showed that sensible heat contributed from 60.5 to 85.5 percent to the total turbulent heat during rain-on-snow periods (Table 2). However, Prowse and Owens (1982) and Zuzel et al. (1983) studied rain-on-snow events which had relatively low precipitation totals (less than 23 mm/day) with high winds (2.7-5.9 m/s), high temperatures (4.0-10.8°C), and low dewpoint temperatures (less than 2.1°C). Thus, the warm temperatures played a larger role in melting snow than did the condensation of water vapor. The results of Moore and Owens (1984) were integrated over a 10-day period of which only six days had rain. Their energy balance was strongly influenced by moderately dry, windy periods which are commonly associated with high fluxes of sensible heat. Unfortunately, Moore and Owens did not include complete weather information, so further speculation of the reasons for high contribution of sensible heat is not possible.

Because the transfers of latent and sensible heats to snowpacks are both dependent on wind as a driving mechanism, they can be combined into an overall turbulent energy flux. In this way, the

importance of wind in melting snow becomes evident. Although the rain-on-snow events studied here did not have high winds (the highest mean hourly windspeed was only 3.0 m/s and the highest instantaneous wind gust was 7.6 m/s), Table 17 shows that except for event 5, snowmelt caused by the turbulent energy fluxes was very important. The low turbulent energy melt of event 5 was caused by very calm conditions during which mean hourly windspeeds never exceeded 0.8 m/s. The case studies of Fitzharris et al. (1980), Prowse and Owens (1982), Zuzel et al. (1983), and Moore and Owens (1984) all show that turbulent energy was the dominant source of snowmelt during rain-on-snow (Table 2). Harr (1981) showed that turbulent heat melt would be consistently higher than longwave radiation melt during a hypothetical rain-on-snow event. The low to moderate winds which prevailed during the study described here accounts for the secondary importance of turbulent energy melt. The threshold mean hourly windspeed where turbulent energy melt became dominant was about 2.0 m/s. However, during the rain-on-snow events studied during the winters of 1983-1984, mean hourly windspeeds equalled or exceeded 2.0 m/s only three percent of the total time studied.

Although turbulent heat melt ranked second in importance to longwave radiation melt, it accounted for a large portion of the difference between predicted snowmelt in the forest and clearcut plots. Turbulent heat melt in the clearcut plot was 226 to 300 percent of the turbulent heat melt of the forest plot. Despite the fact that the periods of energy balance analysis were shorter for the forest plot during events 4 and 5, Figures 7, 11, 15, 20, and 24

show that hourly sensible and latent heat melts were consistently greater in the clearcut plot than in the forest plot when wind was occurring. The major reason for the reduction of turbulent heat melt in the forest was the influence of the forest acting to both reduce winds by its numerous obstacles (trees) and to deflect winds over its canopy.

The variable contribution of snowmelt from the energy of rain (0 to 32 percent of the total snowmelt) reflects the dewpoint temperature and amount of rain that fell during each event. Because event 5 had predominantly low dewpoint temperatures (below 3.0°C) and light rain (less than 2.3 mm/hr), snowmelt caused by rain was negligible. However, during event 4, moderately high dewpoint temperatures (exceeding 5.0°C) and heavy rainfall (exceeding 4.0 mm/hr for over 60 percent of the study period) resulted in a snowmelt contribution of 26.9 to 32.0 percent of the total predicted snowmelt.

The important snowmelt contribution of rain during periods of heavy rainfall (event 4) agrees with the results of other studies. Fitzharris, et al. (1980) determined that rain heat transfer contributed 19 percent of the total heat flow during intense rains of over 10 mm/hr for 25 hours. Anderton and Chinn (1978) found that rainfall provided 19 and 11 percent of the total energy supply on two successive days of rain. Snowmelt resulting from rain was 53 to 91 percent higher in the clearcut than the forest during events 1-4 because of higher rainfall and higher dewpoint temperatures.

Although rain-on-snow is common in the transient snow zone of the Pacific Northwest, it is the larger rain-on-snow events that supply enough water to the soil to initiate major peak flows, channel erosion, and mass movements. These events occur when large amounts of rainfall are augmented by significant snowmelt. This study was designed to analyze the larger rain-on-snow events, those of rainfall magnitudes with return periods greater than two years. It was expected that the energy transfer processes acting to melt snow would be largest during this type of event while large amounts of water could be measured as rain and lysimeter outflow. In this way, the energy transfer processes and measured snowmelt could be most clearly differentiated between the two plots during a potential erosion-causing event. Because of the large energy transfers and water input, predicted and measured snowmelt would be more accurate than for smaller events because relative measurement errors would be low (Appendix A). Of the five rain-on-snow events studied during the winters of 1983-1984, only event 4 (February 11-13, 1984) even approached the annual event in terms of rainfall.

Although the information from all of the rain-on-snow events gives insights into the roles the forest and clearcut plots have on influencing snowmelt, most attention should be placed on event 4 because the results from this event are most likely similar to the larger events of greater return periods. Because of the presence of a snowpack, the peak flows of local streams had return periods of 3-4 years while rainfall had a return period of approximately 2 years. Fortunately, this event was well documented because all of

the equipment was operating properly. Despite the possible errors, snowmelt predicted by the energy balance model agreed reasonably well with both measured snowmelt and snowmelt determined by snow surveys for each plot.

Table 16 shows that during event 4, snowmelt was 55-111 percent greater (depending on the method of measurement) in the clearcut plot. Because the snow in both plots dissappeared, the difference in snowmelt is attributed to both the greater snowpack accumulation and the greater energy inputs into the snowpack of the clearcut plot. Turbulent heat flux was especially important in increasing snowmelt in the clearcut plot between 1300 and 1600 on February 12. If the windspeeds had averaged above 2.0 m/s throughout event 4, it is clear that not only would the turbulent heat snowmelt components have been the dominant components of snowmelt, but also a greater snowmelt differential would have occurred between the clearcut and the forest plots because of the increased turbulent heat acting to melt snow in the clearcut. Because of the greater snowmelt in the clearcut, water input to soil was 21.4 percent greater in the clearcut plot than the forest plot.

CONCLUSIONS

This study has indicated that clearcut timber harvesting has changed the microclimate of the snowpacks in the transient snow zone on the western Cascade Range in Oregon. Conclusions drawn from this study are:

1. The forest canopy played an integral role in trapping snow and allowing the intercepted snow to quickly melt as a result of its high exposure to radiation and moist, relatively warm air. At the same time canopy melt was active, snow that accumulated in the clearcut melted slower because of its lower exposure to the energy inputs associated with radiation and the moist, warm winds. Thus, more snow in the clearcut was available for melt at the commencement of rainfall. The water equivalents of clearcut snowpacks were an average of 29.2 mm greater than forest snowpacks.
2. Energy inputs acting to melt snow on the ground were consistently greater in the clearcut plot than the forest plot. Although longwave radiation was the greatest source of snowmelt, the fluxes of latent and sensible heats accounted for a large portion of the differences between snowmelt in the clearcut and forest plots. Snowmelt caused by the turbulent transfer of sensible and latent heat was greater in the clearcut plot because of its greater exposure to the moist, relatively warm winds which occurred during rainfall. However, because generally low windspeeds (below 2.0 m/s)

characterized the rain-on-snow events in this study, longwave radiation was the dominant source of melt.

3. Although snowmelt predicted by the energy balance model was consistently greater in the clearcut plot, measured snowmelt was greater in the forest plot at times. However, the accuracy of measured melt in the forest plot is questionable. Because of the variability of rainfall and snow accumulation in the forest plot, there is a need for confirmation of proper sampling of both rainfall and snowmelt in future studies of this type.
4. During the largest rain-on-snow event (February 11-13, 1984), approximately 160 mm of rain fell on 35 mm of snow water equivalent in the clearcut and 22 mm of snow water equivalent in the forest. Snowmelt estimated by the energy balance model agreed reasonably well with both measured snowmelt and snowmelt estimated by snow survey information. Snowmelt was 55 to 111 percent greater in the clearcut depending on the method of measurement. The increased snowmelt of the clearcut plot can be attributed to both greater accumulation of snow and greater energy inputs during rainfall.

LITERATURE CITED

Adkins, C. J. 1958. The Summer Climate in the Accumulation Area of the Salmon Glacier. Journal of Glaciology, 3(23): 195-200.

Anderson, E. A. 1968. Development and Testing of Snow Pack Energy Balance Equations. Water Resources Research, 4(1): 19-37.

Anderson, H. W. 1956. Forest-Cover Effects on Snowpack Accumulation and Melt, Central Sierra Snow Laboratory. Transactions, American Geophysical Union, 37(3): 307-312.

Anderson, H. W. 1970. Storage and Delivery of Rainfall and Snowmelt Water as Related to Forest Environments. In: Proceedings of the 3rd Symposium on Forest Microclimate, pp. 51-67.

Anderson, H. W. and C. H. Gleason. 1959. Logging Effects on Snow, Soil Moisture, and Water Losses. In: Proceedings of the 27th Annual Western Snow Conference, pp. 57-65.

Anderson, H. W. and R. L. Hobba. 1959. Forests and Floods in the Northwestern United States. Int. Assoc. Sci. Hydrol., Publ. No. 48, pp. 30-39.

Anderton, P. W. and T. J. Chinn. 1978. Ivory Glacier, New Zealand An I. H. D. Representative Basin Study. Journal of Glaciology, 20(82): 67-83.

Baumgartner, A. 1967. Energetic Bases for Differential Vaporization from Forest and Agricultural Land. In: International Symposium on Forest Hydrology, W. E. Sopper and H. W. Lull (editors), pp. 381-390.

Beaudry, P. and D. L. Golding. 1983. Snowmelt During Rain on Snow in Coastal British Colombia. In: Proceedings of the 51st Annual Western Snow Conference, pp. 55-66.

Boyer, P. B. 1954. Heat Exchange and Melt of Late Season Snow Patches in Heavy Forest. In: Proceedings of the 22nd Annual Western Snow Conference, pp. 54-68.

Campbell, G. S. 1977. An Introduction to Environmental Biophysics. Springer-Verlag, New York, 159p.

Christner, J. and R. D. Harr. 1982. Peak Streamflows from the Transient Snow Zone, Western Cascades, Oregon. In: Proceedings of the 50th Annual Western Snow Conference, pp. 27-38.

Cox, L. M. and J. F. Zuzel. 1976. A Method for Determining Sensible Heat Transfer to Late-Lying Snowdrifts. In: Proceedings of the 44th Annual Western Snow Conference, pp. 23-28.

Davar, K. S. 1970. Peak Flow-Snowmelt Events. In: Handbook on the Principles of Hydrology, D. M. Gray (editor), pp. 9.1-9.25.

de la Casiniere, A. C. 1974. Heat Exchange Over a Melting Snow Surface. Journal of Glaciology, 13(67): 55-72.

DeWalle, D. R. and J. R. Meiman. 1971. Energy Exchange and Late Season Snowmelt in a Small Opening in a Colorado Subalpine Forest. Water Resources Research, 13(67): 55-72.

Dyrness, C. T. 1969. Hydrologic Properties of Soils on Three Small Watersheds in the Western Cascades in Oregon. USDA Forest Service Pacific Northwest Forest and Range Experiment Station Research Note PNW-111, 17p.

Federer, C. A. 1968. Radiation and Snowmelt on a Clearcut Watershed. In: Proceedings of the 25th Annual Eastern Snow Conference, pp. 28-42.

Federer, C. A. and R. E. Leonard. 1971. Snowmelt in Hardwood Forests. In: Proceedings of the 28th Annual Eastern Snow Conference, pp. 95-108.

Fitzharris, B. B., D. Stewart, and W. Harrison. 1980. Contribution of Snowmelt to the October, 1978 Flood of the Pomahaka and Fraser Rivers, Otago. Journal of Hydrology (N.Z.), 19(2): 84-93.

Fredriksen, R. L. 1965. Christmas Storm Damage on the H. J. Andrews Experimental Forest. USDA Forest Service Pacific Northwest Forest and Range Experiment Station Research Note PNW-29, 11p.

Fritschen, L. J. and L. W. Gay. 1979. Environmental Insrumentation. Springer-Verlag, New York, 216p.

Gary, H. W. 1974. Snow Accumulation and Snowmelt as Influenced by a Small Clearing in a Lodgepole Pine Forest. Water Resources Research, 10(2): 348-353.

Gary, H. L. 1975. Airflow Patterns and Snow Accumulation in a Forest Clearing. In: Proceedings of the 43rd Annual Western Snow Conference, pp. 106-112.

Gary, H. L. and C. A. Troendle. 1982. Snow Accumulation and Melt Under Various Stand Densities in Lodgepole Pine in Wyoming and Colorado. USDA Forest Service Rocky Mountain Forest and Range Experiment Station Research Note Rm-417, 6p.

Gates, D. M. 1962. Energy Balance in the Biosphere. Harper and Row Biological Monographs, New York, 151p.

Gerdel, R. W. 1954. Transmission of Water Through Snow. Transactions, American Geophysical Union, 35(6): 475-485.

Gold, L. W. and G. P. Williams. 1961. Energy Balance During the Snowmelt Period at an Ottawa Site. Int. Assoc. Sci. Hydrol., Publ. No. 54, pp, 288-294.

Gray, D. M. 1970. Snow Hydrology of the Prairie Environment. In: Snow Hydrology, Proceedings of the Workshop Seminar, Sponsored by the Canadian National Committee for the International Hydrological Decade and the University of New Brunswick-February 28 and 29, 1968, pp. 21-31.

Gray, D. M. and A. D. J. O'Neill. 1974. Application of the Energy Budget for Predicting Snowmelt Runoff. In: Advanced Concepts and Techniques in the Study of Snow and Ice Resources, National Academy of Sciences, pp.108-118.

Granger, R. J. and D. H. Male. 1978. Melting of a Prairie Snowpack. Journal of Applied Meteorology, 17(12): 1833-1842.

Harr, R. D. 1976. Hydrology of Small Forest Streams in Western Oregon. USDA Forest Service Pacific Northwest Forest and Range Experiment Station General Technical Report PNW-55, 15p.

Harr, R. D. 1977. Water Flux in Soil and Subsoil on a Steep Forested Slope. Journal of Hydrology, 33: 37-58.

Harr, R. D. 1981. Some Characteristics and Consequences of Snowmelt During Rainfall in Western Oregon. Journal of Hydrology, 53: 277-304.

Harr, R. D. and F. M. McCorison. 1979. Initial Effects of Clearcut Logging on Size and Timing of Peak Flows in a Small Watershed in Western Oregon. Water Resources Research, 15(1): 90-94.

Harr, R. D., A. Levno, and R. Mersereau. 1982. Streamflow Changes After Logging 130-Year-Old Douglas Fir in Two Small Watersheds. Water Resources Research, 18(3): 637-644.

Haupt, H. F. 1972. The Release of Water from Forest Snowpacks During Winter. USDA Forest Service Intermountain Forest and Range Experiment Station Research Paper INT-114, 17p.

Haupt, H. F. 1979a. Local Climatic and Hydrologic Consequences of Creating Openings in Climax Timber of North Idaho. USDA Forest Service Intermountain Forest and Range Experiment Station Research Paper INT-223, 26p.

Haupt, H. F. 1979b. Effects of Timber Cutting and Revegetation on Snow Accumulation and Melt in North Idaho. USDA Forest Service Intermountain Forest and Range Experiment Station Research Paper INT-224, 14p.

Hendrie, L. K. and A. G. Price. 1978. Energy Balance and Snow Melt in a Deciduous Forest. In: Modeling of Snow Cover Runoff, S. C. Colbeck (editor), pp. 211-222.

Hoinkes, H. 1955. Measurements of Ablation and Heat Balance on Alpine Glaciers. Journal of Glaciology, 2(17): 497-501.

Holbo, H. R. 1973. Energy Exchange Studies at the Earth's Surface, II, Energy Budget of a Pumice Desert. Department of Forest Engineering Technical Report No. 73-II, Oregon State University, Corvallis, Oregon, 142p.

Holbo, H. R. 1981. A Dew-Point Hygrometer for Field Use. Agricultural Meterology, 24: 117-130.

Holbo, H. R. 1984. Wind Study. Unpublished Study, Comstock Instrument Company, Albany, Oregon, 6p.

Jeffrey, W. W. 1970. Snow Hydrology in the Forest Environment. In: Snow Hydrology, Proceedings of the Workshop Seminar, Sponsored by the Canadian National Committee for the International Hydrological Decade and the University of New Brunswick-February 28 and 29, 1968, pp. 1-19.

Jones, E. B. 1983. Snowpack Ground-Truth Manual. NASA Document CR 170584, 41p.

Jones, E. B., A. Rango, and S. M. Howell. 1983. Snowpack Liquid Water Determinations Using Freezing Calorimetry. Nordic Hydrology, pp. 113-126.

Kittredge, J. 1953. Influences of Forests on Snow in the Ponderosa-Sugar Pine-Fir Zone of the Central Sierra Nevada. Hilgardia, 22(1): 1-96.

Leaf, C. F. 1975. Watershed Management in the Rocky Mountain Subalpine Zone-The Status of our Knowledge. USDA Forest Service Rocky Mountain Forest and Range Experiment Station Research Paper RM-137, 31p.

Male, D. H. and R. J. Granger. 1981. Snow Surface Energy Exchange. Water Resources Research, 17(3): 609-627.

McKay, D. C. 1978. An Energy Budget of a Snow Cover. In: Modeling of Snow Cover Runoff, S. C. Colbeck (editor), pp. 125-134.

McKay, D. C. and G. W. Thurtell. 1978. Measurement of Energy Fluxes Involved in the Energy Budget of a Snow Cover. Journal of Applied Meteorology, 17: 339-349.

Megahan, W. F. 1983. Hydrologic Effects of Clearcutting and Wildfire on Steep Granitic Slopes in Idaho. Water Resources Research, 19(3): 811-819.

Miller, D. H. 1964. Interception Processes During Snowstorms. USDA Forest Service Pacific Southwest Forest and Range Experiment Station Research Paper PSW-18, 24p.

Miller, D. H. 1966. Transport of Intercepted Snow from Trees During Snow Storms. USDA Forest Service Pacific Southwest Forest and Range Experiment Station Research Paper PSW-33, 30p.

Miller, D. H. 1967. Sources of Energy for Thermodynamically-Caused Transport of Intercepted Snow from Forest Crowns. In: International Symposium on Forest Hydrology, W. E. Sopper and H. W. Lull (editors), pp. 201-211.

Miner, N. H. and J. M. Trappe. 1957. Snow Interception, Accumulation, and Melt in Lodgepole Pine Forests in the Blue Mountains of Eastern Oregon. USDA Forest Service Pacific Northwest Forest and Range Experiment Station Research Paper 153, 4p.

Monteith, J. L. 1973. Principles of Environmental Physics. American Elsevier Publication Company, New York, 241p.

Moore, R. D. and I. F. Owens. 1984. Controls on Advective Snowmelt in a Maritime Alpine Basin. Journal of Climate and Applied Meteorology, 23: 135-142.

Niederhof, C. H. and E. G. Dunford. 1942. The Effect of Openings in a Young Lodgepole Pine Forest on the Storage of Melting Snow. Journal of Forestry, 40(10): 802-804.

Obled, C. and H. Harder. 1978. A Review of Snowmelt in the Mountain Environment. In: Modeling of Snow Cover Runoff, S. C. Colbeck (editor), pp. 179-203.

Oke, T. R. 1978. Boundary Layer Climates. John Wiley and Sons, New York, 372p.

O'Neill, A. D. J. and D. M. Gray. 1972. Solar Radiation Penetration Through Snow. In: Proceedings of the Banff Symposium on Snow and Ice in Hydrology, pp. 227-241.

Packer, P. E. 1971. Terrain and Cover Effects on Snowmelt in a Western White Pine Forest. Forest Science, 17(1): 125-134.

Prowse, T. D. and I. F. Owens. 1982. Energy Balance over Melting Snow, Craigieburn Range, New Zealand. Journal of Hydrology (N.Z.), 21(2): 137-147.

Reifsnyder, W. E. and H. W. Lull. 1965. Radiant Energy in Relation to Forests. USDA Technical Bulletin No. 1344, 111p.

Rosenberg, N. J. 1974. Microclimate: The Biological Environment. John Wiley and Sons, New York, 315p.

Rothacher, J. 1963. Net Precipitation Under a Douglas-Fir Forest. Forest Science, 9(4): 423-429.

Rothacher, J. 1965. Snow Accumulation and Melt in Strip Cuttings on the West Slopes of the Oregon Cascades. USDA Forest Service Pacific Northwest Forest and Range Experiment Station Research Note PNW-23, 7p.

Rothacher, J. 1973. Does Harvest in the West Slope Douglas-fir Increase Peak Flow in Small Forest Streams? USDA Forest Service Pacific Northwest Forest and Range Experiment Station Research Paper PNW-163, 13p.

Rothacher, J., C. T. Dyrness, and R. L. Fredriksen. 1967. Hydrologic and Related Characteristics of Three Small Watersheds in the Oregon Cascades. USDA Forest Service Pacific Northwest Forest and Range Experiment Station, 54p.

Satterlund, D. R. and H. F. Haupt. 1970. The Disposition of Snow Caught by Conifer Crowns. Water Resources Research, 6(2): 649-652.

Scarborough, J. B. 1966. Numerical Mathematical Analysis. The Johns Hopkins Press, Baltimore, 600p.

Smith, J. L. 1974. Hydrology of Warm Snowpacks and Their Effects Upon Water Delivery---Some New Concepts. In: Advanced Concepts and Techniques in the Study of Snow and Ice Resources, National Academy of Sciences, pp. 76-89.

Swanson, R. H. and G. R. Hillman. 1977. Predicted Increased Water Yield After Clear-Cutting Verified in West-Central Alberta. National Forest Research Centre Information Report NOR-X-198, 40p.

Swanston, D. N. and F. J. Swanson. 1976. Timber Harvesting, Mass Erosion, and Steepland Forest Geomorphology in the Pacific Northwest. In: Geomorphology and Engineering, pp. 199-221.

Toews, D. A. A. and D. Wilford. 1978. Watershed Management Considerations for Operational Planning on T.F.L. #39 (Blk 6A), Graham Island. Fisheries and Marine Service Manuscript No. 1473, 32p.

USACE (United States Army Corps of Engineers). 1956. Snow Hydrology. U.S. Army Corps of Engineers, Portland, Oregon, 437p.

Vanderwaal, J. A. 1983. Energy Exchange of Transplanted Douglas-fir Seedlings on Two Cutover Sites in Southwestern Oregon, Unpublished M.S. Thesis, Oregon State University, 110p.

Willington, R. P. and A. N. Chatterton. 1983. A Method for Analyzing the Effects of Forest Harvesting on Rain-on-Snow Peak Flows. Unpublished manuscript, Resources Planning Group, British Columbia Forest Products Limited, Crofton, British Columbia.

Yoshida, Z. 1960. A Calorimeter for Measuring the Free Water Content of Wet Snow. Journal of Glaciology, 3: 574-576.

Zuzel, J. F., R. N. Greenwalt, and R. R. Allmaras. 1983. Rain on Snow: Shallow, Transient Snowpacks with Frozen Soils. In: Proceedings of the 51st Annual Western Snow Conference, pp. 67-74.

APPENDICES

APPENDIX A: ERROR ANALYSIS

The evaluation of measurement uncertainties and assumptions are incorporated in an error analysis that follows the technique of Scarborough (1966) as outlined by Holbo (1973), Fritschen and Gay (1979), and Vanderwaal (1983). Because many of the energy balance components used to determine snowmelt are indirect measurements calculated from direct measurements or assumptions, the error in the direct measurements and assumptions must be quantified to determine the error in the energy balance components.

An indirect energy balance measurement, M, is a function of its component variables, X_i, such that:

$$M = f(X_1, X_2, X_3, \ldots, X_n) \tag{1}$$

The errors in the component variables (δX_i) produce errors in the energy budget measurement (δM) such that:

$$M + \delta M = f(X_1 + \delta X_1, X_2 + \delta X_2, \ldots, X_n + \delta X_n) \tag{2}$$

The error in the energy balance measurement can be isolated by expanding this function by Taylor's Theorem, ignoring the small terms and subtracting from equation (2) to yield:

$$\delta M = \delta X_1 \frac{\partial M}{\partial X_1} + \delta X_2 \frac{\partial M}{\partial X_2} + \ldots + \delta X_n \frac{\partial M}{\partial X_n} \tag{3}$$

This is the general formula for calculating the absolute error of a function from the absolute errors in its component variables. If

each component error, δX_i is considered to be a randomly distributed uncertainty within an upper limit, or probable error, rather than the absolute error resulting from the worst possible case, there is the probability that the errors will compensate each other. The overall probable error, δM, is estimated by combining the component probable errors, δX_i, by the principle of least squares:

$$\delta M = [(\delta X_1 \frac{\partial M}{\partial X_1})^2 + (\delta X_2 \frac{\partial M}{\partial X_2})^2 + \ldots + (\delta X_n \frac{\partial M}{\partial X_n})^2]^{1/2} \quad (4)$$

Because of the error compensation, the probable error estimate will be smaller than the absolute error estimate calculated from equation 3. All of the errors discussed will be in terms of meltwater depths.

ERROR IN SHORTWAVE RADIATION MELT

The transfer of heat to a snowpack by shortwave radiation was described previously as:

$$K^* = K\downarrow - K\uparrow \quad (5)$$

Outgoing shortwave radiation may be described by:

$$K\uparrow = \alpha K\downarrow \quad (6)$$

where α is the albedo of the snowpack. Applying the latent heat of fusion and the appropriate unit conversions, snowmelt by shortwave

radiation was determined by:

$$K_M^* = 0.010837(K\downarrow - \alpha K\downarrow) \tag{7}$$

The probable error in shortwave radiation melt is:

$$\delta K_M^* = [(\delta K\downarrow \frac{\partial K_M^*}{\partial K\downarrow})^2 + (\delta\alpha \frac{\partial K_M^*}{\partial \alpha})^2]^{1/2} \tag{8}$$

where the error in shortwave radiation melt, δK_M^*, is the result of the errors in incoming shortwave radiation and albedo. The error of incoming shortwave radiation, $\delta K\downarrow$, was about 10 percent as determined by calibration of the Li Cor Model LI-200S pyranometers with a Kipp solarimeter. Snowpack albedo, α, was estimated to be 0.85 by a Kipp solarimeter. An analysis of the data resulted in an error of 0.04.

Differentiating shortwave radiation with respect to incoming shortwave radiation gives:

$$\frac{\partial K_M^*}{\partial K\downarrow} = 0.010837 - 0.010837\alpha \tag{9}$$

Differentiating shortwave radiation melt with respect to albedo gives:

$$\frac{\partial K_M^*}{\partial \alpha} = -0.010837K\downarrow \tag{10}$$

The probable error of shortwave radiation melt can now be estimated by:

$$\delta K_M^* = [(0.10K\downarrow(0.010837-0.010837\alpha))^2+(0.04(-0.010837K\downarrow))^2]^{1/2} \quad (11)$$

using the derived expressions and values given above.

Error magnitudes are given in Table A1 for several sets of values that are in the range of measurements. The relative probable error of shortwave radiation melt, $\partial K_M^*/K_M^*$, was 28 percent with about 73 percent of that error caused by the error of albedo. The errors in shortwave radiation melt do not strongly affect the energy balance model because of the low shortwave radiation input during most rain-on-snow periods (generally less than 50 W/m^2).

ERROR IN LONGWAVE RADIATION MELT

The heat transfer of longwave radiation (L^*) to a snowpack was given by:

$$L^* = \sigma(T_a^4 - T_s^4) \quad (12)$$

Converted to melt water depth by applying the latent heat of fusion and the appropriate unit conversions, the expression becomes:

$$L_M^* = 0.010837\sigma(T_a^4 - T_s^4) \quad (13)$$

where the cloud base and forest canopy temperatures were approximated

Table A1. Probable Errors (δK_M^*) and Relative Probable Errors ($\delta K_M^*/K_M^*$) of Shortwave Radiation Melt for a Range of Incoming Shortwave Radiation Magnitudes ($K\downarrow$).

$K\downarrow$ (W/m^2)	K_M^* (mm/hr)	δK_M^* (mm/hr)	$\delta K_M^*/K_M^*$ (%)
1	0.002	0.001	28
5	0.008	0.002	28
10	0.016	0.005	28
20	0.032	0.009	28
50	0.081	0.023	28
100	0.163	0.046	28
200	0.325	0.093	28
300	0.488	0.139	28

Table A2. Probable Errors (δL_M^*) and Relative Probable Errors ($\delta L_M^*/L_M^*$) of Longwave Radiation Melt for a Range of Commonly Occurring Air Temperatures.

Plot	Air Temperature (°C)	L_M^* (mm/hr)	δL_M^* (mm/hr)	$\delta L_M^*/L_M^*$ (%)
Clearcut				
	2	0.101	0.074	73
	4	0.205	0.075	37
	6	0.311	0.077	25
Forest				
	2	0.101	0.045	44
	4	0.205	0.046	22
	6	0.311	0.047	15

by air temperature. However, field verification by a Telatemp AG-42 infrared thermometer revealed that the cloud base and forest canopy termperatures deviated from air temperature. During periods of rain with low, thick clouds, air temperature overestimated cloud base temperature by an average of 0.79°C. Similarly, the air temperature overestimated the temperature of the forest canopy by an average of 0.22°C. The specifications of the Campbell Model 101 thermistors indicated an error in air temperature measurements of 0.15°C and the specifications of the Telatemp Ag-42 infrared thermometer indicated temperature errors of 0.5°C. Thus, the overall errors were 1.44°C for the clearcut and 0.88°C for the forest plot. Because the errors of cloud base and forest canopy temperatures were not identical, the probable errors of longwave radiation melt in the forest and clearcut were analyzed separately. Longwave radiation melt for the clearcut may be written as:

$$L_M^* = 0.010837\sigma(T_c^4 - T_s^4) \tag{14}$$

The probable error in L_M^* is:

$$\delta L_M^* = \delta T_c \frac{\partial L_M^*}{\partial T_c} \tag{15}$$

Differentiating longwave radiation melt with respect to cloud temperature (T_c), and applying the 1.44°C error in cloud base temperature (δT_c) gives the equation to estimate the overall

probable error in longwave radiation melt for the clearcut:

$$\delta L_M^* = 0.0624\sigma T_c^3 \tag{16}$$

Error magnitudes are given in Table A2 for a range of air temperatures most common during rain-on-snow periods. Although the relative probable errors of longwave radiation melt ($\delta L_M^*/L_M^*$) were quite high for low temperatures, it must be noted that snowmelt attributed to longwave radiation was quite low during these periods. As a result, the relative probable errors were large. The probable error of longwave radiation melt was about 0.074 to 0.077 mm/hr for the range of air temperatures analyzed.

Longwave radiation melt errors for the forest plot were analyzed in a similar fashion, but the absolute error for the forest canopy temperature (δT_f) was 0.88°C. The probable error in forest longwave radiation melt can then be written as:

$$\delta L_M^* = 0.0381\sigma T_f^3 \tag{17}$$

It is not surprising that large relative errors in longwave radiation melt ($\delta L_M^*/L_M^*$) occurred in the forest (Table A2). As in the clearcut, the longwave radiation melt in the forest was low during periods of low temperatures. Although probable errors were nearly constant at about 0.05 mm/hr, the effect of dividing the probable errors by low longwave radiation melt rates greatly increased the relative probable errors.

ERROR IN SENSIBLE HEAT MELT

The U. S. Army Corps of Engineers (USACE, 1956) developed the equation used in this study to estimate snowmelt by sensible heat flux:

$$M_H = 1.80 \times 10^{-2} \left(\frac{P_a}{P_o}\right) (Z_a \times Z_t)^{-1/6} (T_a - T_s) V \qquad (18)$$

where P_a/P_o was approximated by 0.902 and $(Z_a \times Z_t)^{-1/6}$ was set to 0.847. Incorporating the constants into equation 18 yields the simplified equation:

$$M_H = 0.0138\ VT_a - 0.0138\ VT_s \qquad (19)$$

As discussed previously, the error of air temperature measurements, δT_a, was 0.15°C. Calibration of the Weathertronics Model 2031 3-cup anemometers in a wind tunnel revealed errors in windspeed measurement. Minimum windspeeds necessary to initiate anemometer spinning was 0.9 m/s for the clearcut anemometer and 0.7 m/s for the forest anemometer. The errors of wind measurements, δV, were 0.21 m/s for the clearcut anemometer and 0.24 m/s for the forest anemometer. The errors were determined by comparing the anemometer outputs to the calibration equation values for a range of windspeeds. Because errors in sensible heat melt were related to measurement errors of air temperature and wind, the overall probable

error is described by:

$$\delta M_H = [(\delta T_a \frac{\partial M_H}{\partial T_a})^2 + (\delta V \frac{\partial M_H}{\partial V})^2]^{1/2} \quad (20)$$

The differentiation of M_H with respect to T_a is simply 0.01380V, and the differentiation of M_H with respect to V is $0.01380T_a$. Combining the measurement errors with the differentiated terms yields the overall probable error for sensible heat melt:

$$\delta M_H = [(0.15 \times 0.01380V)^2 + (0.21 \times 0.01380T_a)^2]^{1/2} \quad (21)$$

for the clearcut and:

$$\delta M_H = [(0.15 \times 0.01380V)^2 + (0.24 \times 0.01380T_a)^2]^{1/2} \quad (22)$$

for the forest plot. It is important to note that during periods of windspeeds below the anemometer thresholds, but above 0.0 m/s, the sensible heat melt was computed as zero resulting in a 100 percent relative probable error. However, sensible heat melt during these periods was not large compared to windier periods. Consequently, unless low wind periods were of long duration, the probable errors of sensible heat melt would not be great. Probable and relative probable error magnitudes are given in Table A3 for a range of temperatures and windspeeds most common during the rain-on-snow periods studied. Probable errors were generally less than 0.02 mm/hr, but relative probable errrors were as high as 25 percent during cool, low wind periods when sensible heat melt was not great.

Table A3. Probable Errors (δM_H) and Relative Probable Errors ($\delta M_H/M_H$) of Sensible Heat Melt for a Range of Commonly Occurring Air Temperatures and Windspeeds.

Plot	Air Temperature (°C)	Windspeed (m/s)	M_H (mm/hr)	δM_H (mm/hr)	$\delta M_H/M_H$ (%)
Clearcut					
	2	1	0.028	0.006	22
	2	2	0.055	0.007	13
	2	3	0.083	0.008	10
	4	1	0.055	0.012	21
	4	2	0.110	0.012	11
	4	3	0.166	0.013	8
	6	1	0.083	0.018	21
	6	2	0.166	0.018	11
	6	3	0.248	0.018	7
Forest					
	2	1	0.028	0.007	25
	2	2	0.055	0.008	14
	2	3	0.083	0.009	11
	4	1	0.055	0.013	24
	4	2	0.110	0.014	13
	4	3	0.166	0.015	9
	6	1	0.083	0.020	24
	6	2	0.166	0.020	12
	6	3	0.248	0.021	8

ERROR IN LATENT HEAT MELT

Snowmelt by latent heat transfer was estimated by an equation developed by the U. S. Army Corps of Engineers (USACE, 1956) given previously as:

$$M_E = 8.63 \times 10^{-4} (Z_a \times Z_d)^{-1/6} (e_a - e_s)V \quad (23)$$

In this study, the constant $(Z_a \times Z_d)^{-1/6}$ is 0.847 and the vapor pressure of snow (e_a) is 610.78 Pa. Thus, equation 23 simplifies to:

$$M_E = 7.3 \times 10^{-4} (e_a - 610.78)V \quad (24)$$

The overall probable error of latent heat melt is:

$$\delta M_E = [(\delta e_a \frac{\partial M_E}{\partial e_a})^2 + (\delta V \frac{\partial M_E}{\partial V})^2]^{1/2} \quad (25)$$

where the probable error of latent heat melt (δM_E) is a function of the probable errors in the air vapor pressure (δe_a) and the windspeed (δV) terms.

The vapor pressure of air is a function of dewpoint termperature and its probable error can be written as:

$$\delta e_a = \delta T_d \frac{\partial e_a}{\partial T_d} \quad (26)$$

The uncertainty of the dewpoint temperature measurements (δT_d) was

a combination of the measurement error of the dewcels and the measurement error of the E. G. and G. Model 880 mirror hygrometer used to calibrate the dewcels. Specifications for the E. G. and G. Model 880 mirror hygrometer gave a probable error of 0.83°C. Calibration of the dewcels with the mirror hygrometer under different humidity levels resulted in probable errors of 0.34°C for the clearcut dewcel and 0.29°C for the forest dewcel. Thus, the overall probable errors of dewpoint temperature measurements (δT_d) were 1.17°C for the clearcut plot and 1.12°C for the forest plot.

The water vapor pressure of the air was calculated by:

$$e_a = 610.78 \exp\left[\frac{(17.269T_d)}{(237.3 + T_d)}\right] \tag{27}$$

which, when differentiated with respect to T_d, gives:

$$\frac{\partial e_a}{\partial T_d} = \frac{[(237.3+T_d)17.269-17.269T_d]}{(237.3+T_d)^2} \times 610.78\exp\left[\frac{(17.269T_d)}{(237.3+T_d)}\right] \tag{28}$$

The differentiation of latent heat melt (M_E) with respect to the vapor pressure of air ($\partial M_E/\partial e_a$) is simply $7.3 \times 10^{-4}V$. Therefore, the first term on the right side of equation 25 becomes:

$$\delta e_a \frac{\partial M_E}{\partial e_a} = \delta T_d \times (\text{equation 28}) \times 7.3 \times 10^{-4}V \tag{29}$$

As discussed previously, probable errors in windspeed measurement

were determined to be 0.21 m/s for the clearcut plot and 0.24 m/s for the forest plot. The anemometer thresholds were 0.9 m/s for the clearcut anemometer and 0.7 m/s for the forest anemometer. Differentiating latent heat melt with respect to windspeeds gives:

$$\frac{\partial M_E}{\partial V} = (7.3 \times 10^{-4} e_a) - (7.3 \times 10^{-4} e_s) \quad (30)$$

Thus, the overall probable error of latent heat melt may be written as:

$$\delta M_E = [(1.17(\text{eqn. } 28)(7.3\text{x}10^{-4}V))^2 + (0.21(7.3\text{x}10^{-4}e_a - 0.4457))^2]^{1/2} \quad (31)$$

for the clearcut plot and:

$$\delta M_E = [(1.12(\text{eqn. } 28)(7.3\text{x}10^{-4}V))^2 + (0.24(7.3\text{x}10^{-4}e_a - 0.4457))^2]^{1/2} \quad (32)$$

for the forest plot. As previously noted, during periods of windspeeds below the anemometer thresholds, the latent heat was computed to be zero resulting in a relative probable error of 100 percent.

The probable and relative probable errors of latent heat melt are given in Table A4 for a range of frequently occurring dewpoint temperatures and windspeeds. The probable errors were large, ranging from 0.04 mm/hr to 0.16 mm/hr. The relative probable errors for dewpoint temperatures above 0°C were especially large during periods of low dewpoint temperatures. This was because the large probable

Table A4. Probable Errors (δM_E) and Relative Probable Errors ($\delta M_E/M_E$) of Latent Heat Melt for Ranges of Commonly Occurring Dewpoint Temperatures and Windspeeds.

Plot	Dewpoint Temperature (°C)	Windspeed (m/s)	M_E (mm/hr)	δM_E (mm/hr)	$\delta M_E/M_E$ (%)
Clearcut					
	1	1	0.034	0.041	122
	1	2	0.067	0.081	121
	1	3	0.100	0.121	121
	3	1	0.107	0.051	48
	3	2	0.214	0.095	44
	3	3	0.322	0.140	43
	5	1	0.191	0.066	34
	5	2	0.382	0.111	29
	5	3	0.572	0.161	28
Forest					
	0	1	0.000	0.036	∞
	0	2	0.000	0.073	∞
	0	3	0.000	0.109	∞
	1	1	0.034	0.040	118
	1	2	0.067	0.078	116
	1	3	0.100	0.117	116
	3	1	0.107	0.049	46
	3	2	0.214	0.092	43
	3	3	0.322	0.134	42

errors of dewpoint temperatures (1.12°C and 1.17°C) exceeded or equalled the magnitudes of the commonly occurring dewpoint temperatures. Because snowmelt attributed to latent heat was near-zero during these periods, dividing the probable errors by snowmelt resulted in large relative probable errors. Therefore, it is not surprising that errors in dewpoint temperature measurements accounted for up to 97 percent of the overall probable error of latent heat melt during low dewpoint temperatures.

ERROR IN RAIN MELT

The heat transfer from rainfall to a snowpack is described by:

$$F = \rho_w C_w T_d P \tag{33}$$

Applying the appropriate unit conversions, the latent heat of fusion, and applicable constants yields the equation:

$$F_M = 0.01264 T_d P \tag{34}$$

The probable error in F_M can be written as:

$$\delta F_M = [(\delta T_d \frac{\partial F_M}{\partial T_d})^2 + (\delta P \frac{\partial F_M}{\partial P})^2]^{1/2} \tag{35}$$

Probable errors in the measurements of dewpoint temperature and rainfall resulted in an overall probable error of snowmelt caused by rainfall.

The probable errors in measurements of dewpoint temperature (δT_d) were previously given as 1.17°C for the clearcut plot and 1.12°C for the forest plot. Differentiating snowmelt caused by rain with respect to dewpoint temperature gives:

$$\frac{\partial F_M}{\partial T_d} = 0.01264P \tag{36}$$

The probable errors of precipitation measurement (δP) were dependent on the method of measuring precipitation. As discussed previously, storage gages were installed in both plots to account for the spatial variation in rainfall. In addition, these gages served as standards of calibration for the heated tipping bucket raingages because the storage gages were located on the ground adjacent to the snowmelt pans. As a result, heated tipping bucket raingage errors caused by evaporation and wind could be measured and removed from the analysis. Thus, it was assumed that no measurement errors occurred when the storage gages and heated tipping bucket raingages were both operating. Unfortunately, the storage gages were not utilized in the forest until the rain-on-snow event of December 28-31, 1983 or in the clearcut until the February 11-13, 1984 rain-on-snow event. Therefore, precipitation information from the heated tipping bucket raingage in the clearcut was adjusted by an average calibration coefficient calculated from data obtained when the storage gages and heated tipping bucket raingage were operating.

The probable error for the clearcut precipitation measurements, which was conservatively estimated to be 10 percent, accounted for

the variation of the raingage calibration coefficients. A large factor that influenced the rainfall information in the forest was that the heated tipping bucket raingage did not operate properly for events 1, 2, 3, and 5. As a result, hourly rainfall information had to be synthesized by the rainfall information from the clearcut and the rainfall information from the forest storage gages when it was available. Thus, the 10 percent clearcut rainfall error had to be included. To synthesize forest precipitation, an interception coefficient (0.94) was applied to the clearcut precipitation. The forest canopy interception averaged 6.2 percent, but was as high as 12.4 percent and as low as zero. As a result, an additional interception error of 6.2 percent had to be applied for a total probable error of 16.2 percent. This probable error was assigned to the forest plot whenever the heated tipping bucket raingage was not operating. Differentiating snowmelt caused by rain with respect to rainfall measurement gives:

$$\frac{\partial F_M}{\partial P} = 0.01264 T_d \tag{37}$$

The overall probable error of snowmelt caused by rainfall for the clearcut when storage gages were present then becomes:

$$\delta F_M = 1.17 \times 0.01264 P \tag{38}$$

For the clearcut when storage gages were not used, overall probable

error becomes:

$$\delta F_M = [(1.17 \times 0.01264P)^2 + (0.10P \times 0.01264T_d)^2]^{1/2} \quad (39)$$

For the forest when the heated tipping bucket was operating, overall probable error becomes:

$$\delta F_M = 1.12 \times 0.01264P \quad (40)$$

For the forest when the heated tipping bucket raingage was not operating, overall probable error becomes:

$$\delta F_M = [(1.12 \times 0.01264P)^2 + (0.162P \times 0.01264T_d)^2]^{1/2} \quad (41)$$

Because there was only a slight difference in errors when the heated tipping bucket was not operating in the forest plot, a separate error was not calculated for the times storage gages were used when the raingage was not operating.

The probable and relative probable errors of snowmelt resulting from rainfall are given in Table A5 and A6. Like the errors of latent heat melt, relative probable errors were large, especially when the dewpoint temperatures were low. This was because of the large errors in measurement of dewpoint temperature. In fact, comparing the errors when the storage gages were in use with the errors when they were not indicates that the largest component of the probable errors consisted of the dewpoint temperature errors.

Table A5. Probable Errors (δF_M) and Relative Probable Errors ($\delta F_M/F_M$) of Snowmelt Resulting from Rainfall for Ranges of Commonly Occurring Dewpoint Temperatures and Rainfall Intensities in the Clearcut Plot. (C/G = clearcut plot with storage raingages and C = clearcut plot without storage raingages.)

Plot	Dewpoint Temperature (°C)	Rainfall (mm/hr)	F_M (mm/hr)	δF_M (mm/hr)	$\delta F_M/F_M$ (%)
C/G	1	0.5	0.006	0.007	117
C	1	0.5	0.006	0.007	117
C/G	1	1.0	0.013	0.015	117
C	1	1.0	0.013	0.015	117
C/G	1	2.0	0.025	0.030	117
C	1	2.0	0.025	0.030	117
C/G	1	4.0	0.051	0.059	117
C	1	4.0	0.051	0.059	117
C/G	3	0.5	0.019	0.007	39
C	3	0.5	0.019	0.008	40
C/G	3	1.0	0.038	0.015	39
C	3	1.0	0.038	0.015	40
C/G	3	2.0	0.076	0.030	39
C	3	2.0	0.076	0.030	40
C/G	3	4.0	0.152	0.059	39
C	3	4.0	0.152	0.061	40
C/G	3	6.0	0.228	0.089	39
C	3	6.0	0.228	0.092	40
C/G	5	0.5	0.032	0.007	23
C	5	0.5	0.032	0.008	25
C/G	5	1.0	0.063	0.015	23
C	5	1.0	0.063	0.016	25
C/G	5	2.0	0.126	0.030	23
C	5	2.0	0.126	0.032	25
C/G	5	4.0	0.253	0.059	23
C	5	4.0	0.253	0.064	25
C/G	5	6.0	0.379	0.089	23
C	5	6.0	0.379	0.097	25

Table A6. Probable Errors (δF_M) and Relative Probable Errors ($\delta F_M/F_M$) of Snowmelt Resulting from Rainfall for Ranges of Commonly Occurring Dewpoint Temperatures and Rainfall Intensities in the Forest Plot. (F/T = forest plot when the heated tipping bucket raingage was operating and F = forest plot when the heated tipping bucket raingage was not operating.)

Plot	Dewpoint Temperature (°C)	Rainfall (mm/hr)	F_M (mm/hr)	δF_M (mm/hr)	$\delta F_M/F_M$ (%)
F/T	0	0.5	0.000	0.007	∞
F	0	0.5	0.000	0.007	∞
F/T	0	1.0	0.000	0.014	∞
F	0	1.0	0.000	0.014	∞
F/T	0	2.0	0.000	0.028	∞
F	0	2.0	0.000	0.028	∞
F/T	0	4.0	0.000	0.057	∞
F	0	4.0	0.000	0.057	∞
F/T	1	0.5	0.006	0.007	112
F	1	0.5	0.006	0.007	113
F/T	1	1.0	0.013	0.014	112
F	1	1.0	0.013	0.014	113
F/T	1	2.0	0.025	0.028	112
F	1	2.0	0.025	0.029	113
F/T	1	4.0	0.051	0.057	112
F	1	4.0	0.051	0.057	113
F/T	3	0.5	0.019	0.007	37
F	3	0.5	0.019	0.008	40
F/T	3	1.0	0.038	0.014	37
F	3	1.0	0.038	0.015	40
F/T	3	2.0	0.076	0.028	37
F	3	2.0	0.076	0.031	40
F/T	3	4.0	0.152	0.057	37
F	3	4.0	0.152	0.062	40
F/T	3	6.0	0.228	0.085	37
F	3	6.0	0.228	0.092	40

ERROR IN MEASURED MELT

Measured melt was determined simply by comparing the snowmelt lysimeter data with the rainfall data. Because of prior calibration, there was little error evident in the lysimeter tipping bucket data. However, rainfall data was in error during periods when the storage gages were not in use or when the heated tipping bucket raingage in the forest was not operating properly. Therefore, there was a 10 percent absolute error of measured snowmelt for the clearcut plot prior to the February 11-13, 1984 rain-on-snow event. A probable error of 16.2 percent for the forest plot was assigned to all of the rain-on-snow events except the February 11-13, 1984 rain-on-snow event.

Discussion of Measurement Errors

It is not surprising that the relative errors were large in this study. During most of the rain-on-snow periods, there were periods when air temperatures, dewpoint temperatures, and windspeeds were lower than the errors associated with their measurement. However, during these periods, snowmelt rates were low because energy inputs into the snowpacks were low. It is evident from the error tables that during periods of high melt rates, the relative probable errors decreased. Although there were periods during each rain-on-snow event where energy inputs were lower than the measurement errors, the periods of higher energy inputs and snowmelt were the major concern

of this study. Thus, the relative probable errors did not usually reach their upper limits during the periods of rapid snowmelt.

APPENDIX B: SYMBOLS AND DEFINITIONS

Symbol	Definition
C_a	Specific heat of air (1.005 kJ/kg-°C)
C_w	Specific heat of water (4.218 kJ/kg-°C)
E	Water vapor flux density (kg/m^2-min)
F	Heat transfer from rain water (kJ/m^2)
F_M	Snowmelt resulting from rainfall (mm/hr)
FWC	Free water content of snow (percent by weight)
G_b	Heat transfer from the ground (W/m^2)
H	Turbulent transfer of sensible heat (W/m^2)
I	Mass of ice (kg)
K	General turbulent exchange coefficient (m^2/s)
K_H	Exchange coefficient for sensible heat (m^2/s)
K_E	Exchange coefficient for latent heat (m^2/s)
K*	Net shortwave radiation flux density (W/m^2)
K_M*	Shortwave radiation melt (mm/hr)
K↓	Incoming shortwave radiation flux density (W/m^2)
K↑	Outgoing shortwave radiation flux density (W/m^2)
L*	Net longwave radiation flux density (W/m^2)
L_M*	Longwave radition melt (mm/hr)
L↓	Incoming longwave radiation flux density (W/m^2)
L↑	Outgoing longwave radiation flux density (W/m^2)
M_E	Latent heat melt (mm/hr or m/day)
M_H	Sensible heat melt (mm/hr or m/day)

Symbol	Definition
P	Rainfall (m)
P_a	Local atmospheric pressure (Pa)
P_o	Atmospheric pressure at sea level (Pa)
Q_m	Heat equivalent of snowmelt (W/m^2)
T	General temperature term (°C or °K)
T_a	Air temperature (°C or °K)
T_c	Cloud base temperature (°C or °K)
T_d	Dewpoint temperature (°C or °K)
T_f	Forest canopy temperature (°C or °K)
T_p	Rain temperature (°C or °K)
T_s	Snow temperture (°C or °K)
V	Windspeed (m/s)
W	General mass term (kg)
X	Flux density of general property (W/m^2)
Z	Vertical distance from exchange surface (m)
Z_a	Height of windspeed measurement (m)
Z_d	Height of humidity measurement (m)
Z_t	Height of air temperature measurement (m)
d_s	Depth of snow (m)
d_w	Depth of water (m)
e_a	Vapor pressure of air (Pa)
e_s	Vapor pressure of snow (Pa)
q	Specific humidity (kg/kg)

Symbol	Definition
w	Water equivalent of calorimeter (kg)
α	Albedo (dimensionless)
ε	Emissivity of surface or object (dimensionless)
λ	Latent heat of vaporization (2708.7 kJ/kg)
λE	Turbulent transfer of latent heat (W/m^2)
ρ_a	Density of air (1.29 kg/m^3)
ρ_s	Density of snow (kg/m^3)
ρ_w	Density of water (1000 kg/m^3)
σ	Stefan-Boltzmann constant (5.67×10^{-8} $W/m^2\text{-}°K^4$)